SYNTHESIS AND CHARACTERISATION OF BIODEGRADABLE SUPERABSORBENT POLYMER DERIVED FROM SODIUM ALGINATE

PHANG YING NING

MASTER OF SCIENCE

FACULTY OF ENGINEERING AND SCIENCE
UNIVERSITI TUNKU ABDUL RAHMAN
JULY 2011

SYNTHESIS AND CHARACTERISATION OF BIODEGRADABLE SUPERABSORBENT POLYMER DERIVED FROM SODIUM ALGINATE

By

PHANG YING NING

A thesis submitted to Faculty of Engineering and Science,
Universiti Tunku Abdul Rahman,
in partial fulfillment of the requirements for the degree of
Master of Science in Chemistry,
July 2011

ABSTRACT

SYNTHESIS AND CHARACTERISATION OF BIODEGRADABLE SUPERABSORBENT POLYMER DERIVED FROM SODIUM ALGINATE

Phang Ying Ning

Superabsorbent polymers (SAPs) based on sodium alginate (NaAlg), acrylamide (AM), itaconic acid (IA) and acrylic acid (AA) were synthesised. The graft copolymerisation of AM/IA and also AM/IA/AA onto commercial NaAlg was carried out with potassium persulphate (KPS) and SFX or tert-butyl hydroperoxide (tBHP) and SFX as the redox initiators and N,N'-methylenebisacrylamide (N-MBA) and sodium bicarbonate (SBC) as the crosslinking agent and neutralising agent respectively. Ethanol or calcium chloride ($CaCl_2$) was employed as the precipitating agent. The SAPs produced in small-scale synthesis included Alg-*g*-P(AM-*co*-IA) (with and without crosslinking), Alg-*g*-P(AM-*co*-IA-*co*-AA) and Alg-*g*-P(AM-*co*-IA-*g*-AA) (with and without crosslinking), whereas in bigger-scale synthesis, crosslinked-Alg-*g*-P(AM-*co*-IA-*g*-AA) was synthesised. The effects of molar ratio of AM:IA:AA, concentration of KPS or tBHP, grafting of AA, concentration of $CaCl_2$, concentration of N-MBA, volume ratio of $CaCl_2$ to SAP solution and duration of swelling on the swelling capacity of the SAPs prepared in small-scale syntheses were investigated. As 1.0×10^{-4} moles and 2.5×10^{-5} moles of N-MBA were added to the syntheses, crosslinked-Alg-*g*-

P(AM-*co*-IA) and crosslinked-Alg-*g*-P(AM-*co*-IA-*g*-AA) swelled as high as 654.0 and 754.0 gg^{-1}, respectively. On the other hand, the effect of concentration of $CaCl_2$, dilution of SAP solution and particle size of dry polymer on swelling capacity of crosslinked-Alg-*g*-P(AM-*co*-IA-*g*-AA) produced via bigger-scale synthesis were inspected. In the absorbency under load (AUL) test, the AUL throughout all the different durations of swelling (1 to 8 hours) decreased as the applied pressure increased from 0 to 40 g/cm^2. In the test of total solids content (TSC), the percentage monomer conversion was found to be 96.7 %. The SAP showed excellent biodegradability within a short period of time, i.e. up to 83.0 % of weight loss in 40 days. In addition, Infra-red (IR) spectroscopy, thermogravimety analysis (TGA) and scanning electron microscopy (SEM) were done on the SAPs.

ACKNOWLEDGEMENTS

I would like to take this opportunity to express my sincere gratitude to my supervisor, Dr. Chee Swee Yong, who graciously gave her time to guide me throughout this research project. Her helpful suggestions and corrections are gratefully acknowledged.

I would also like to express my appreciation to the government of Malaysia, represented by the Ministry of Science, Technology and Innovation (MOSTI) for funding, Kuok Foundation for offering scholarship to my study, and Green Wish Vegi Garden, Chenderiang, Perak, Malaysia for providing the indigenous microorganism soil.

I owe my thanks to my coursemates for their invaluable comments throughout this project. My special thanks must be reserved to John, my supervisor's research assistant, who helped in carrying out the tests of microbial degradation, and also my friend, Chloe, who solved a lot of my queries on software-related problems.

Last but not least, special thanks to my family, especially my parents, for their willingness to understand and support me from start to finish.

FACULTY OF ENGINEERING AND SCIENCE

UNIVERSITI TUNKU ABDUL RAHMAN

Date: _____

SUBMISSION OF THESIS

It is hereby certified that **PHANG YING NING** (ID No: **09UEM02285**) has completed this thesis/dissertation entitled "**SYNTHESIS AND CHARACTERISATION OF BIODEGRADABLE SUPERABSORBENT POLYMER DERIVED FROM SODIUM ALGINATE**" under the supervision of Assistant Prof. Dr. Chee Swee Yong from the Department of Chemical Science, Faculty of Science.

I understand that University will upload softcopy of my thesis in pdf format into UTAR Institutional Repository, which may be made accessible to UTAR community and public.

Yours truly,

_____

(PHANG YING NING)

APPROVAL SHEET

This dissertation/thesis entitled "**SYNTHESIS AND CHARACTERISATION OF BIODEGRADABLE SUPERABSORBENT POLYMER DERIVED FROM SODIUM ALGINATE"** was prepared by **PHANG YING NING** and submitted as partial fulfillment of the requirements for the degree of Master of Science at Universiti Tunku Abdul Rahman.

Approved by:

_____
(Assistant Prof. Dr. Chee Swee Yong)
Date:……..
Supervisor
Department of Chemical Science
Faculty of Science
Universiti Tunku Abdul Rahman

LIST OF TABLES

LIST OF FIGURES

LIST OF APPENDICES

LIST OF ABBREVIATIONS

µL	microlitre
AA	acrylic acid
Alg-*g*-P(AM-*co*-IA)	alginate-*g*-poly[acrylamide-*co*-(itaconic acid)]
Alg-*g*-P(AM-*co*-IA-*co*-AA)	alginate-*g*-poly[acrylamide-*co*-(itaconic acid)-*co*-(acrylic acid)]
Alg-*g*-P(AM-*co*-IA-*g*-AA)	alginate-*g*-poly[acrylamide-*co*-(itaconic acid)-*g*-(acrylic acid)]
Alg-*g*-PAA	alginate-*g*-poly(acrylic acid)
Alg-*g*-PAM	alginate-*g*-polyacrylamide
Alg-*g*-PIA	alginate-*g*-poly(itaconic acid)
AM	acrylamide
AN	acrylonitrile
APS	ammonium persulphate
AUL	absorbency under load
Ca^{2+}	calcium (II) ion
$CaCl_2 \cdot 2H_2O$ (or $CaCl_2$)	calcium chloride dichloride
$CaCO_3$	calcium carbonate
$CaSO_4$–$CaCO_3$–GDL	calcium sulphate-calcium carbonate-glucono-d-lactone
CMC	carboxymethylcellulose
COD	chemical oxygen demand
$-COO^-$	carboxylate
-COOH	carboxylic acid
crosslinked-Alg-*g*-P(AM-*co*-IA)	crosslinked-alginate-*g*-poly[acrylamide-*co*-(itaconic acid)]
crosslinked-Alg-*g*-P(AM-*co*-IA-*g*-AA)	crosslinked-alginate-*g*-poly[acrylamide-*co*-(itaconic acid)-*co*-(acrylic acid)]
G	(1,4)-α-L-gulopyranuronic acid
IA	itaconic acid
IPN	interpenetrating network
IR	Infra-red
IUPAC	International Union of Pure and Applied Chemistry
KBr	potassium bromide
kDa	kiloDalton
kPa	kilopascal
KPS	potassium persulphate
M	(1,4)-β-D-mannopyranuronic acid
M	monomer molecule
$M_1\bullet$	chain initiating species

MAA	methacrylic acid
mPa.s	millipascal seconds
Na_2CO_3	sodium carbonate
NaAlg	sodium alginate
NaAlg-*g*-PAA	sodium alginate-*g*-poly(acrylic acid)
NaAlg-*g*-PIA	sodium alginate-*g*-poly(itaconic acid)
NaCl	sodium chloride
N-MBA	N,N'-methylenebisacrylamide
ORD-reaction	oxidative–reductive free radical depolymerisation
OSA	oxidised sodium alginate
PAA	poly(acrylic acid)
PAM	polyacrylamide
PIA	poly(itaconic acid)
psi	pound per square inch
PVP	polyvinylpyrolidone
R•	initiator radical
rpm	revolutions per minute
SAP	superabsorbent polymer
SBC	sodium bicarbonate
SEM	scanning electron microscopy
Semi-IPN	semi-interpenetrating network
SGF	simulated gastric fluid
SH	sodium humate
SIF	simulated intestinal fluid
tBHP	tert-butyl hydroperoxide
T_d	thermal decomposition temperature
T_g	glass transition temperature
TG	thermogravimetry
TGA	thermogravimetric analysis
TSC	total solids content
UV	ultraviolet
wt.%	weight percent

TABLE OF CONTENTS

CHAPTER 1.0

INTRODUCTION

1.1 Polysaccharide

Sustainable development requires a friendly environment. It is the general consensus that non-biodegradable waste has to be evaded, and biodegradable product has to be utilised as far as possible under reasonable ecological and economical conditions. Hence, in recent years, interest in polymer production has shifted towards the synthesis of biodegradable polymers because of their environmental benefits. Among them, carbohydrates have attracted growing interest for the development of carbohydrate-based products.

Carbohydrates are plentiful, as they comprise more than 90% of the dry mass of all biomass, and more than 90% of the carbohydrate mass is in the form of carbohydrate polymers (polysaccharides) (Zohuriaan and Shokrolahi, 2004). Polysaccharides, which are the stereoregular polymers of monosaccharides, are distinctive raw materials. The uniqueness of polysaccharides lies on the facts that they are natural biopolymers which are inexpensive (economic) and widely available in many countries. Being stable, hydrophilic and amenable to both chemical and biochemical modification

(Crini, 2005), polysaccharides are obtainable from renewable resources, which caused them to be exploited for decades in numerous applications.

Apart from the above-mentioned, polysaccharides also have superior biological and chemical properties. These advantageous properties include biodegradability, polyfunctionality, non-toxicity, high chemical reactivity, biocompatibility, chirality, chelation and adsorption capacities. The factors which contribute to the extraordinary adsorption behavior of polysaccharides include high hydrophilicity of the polymer due to hydroxyl groups of glucose units, presence of a large number of functional groups (acetamido, primary amino and/or hydroxyl groups), high chemical reactivity of the functional groups and flexible structure of the polymer chain (Crini, 2005).

1.2 Alginates

1.2.1 Source of Alginic Acid

Alginic acid is a naturally occurring acidic polysaccharide majorly extracted from the brown algae (phylum Phaeophyta). It exists as the most abundant polysaccharide in the brown algae, consisting of up to 40% of the dry matter (Draget, 2009). The extracts of polysaccharides from marine macroalgae are commonly called hydrocolloids or phycocolloids because they display colloidal properties when dissolved in water and are extracted from seaweed (the Greek word for seaweed is ‘phykos’) (Lewis *et al.*, 1988).

Although this gelling polysaccharide is found in all species of brown seaweeds (Chandia *et al.*, 2005), the main species of commercial importance are *Laminaria hyperborea*, *Laminaria digitata*, *Laminaria japonica*, *Macrocystis pyrifera*, *Ascophyllum nodosum*, *Eclonia maxima*, *Lessonia nigrescens*, *Durvillaea antarctica*, and *Sargassum spp* (Cui and Wang, 2006). Alginic acid is also found in the family Corallinaceae of the red algae (phylum Rhodophyta) (Davis *et al.*, 2003).

Alginate is present within the inner layer of the cell wall matrix and in the mucilage or intercellular matrix as a gel containing sodium, calcium, magnesium, strontium and barium ions (Davis *et al.*, 2003; Draget, 2009). As the major structural polysaccharide of brown seaweed, alginate imparts flexibility in addition to contributing to the strength of the cell wall. The abundance of alginic acid varies between 10% and 40% of the dry weight of untreated algae, depending on the seasonal variations and the depth at which the algae grows in the water (Davis *et al.*, 2003, Sabra and Deckwer, 2004).

Apart from being present in natural seaweeds that are found in the shallow waters of temperate zones, alginic acid is also synthesised as capsular polysaccharides by two types of soil bacteria, *Pseudomonas aeruginosa* and *Azotobacter vinelandii* (Draget *et al.*, 2005; Robyt, 1998). However, all commercial alginates are extracted from algal sources (Draget, 2009). Although the mechanism involved in producing this polymer is not elucidated up to date, the fact that these bacteria synthesised alginic acid resembling alginates from brown algae is undisputed.

1.2.2 Chemical Structure of Alginic Acid

Alginic acid is an unbranched block copolymer consisting of two distinct monosaccharide residues, (1,4)-β-D-mannopyranuronic acid (M) (Figure 1.1) and (1,4)-α-L-gulopyranuronic acid (G) (Figure 1.2). Although Robyt (1998) described that the amounts of M and G are in the ratio of 2:1 for most alginic acids, the ratio or composition of the uronic acids can differ widely with the algal species, season, type of the tissue, age of the plant and habitat (Chandia *et al.*, 2005; Leal *et al.*, 2008; Robyt, 1998).

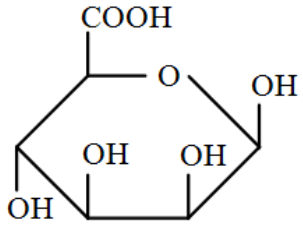

Figure 1.1 (1,4)-β-D-mannopyranuronic acid (M)

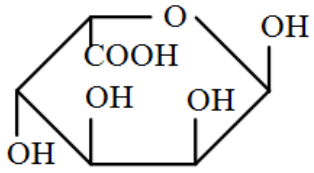

Figure 1.2 (1,4)-α-L-gulopyranuronic acid (G)

The polymer could be broken up into three distinct portions simply by partial acid hydrolysis (Draget *et al.*, 2005). Repeating units of the respective M and G molecules made up the homopolymeric M- and G-blocks. These

homopolymeric regions of M- and G-blocks are in turn strictly separated by alternating repeating units of M and G, the so-called MG blocks (Figure 1.3).

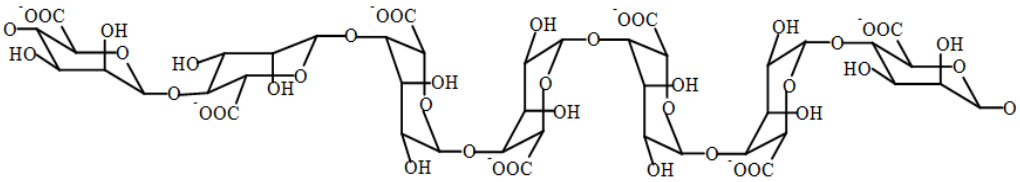

Figure 1.3 Chair conformation of MG block

Draget *et al*. (2005) cited Larsen *et al.* (1970), Painter *et al.* (1968), and Smidsrød and Whittington (1969) as proving that the sequential structure of an alginic acid polymer takes no regular pattern, hence the Bernoullian statistics could not explain the distribution of monomers along the polysaccharide chain. This finding was further supported by Orive *et al*. (2006). However, Larsen *et al.* (1970) proposed that a second-order Markov model would be appropriate to generally describe the monomer sequence in alginates.

According to Skjåk-Bræk *et al*. (1986) (as cited by Draget *et al*. (2005)), the main distinction at the molecular level between algal and bacterial alginates is the existence of *O*-acetyl groups found at C2 and/or C3 in the bacterial alginates. The source of the algae, part of the algae from which the alginate is extracted, as well as the place and season of collection determine the sequences and lengths of the three blocks (Cui and Wang, 2006).

Alginates are the salts and derivatives of alginic acid. If the acid groups are in the acid form (-COOH), the polysaccharide is called alginic acid, which

is water insoluble. Oppositely, if the acid groups are in the carboxylate form ($-COO^-$), it is known as the alginate or sodium alginate (Figure 1.4), which is water soluble. Since alginic acid is insoluble, the soluble sodium, potassium or ammonium salts become the preferable compounds for industrial and food purposes. Among these, sodium alginate is the most widely used compound (Glicksman, 1953).

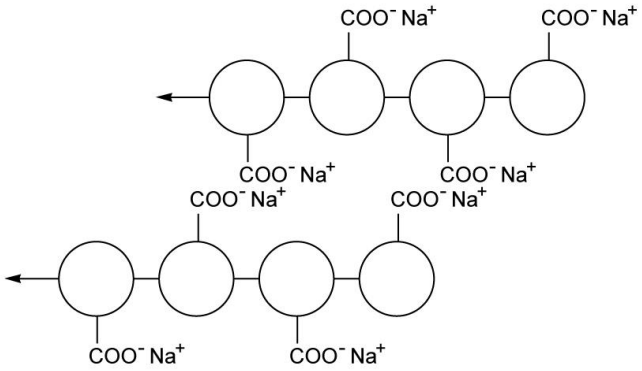

Figure 1.4 Model of sodium alginate

1.2.3 Physical Properties of Alginate

In general, the molecular masses of alginates range between 500 and 1000 kDa. They are readily soluble in cold or hot water – their solubility is influenced by factors such as pH, concentration, ions in solution, the presence of divalent ions (Moe *et al.*, 1995) and ionic force (Rioux *et al.*, 2007).

The viscosities of alginates could reach up to 5000 mPa.s for a 1 % solution. As alginate solutions are known to be pseudoplastic, a drop in viscosity is expected as higher shear is applied. Temperature, shear rate,

concentration, and polymer size are among some known physical variables that affect the flow characteristics of alginate solutions, while chemical variables include pH, sequestrants, monovalent salts and polyvalent cations (Lewis *et al*., 1988).

Compared with other gelling polysaccharides, alginate gels are well-known to be cold setting. This in turn signifies that alginate gels set more or less independent of temperature. However, the kinetics of the gelling process may be strongly modified by a change in temperature. Being non-equilibrium gels, alginates are dependent upon the history of formation. Thus, the properties of the final gel will change if gelation occurs at different temperature (Draget, 2009). The thermoirreversibility of alginate gels also indicates that the gels are heat stable, hence they can be heat treated without melting, although they may ultimately degrade (Cui and Wang, 2006).

Perhaps the most remarkable feature of alginate's physical property is its selective binding of multivalent cations (Draget *et al*., 2005). As soon as it comes into contact with divalent metal ions, the sodium ions in sodium alginate are replaced by the ions and the polysaccharide is crosslinked by the metal ions to form gels. The divalent metal ions are such as calcium, barium, strontium, cadmium, copper, cobalt, lead, nickel or zinc. Among these ions, calcium is the most frequently used cation to form gels (Figure 1.5) (Robyt, 1998).

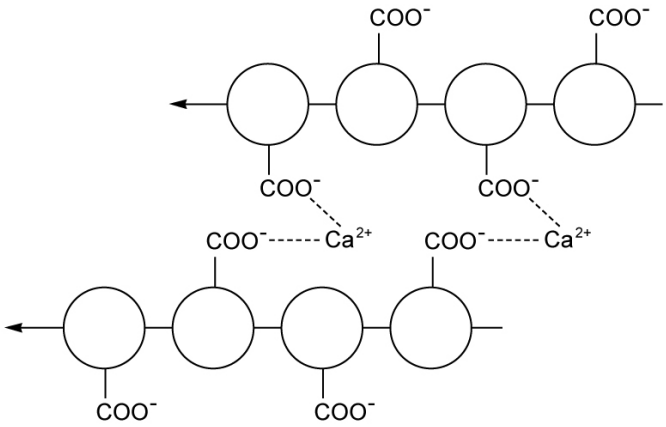

Figure 1.5 Model of calcium alginate

The affinity for divalent cations and the formation of gels in alginates are largely due the presence of G residues. The binding sites for the calcium ions are believed to be formed by two axially linked G residues, and that sequence of G between two or more alginate molecules creates a gel network of calcium crosslinking the alginate molecules. This description is known as the "egg-box" model, since the calcium ions resembled eggs fitting into a box made by the alginate chains (Figure 1.6) (Robyt, 1998).

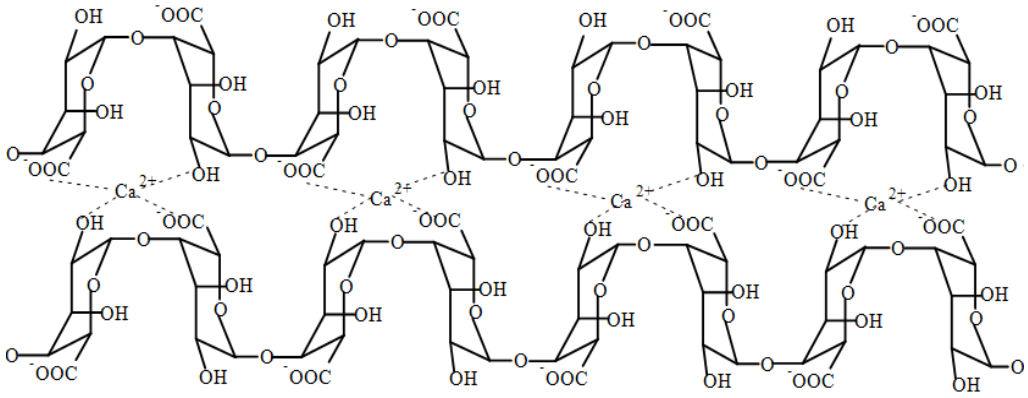

Figure 1.6 "Egg-box" model

Nevertheless, it is worthwhile to keep in mind that the chemical and physical properties of the alginic acid molecules are determined by the distribution, proportion and length of the M-, G- and MG-blocks (FMC Biopolymer, 2010).

1.2.4 Industrial Production of Alginate

Upon harvest and delivery to the factory, seaweeds are milled and washed to prepare them for alginate removal. Since alginate is insoluble due to its salt derivatives obtained during growth in seawater, a pre-extraction treatment is needed to convert the insoluble cations into protons. Therefore, in algae production, the first step is an ion-exchange with protons by extracting the milled algal tissue with 0.1 – 0.2 M mineral acid in order to recover purified alginate (Draget, 2009).

The second step is to convert the water insoluble alginic acid into water soluble sodium salt by neutralisation with alkali such as sodium carbonate or sodium hydroxide (Cui and Wang, 2006). The algal cell structure is broken down upon further dilution of the mixture with fresh water, releasing sodium alginate into the solution. Separation of the insoluble seaweed particles from the sodium alginate solution is achieved via standard solid-liquid clarification techniques such as sifting, floatation, sedimentation, filtration and centrifugation (Lewis *et al*., 1988).

After these extensive separation procedures, alginate is recovered from the clarified sodium alginate solution by direct precipitation with alcohol, calcium chloride or mineral acids such as sulphuric acid. The alginate is converted to the desired form by neutralisation with appropriate cation bases, then dried and milled to produce the final product (Lewis *et al*., 1988). In addition to alginic acid, sodium, potassium, ammonium and calcium salts are other commercially available alginates.

1.2.5 Applications of Alginates

1.2.5.1 Food

Consuming about 50 % of the alginate produced (Sabra and Deckwer, 2004), the food industry witnesses the growing demand of alginates in the market. The alginates used in food industry are currently produced from harvested brown algae, and the global market for this polysaccharide is about 30,000 tons (Sabra and Deckwer, 2004).

Alginates do not have any nutritional value; nevertheless, they are frequently used as additives to alter and stabilise the texture of foods. The fact that the most significant properties of alginate are its ability to form a gel and stabilise aqueous mixtures and emulsions (Torres *et al*., 2007), alginates are widely used as additives capable of viscosifying, stabilising, emulsifying and gelling aqueous solutions. They are used extensively in foods such as bakery products, dessert gels, salad dressings, dairy products, beverages, fabricated foods and frozen desserts (Lewis *et al*., 1988). Ice cream production witnesses

the most important application of alginate, in which it is used to prevent crystallisation and shrinkage, thus rendering a more homogenous product (Sabra and Deckwer, 2004).

The high level of safety of alginates in food use has been proven through several toxicological studies. In 1982, the U.S. Federation of American Societies for Experimental Biology (FASEB) affirmed the status of alginates as "generally recognised as safe". The European common market (EC) regulations and the Codex Alimentarius Commission of the United Nations Food and Agriculture Organisation/World Health Organisation also permit the usage of alginates in foods (Lewis *et al*., 1988).

1.2.5.2 Medicine

For decades, alginates are renowned as helping agents in human-health applications. The salts of alginic acid have a long history in the management of wounds, and huge amounts of alginates are used each year for the treatment of exuding wounds, such as leg ulcers, pressure ulcers and infected surgical wounds (Thomas, 2004). Other than being used as traditional wound dressings, alginates are also used in dental impression material and in some formulations preventing gastric reflux (Draget *et al.*, 2005).

The fiery increase in the use of alginate in medical applications began with the acknowledgment of its use as a scaffold for the encapsulation and

immunoprotection of transplanted cells. In various biotechnological processes, alginates are well-known as immobilisation matrices (Wong, 2004).

Calcium alginate gel has become the most extensively used medium for immobilising living cells such as bacteria, algae, yeast, and plant and animal cells (Sabra and Deckwer, 2004). The immobilisation of living cells by entrapment of cells within calcium alginate gel-spheres is carried out in a single-step procedure under very mild conditions, and is thus compatible with most cells (Draget *et al.*, 2005). From production of ethanol by yeast, to production of monoclonal antibodies by hybridoma cells, to mass production of artificial seed by entrapment of plant embryos, the use of this immobilisation technique is vast.

Similarly, alginate has been used to immunoprotect recombinant cells delivering tumor-suppressing agents and growth hormone. Chondrocytes, bone-marrow stromal cells, islets, myoblasts, fibroblasts, kidney cells and epithelial cells are the cell types that have been achieved as stable cultures in alginate beads (Wong, 2004).

1.2.5.3 Technical utilisation

The technical applications of alginates could be described as scarce. Quantitatively, the role of alginates in textile printing is the most significant technical application of alginates. Alginate has gained a high popularity in

textile printing as a shear-thinning viscosifyer because of its resulting colour yield, brightness and print levelness.

In paper industry, alginates are used as "sizes" to obtain surface uniformity on papers. This is to enable the deposition and adherence of dyes and ink substances prior to printing (Sabra and Deckwer, 2004). Furthermore, alginates are also used as binding agents in the production of welding rods. In the wet stage, alginate gives stability; during the extrusion process, it functions as a plasticiser (Draget *et al.*, 2005).

Apart from these, alginates are also used in water treatment processes because they help in increasing the aggregate sizes in flocculation processes (Sabra and Deckwer, 2004). Ammonium alginate is used in can sealing. The ammonium form is used because of its very low ash content (Draget *et al.*, 2005).

1.3 Superabsorbent Polymers

Superabsorbent polymers (SAPs) were first introduced into the agriculture and diaper industries about four decades ago (Omidian *et al.*, 2005). Since then, where an excellent water-holding property was of primary concern, SAPs extended their applications to other industries.

SAPs are structurally crosslinked, highly swollen and hydrophilic polymer networks capable of absorbing a large amount of water or aqueous

saline solutions, practically 10 to 1000 times of their original weight or volume (Ramazani-Harandi *et al*., 2006), in relatively short periods. SAPs are not dissolved in the media they are in due to their three-dimensional structure. The electrostatic repulsion of the ionic charges of the polymer networks induces swelling by the dissociation of the carboxylic groups (-COONa or -COOK) in solution (Karadag and Saraydin, 2002), allowing the water to enter the matrix.

Kabiri *et al*. (2003) and Ramazani-Harandi *et al*. (2006) described that the desired features of SAPs include high swelling capacity, high swelling rate and good strength of the swollen gel. The water absorbency of a SAP is greatly influenced by its composition, molecular weight, degree of crosslinking, the molecular conformation of the polymer, and by the properties of liquids to be absorbed (Chen and Tan, 2006).

SAPs are commonly based on acrylic monomers such as acrylamide, acrylic acid and salts of the acid (Omidian *et al*., 1998). Commercially, SAPs are majorly produced with acrylic acid as a key component (Lanthong *et al*., 2006). The super-swelling characteristics of SAPs equipped them for use in water absorbing applications such as disposable diapers, feminine napkins, agriculture, cosmetic and absorbent pads.

Recently, the diverse applications of superabsorbent polymers are still being expanded to many fields including agriculture and sealing composites, horticulture, drilling fluid additives, artificial snow, medicine, and so on (Li and Wang, 2005). The applications found in medical field can be further

divided roughly into three categories: drug delivery systems, wound closure and healing products, and surgical implant devices (Van de Velde and Kiekens, 2002).

Diapers or other absorbent articles incorporated with biodegradable SAPs might be disposed of in municipal composting facilities or directly flushed down the toilet to degrade in domestic septic tanks or at municipal wastewater treatment plants. Thus, SAP producers have shifted their attention to the development of biodegradable SAPs in order to suit the growing demand for biodegradable products.

1.4 Scope

In this project, the synthesis of a novel biodegradable superabsorbent polymer derived from sodium alginate is emphasised. The sodium alginate-based superabsorbent polymers are achieved by grafting of poly[acrylamide-*co*-(itaconic acid)] (P(AM-*co*-IA)), poly[acrylamide-*co*-(itaconic acid)-*co*-(acrylic acid)] (P(AM-*co*-IA-*co*-AA)) and poly[acrylamide-*co*-(itaconic acid)-*g*-(acrylic acid)] (P(AM-*co*-IA-*g*-AA)) onto sodium alginate.

Publications on the syntheses of sodium alginate-based biodegradable SAPs are scarce if compared with SAPs incorporated with other carbohydrates, such as cellulose (Chang *et al*., 2010; Wang, 2007) and starch (Lanthong *et al*., 2006; Pourjavadi *et al*., 2010a). Even if there were a few publications on sodium alginate-based SAPs (Hua and Wang, 2009; Lee *et al*.,

2005b; Pourjavadi *et al*., 2006; Pourjavadi *et al*., 2010b), the prepared SAPs were not synthesised with AM, IA and AA as constituent polymers. Thus the current study is pivotal to get an in-depth idea on the swelling capacity, biodegradability and other related properties of the SAPs which are synthesised based on sodium alginate and grafted with acrylamide (AM), itaconic acid (IA) and acrylic acid (AA) – Alg-*g*-P(AM-*co*-IA) (with and without crosslinking), Alg-*g*-P(AM-*co*-IA-*co*-AA) and Alg-*g*-P(AM-*co*-IA-*g*-AA) (with and without crosslinking).

In this research, small-scale syntheses of all the above-mentioned SAPs were carried out before bigger-scale syntheses of crosslinked-Alg-*g*-P(AM-*co*-IA-*g*-AA) were performed. The bigger-scale synthesis was carried out to observe the similarities or differences in the swelling capacities of the samples, between small scale and bigger-scale syntheses.

The small-scale synthesis was carried out to obtain the ratios of the constituting monomers and other ingredients which would result in maximum swelling capacity in the SAP, so as to prevent wastage of chemicals. Once the recipe for the SAP had been established, the scale-up synthesis was performed instead. Synthesising the SAP in a bigger scale would produce results which are more reproducible and representative. More detailed discussions on small-scale and bigger-scale syntheses are provided in Section 4.1.

An effective SAP could easily be defined as an SAP which could absorb high degree of water. In order to establish the ratio of the components

of the SAPs that would produce highest swelling capacity, the effects of the molar ratio of monomer, concentration of initiators, grafting of acrylic acid, concentration of precipitating agent, concentration of crosslinking agent, volume ratio of precipitating agent to SAP solution and duration of swelling on the swelling capacity of the sodium alginate-based SAPs produced via small-scale syntheses would be studied.

In bigger-scale syntheses, the effect of concentration of precipitating agent, dilution of SAP solution and particle size of dry polymer on the swelling capacity of crosslinked-Alg-*g*-P(AM-*co*-IA-*g*-AA) were investigated.

Characterisation of the synthesised SAP – crosslinked-Alg-*g*-P(AM-*co*-IA-*g*-AA) – would be the next step, in which the swollen gel strength, functional groups, thermal stability, total solids content, morphology and biodegradability of the SAP would be respectively verified through absorbency under load (AUL) test, Fourier transform infrared (FTIR) analysis, thermogravimetric analysis (TGA), total solids content (TSC) test, scanning electron microscopy (SEM), and weight loss test using soil supernatant.

In all applications such as diapers or agricultural field which involve SAPs, the swelling products are meant to absorb aqueous solutions while they are under pressure, e.g. the weight of baby, soil, etc. However, the swelling capacities of SAPs are always reported as free-swelling data, i.e. load-free swelling (usually in distilled water). Although the free-swelling data are equally important, the absorbency under load (AUL) data are usually provided

in patent literatures and technical data sheets offered by industrial SAP manufacturers (Ramazani-Harandi *et al*., 2006). In view of the fact, besides measurement of water swelling capacity, the AUL value of the SAP crosslinked-Alg-*g*-P(AM-*co*-IA-*g*-AA) was also obtained in this study.

FTIR analysis provides valuable collection of data on the functional groups which could be found in a substance. Although the FTIR spectrum of commercial sodium alginate had been presented elsewhere (Işıklan *et al*., 2010; Yang *et al*., 2007), the SAPs synthesised in this study are unprecedented. FTIR spectra of Alg-*g*-P(AM-*co*-IA), Alg-*g*-P(AM-*co*-IA-*g*-AA) and crosslinked-Alg-*g*-P(AM-*co*-IA-*g*-AA) were therefore obtained, so as to identify the functional groups which constituted the SAPs.

Thermogravimetry is a well-established experimental technique used in a complete evaluation and interpretation of results when it is known as thermogravimetric analysis (TGA). The significance of TGA in the characterisation of a polymer lies on the fact that it will provide information on the nature and extent of degradation of the polymer as a function of temperature. Thus, in this study, TGA was performed to study the thermal property of the SAP, crosslinked-Alg-*g*-P(AM-*co*-IA-*g*-AA).

Other than the above, the total solids content (TSC) of the polymer samples would also be studied. From the economical aspect, it is important to be aware of the total percentage of solids contained by the SAP, which gives

an indication on the percentage of monomer which has been successfully converted into polymer.

Scanning electron microscopy (SEM) would be used to examine the surface morphology of the SAP. There are quite a few literatures that revealed the SEM picture(s) of a NaAlg-based SAP (Hua and Wang, 2009; Işıklan *et al*., 2010; Pourjavadi *et al*., 2006) if compared to the polymers incorporated with other natural polysaccharides such as cellulose (Sannino and Nicolais, 2005), carboxymethyl cellulose (Biswal and Singh, 2004), mucilage (Mishra *et al*., 2006), sago starch (Danjaji *et al*., 2002), and starch (Lanthong *et al*., 2006). However, it is advantageous to have an idea on the surface morphology of the current SAP, crosslinked-Alg-*g*-P(AM-*co*-IA-*g*-AA), which is based on NaAlg and grafted with PAM, PIA and PAA.

The biodegradability of the SAP synthesised would be analysed via microbial degradation by the means of weight loss test. The utilisation of natural polysaccharides such as alginates in different aspects, such as food, medicine and so on continues to be a subject of intense investigation mostly because of its biodegradability.

Although there are numerous literatures which discussed on different biodegradability tests used for polysaccharide-based polymer (Danjaji *et al*., 2002; Lanthong *et al*., 2006; Mishra *et al*., 2006; Preechawong *et al*., 2004; Rosa *et al*., 2005; Yoshimura *et al*., 2005), there are, however, limited amount of literatures (Lee *et al*., 2005b) on the measurement of biodegradability of

SAPs based on sodium alginate. Therefore, the biodegradability of the SAP would be examined and hence ascertained by microbial degradation.

1.5 Objectives of Study

The objectives of this study are as follows:

(i) To synthesise a biodegradable SAP derived from sodium alginate, namely crosslinked-Alg-*g*-P(AM-*co*-IA-*g*-AA).

(ii) To study the effects of the molar ratio of monomer, concentration of initiators, grafting of acrylic acid, concentration of precipitating agent, concentration of crosslinking agent, volume ratio of precipitating agent to SAP solution, duration of swelling, dilution of SAP solution and particle size of dry polymer on the swelling capacity of the sodium alginate-based SAPs.

(iii) To characterise the SAP, crosslinked-Alg-*g*-P(AM-*co*-IA-*g*-AA), by determining the swollen gel strength, functional groups, thermal stability, total solids content, morphology and biodegradability through absorbency under load (AUL) test, Fourier transform infrared (FTIR) analysis, thermogravimetric analysis (TGA), total solids content (TSC) test, scanning electron microscopy (SEM), and weight loss test using soil supernatant, respectively.

CHAPTER 2.0

LITERATURE REVIEW

2.1 Polymer, Copolymer and Graft Copolymer

The term polymer (Greek words: *poly* meaning many, and *meros* meaning parts) is generally used to describe macromolecules possessing relative molecular masses in excess of 5000 g/mol, which are certainly composed of a minimum of several hundred repeating chemical units (Murray, 1977). The individual repeating units which comprise a polymer are referred to as monomer molecules. A polymer is thus a substance with large molecular mass composed of molecules with repeating structural units, or monomers, which are connected by chemical covalent bonds.

Macromolecules may be classified according to different criteria. One criterion is according to the number of different types of monomers they are prepared from (Braun *et al*., 2005). Polymers are called "homopolymers" when they are produced from one single type of monomer. The resulting materials are called "binary, ternary, … copolymers" if a second or third type of monomer is involved in the polymer synthesis. Depending on how the different monomers are arranged in the resulting copolymer chains, these copolymers are categorised into alternating-, statistic-, block-, and graft-copolymers.

Graft copolymer is a type of copolymer in which one or more blocks of homopolymer B are grafted as branches onto a main chain of homopolymer A, meaning it is a branched copolymer with one or more side chains of a homopolymer B attached to the backbone of homopolymer A. It is named by mentioning the main chain first, with the word "-*graft*-" being inserted in between the names of the corresponding homopolymers, e.g. polyA-*graft*-polyB (Odian, 1991).

2.2 Polyacrylamide, Poly(acrylic acid) and Poly(itaconic acid)

The polymers and copolymers of acrylamide (C_3H_5NO; IUPAC name: prop-2-enamide; common synonyms: acrylic amide, 2-propenamide) and acrylic acid ($C_3H_4O_2$; IUPAC name: prop-2-enoic acid; common synonyms: acroleic acid, ethylenecarboxylic acid, propene acid, propenoic acid, vinylformic acid) are included in the acrylic family of polymers.

Frequently including ionic comonomers, polyacrylamide (Figure 2.1) is used as flocculant in papermaking, mining, and treatment of municipal drinking water and industrial wastes. Meanwhile, gel electrophoresis is known to be using crosslinked polyacrylamide (Odian, 1991).

Poly(acrylic acid) (Figure 2.2) is employed as adhesives, crosslinked ion-exchange resins, and in paints, it is found useful as dispersants for inorganic pigments. It is also used as thickening agents – water used in secondary recovery of oil, rubber emulsions applied to fabrics to produce

nonslip backing for floor covering. Other than these applications, PAA is used as flocculants to aggregate suspended particles in metal recovery and clarification of waste and potable waters (Odian, 1991).

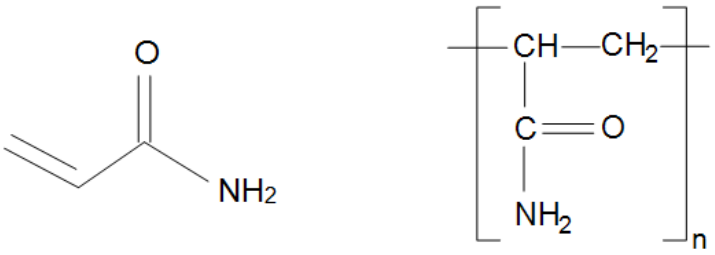

Figure 2.1 Acrylamide (AM) and polyacrylamide (PAM)

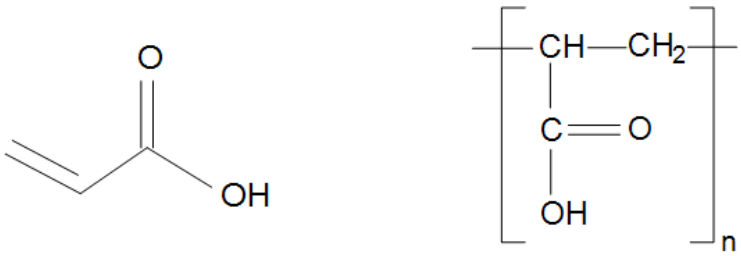

Figure 2.2 Acrylic acid (AA) and poly(acrylic acid) (PAA)

PAA is well-recognised as a polyelectrolyte which has been extensively used in the area of site-specific drug delivery to specific regions of the gastrointestinal tract. Nevertheless, due to its high water solubility, PAA's usage as a drug carrier has been constrained to a certain extent because of dissolution before the drug can be transported. Although PAA is usually crosslinked with organic cross-linkers to form interpenetrating networks (IPNs) as a way to overcome this disadvantage, there appears to be restrictions in the morphology and properties such as morphological inhomogeneity and mechanical weakness in the mentioned systems (Huang *et al*., 2007).

However, the existence of carboxylic acid groups in PAA enables it to develop different intermolecular interaction like electrostatic interaction, hydrogen bonds, and dipole-ion with other polymers, notably ionic natural polysaccharides. The swelling behavior of the hydrogels is shown to be greatly influenced by these interactions, according to various investigations, hence giving the PAA hydrogels ability to be applied in pharmaceutical preparations, particularly in drug delivery systems (Huang *et al*., 2007, Yin *et al*., 2008).

Through the action of *Aspergillus terreus* in the fermentation of carbohydrate materials such as molasses and hydrolysed starch, itaconic acid ($C_5H_6O_4$; IUPAC name: 2-methylidenebutanedioic acid; common synonyms: methylene butanedioic acid methylenesuccinic acid, 3-carboxy-3-butanoic acid, propylenedicarboxylic acid) is easily obtainable from renewable resources by biosyntheses (Krusic *et al*., 2004; Işıklan *et al*., 2010). *Aspergillus terreus* is a fungus commonly used in industry to produce important organic acids.

Being one of the monomers which is frequently used in copolymerisation with acrylates (Ebewele, 2000) and readily available at low cost, poly(itaconic acid) (PIA) is unique as a polyelectrolyte having different pK_a values (3.84 and 5.55) because of the presence of two ionisable carboxylic groups which can form H-bonds (Figure 2.3). Under certain circumstances, these groups bring additional potential of chelate formation.

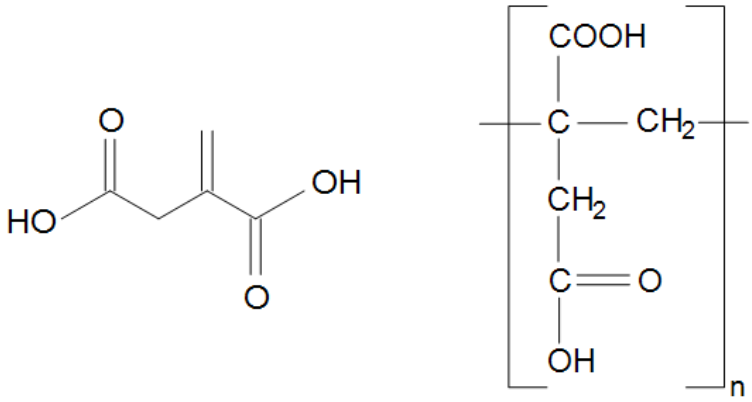

Figure 2.3 Itaconic acid (IA) and poly(itaconic acid) (PIA)

2.3 Graft Copolymerisation

Grafting reaction involves the copolymerisation of a monomer onto the polymer backbone – it originates from the formation of an active site at a point on a polymer chain other than its end, followed by the exposure of this site to a monomer (Han *et al*., 2003).

2.3.1 Advantages of Graft Copolymerisation

In recent years, the modification of polymers has received much attention. Grafting is one of the universal, effective, accessible and promising methods among all the methods of chemical modification of high molecular weight compounds, and natural polymers in particular (Lee *et al*., 2005a). Işıklan *et al*. (2010) described grafting as a well-established and powerful method for the preparation of natural-synthetic polymer hybrid materials. Generally speaking, grafting has been used as an important technique to improve the functional properties of polymers by modifying their physical and

chemical properties. With grafting, the properties of the pendant chains can be implemented to those of the substrate polymers without changing the latter to a great extent (Lee *et al*., 2005a).

In the presence of crosslinker, graft copolymerisation formed three-dimensional polymeric networks, those that swell quickly by absorbing a large amount of water (Singh *et al*., 2007). Monomer concentration, pH, and ionic strength are the factors which significantly influence the network formation made via the free radical polymerisation mechanism. Singh *et al*. (2007) quoted Elliott *et al*. (2004) as explaining that the degree of crosslinking and primary cyclisation during the network formation of multifunctional monomers are controlled by these factors.

Zhu *et al*. (1996) commented that polymer grafting allows the conversion of commodity polymers to value-added specialty polymers. Instances given are, for example, the grafting of highly charged ionic polymers onto high molecular weight polyacrylamide to give better flocculation effects, the grafting of elastomers onto polypropylene to enhance impact strength for applications in the automobile industry and the grafting of maleic anhydride oligomers onto polyolefins to improve the adhesion of the base polymers to metals and glass fibers.

Alginate graft copolymers are becoming increasingly important because of their potential application in industry. The wide range of available vinyl and other monomers suggests that grafting is a powerful method for

effecting substantial modification to alginate properties, thereby enlarging its collection of applications and utilisation. Işıklan *et al*. (2010) stated that desired properties could be introduced following the graft copolymerisation of vinyl monomers onto alginate. By choosing a variety of types of side chains, the field of potential application of alginate is expanded.

The grafting of vinyl monomers such as itaconic acid (Işıklan *et al*., 2010), methyl acrylate (Patel *et al*., 1999), acrylamide (Tripathy *et al*. 1999; Xu *et al*., 2006), acrylic acid (Yin *et al*., 2008), and acrylonitrile (Lee *et al*., 2005b; Pourjavadi and Zohuriaan-Mehr, 2002) onto alginate has gained significant attention and proved of value in developing new polymeric materials with unique properties and widening the range of its utilisation. In this study, instead of grafting either one type of the monomer onto alginate like the above-mentioned authors, the grafting reaction was carried out by grafting altogether acrylamide, itaconic acid and acrylic acid onto alginate.

2.3.2 Synthesis Methods of Graft Copolymerisation

The methods for the synthesis of graft copolymers can be categorised into three divisions (Braun *et al*., 2005). The first method to prepare graft copolymers is the homo- and copolymerisation of macromonomers (Figure 2.4). An instance of preparation of such macromonomers is via anionic polymerisation where the reactive chain end is modified with a reactive vinyl monomer, and examples of macromonomers are the methacrylic acid esters of long chain aliphatic alcohols or monofunctional polyethylene oxides.

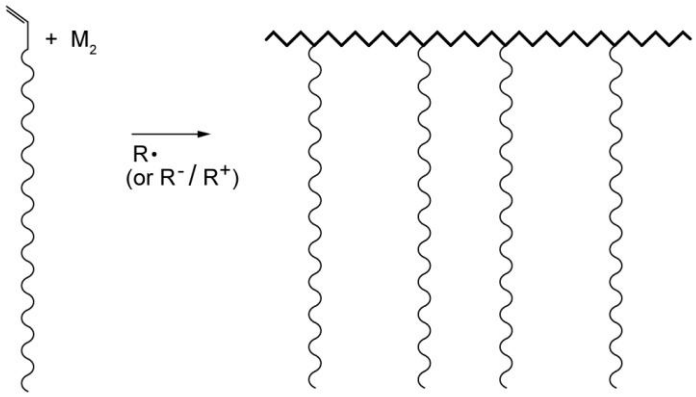

Figure 2.4 Copolymerisation of macromonomers (Braun *et al*., 2005)

The second possibility of synthesising graft copolymers is termed "grafting from", in which the long chain branches are achieved when the active sites generated at the polymer backbone A initiated the polymerisation of monomer B (Braun *et al*., 2005), as depicted in Figure 2.5. The radical center on the backbone of polymer A could be generated with irradiation using UV radiation or with high energy radiation.

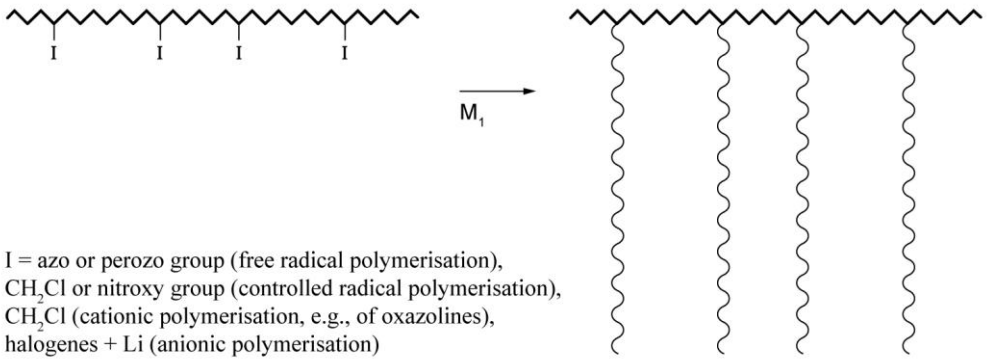

Figure 2.5 Copolymer grafted from polymer A (Braun *et al*., 2005)

The last possible route is called "grafting onto" (Figure 2.6). A long branch is formed when the polymer backbone A is attacked by a growing

chain B, with the attack being either a chain-transfer reaction or a "copolymerisation" with unsaturated groups, for instance, in polydienes. The reaction of monofunctional oligomers with the reactive side groups of a polymer backbone is also a "grafting onto" reaction.

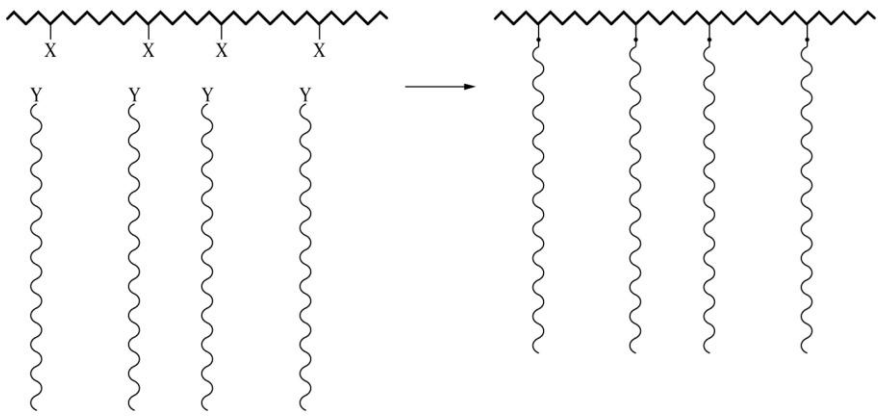

Figure 2.6 Grafting of growing chain B onto polymer backbone A (Braun *et al*., 2005)

Meanwhile, Da Silva *et al*. (2007) described that the copolymerisation mechanism of AM grafting onto polysaccharides, using persulphate as the initiator, has been well studied. According to the authors, upon heating, the persulphate initiator is decomposed to generate sulphate ion radicals, which are well known as chain carriers (refer to Section 2.4.2.1 for details). A hydrogen radical is then abstracted from the hydroxyl group of the polysaccharide to form alkoxy radicals on the substrate and results in active centres on the substrate, which in turn initiates a radical polymerisation of AM and leads to a graft copolymer.

On the other hand, the free radical graft copolymerisation of poly(methacrylic acid) (PMAA) onto carboxymethyl starch (CMS) was carried out at 70^{o}C by Saboktakin and co-workers (2009), with bis-acrylamide as the crosslinking agent and persulfate as an initiator. The authors, in the paper, revealed that equilibrium swelling studies were carried out in enzyme-free simulated gastric and intestinal fluids (SGF and SIF, respectively). The swelling and hydrolytic behavior of the hydrogels was dependent on the content of MAA groups, which caused a decrease in gel swelling in SGF or an increase in gel swelling in SIF.

The graft copolymers of NaAlg and PAM are found out to be flocculation-efficient. Tripathy *et al*. (1999) prepared graft copolymers of NaAlg with PAM using a ceric ion initiated solution polymerisation technique at 27 ± 1°C. Six graft copolymers have been synthesised with a variation in the number and length of grafted PAM chains. It was observed that the graft copolymers containing longer PAM chains were the most efficient as being flocculants.

Xu *et al*. (2006) carried on the effort of Tripathy and co-workers (1999) on synthesising graft copolymers of NaAlg using a ceric ion initiated solution polymerisation technique. They found out that the graft copolymer was more efficient in flocculation behavior as compared to PAM and NaAlg in kaolin suspension, and in removal capacities for chemical oxygen demand (COD) and colority in dyeing wastewater.

2.4 Chain Growth Polymerisation

Chain-growth polymerisation (also known as addition polymerisation) is distinguished by the occurrence of activated species (initiators) or active centers, and it involves the linking together of molecules having double or triple chemical bonds or are cyclic and having a sufficiently high ring strain. Chain growth polymerisation is further divided into different categories based on the mechanism of initiation – whether the initiation of chains occur via radical, ionic (cationic, anionic), or so-called coordinative-acting (found in transition-metal mediated polymerisation) initiators (Braun *et al*., 2005). Initiators are regularly but inaccurately identified as catalysts. It should be noted that initiators are consumed in the reaction, whereas catalysts are regenerated at the end of the reaction (Ebewele, 2000).

Since the initiation system employed in this study is made up of redox system which would generate radicals in the initiation step, the chain growth polymerisation naturally proceeds via the radical polymerisation pathway. Therefore, only radical polymerisation is described in the following section.

2.4.1 Radical Chain Polymerisation

The three distinctive kinetic steps involved in a typical free radical chain reaction are initiation, propagation and termination. After the generation of active centers in the initiation step, the reaction will propagate very rapidly

via the action of macroradicals or macroions until the termination stage that produces inactive macromolecules is achieved (Braun *et al*. 2005).

Initiation of free radical chain polymerisation comprises two reactions: formation of initiator radical (which is the rate-determining step in initiation stage) and addition of the initiator radical to monomer. The initiator radicals of chain reactions are formed by the homolytic dissociation of the relatively weak covalent bond in the initiator, I, to acquire a pair of initiator (or primary) radicals, R•.

The initiation step proceeds to the succeeding part where the primary radical formed binds to the first monomer molecule (M) to yield a new radical, the chain initiating species, M_1•.

The growth of M_1• by the successive additions of hundreds and perhaps thousands of monomer molecules marked the beginning of the second step – the propagation step. With each addition, a new radical that is larger by one monomer unit than the previously described primary radical is formed (Odian, 1991).

In chain-reaction polymerisation, the reaction propagates at the reactive chain ends and ceases only when termination reaction causes the chain ends to be inactive, or until the monomer has been consumed completely. Technically, termination could either occur by the molecular reaction between radicals by combination (coupling), or, more rarely, by disproportionation in which a beta

hydrogen radical of one radical center is shifted to another radical center (Odian, 1991).

Both combination and disproportionation reactions are kinetically identical. The only difference of these two termination reactions lies with the products, in which combination generates a single polymer chain, while disproportionation results in two chains, each with half the molecular mass of the product from recombination (Braun *et al*., 2005; Buchholz and Graham, 1998).

2.4.2 Redox Initiation

Free radicals needed to initiate a polymerisation reaction can be generated through various kinds of pathways, including thermal or photochemical decomposition of organic peroxide compounds, dissociation of covalent bonds by high-energy irradiation, and redox reactions (Ebewele, 2000). When the radicals are generated via oxidation-reduction reactions, these initiation reactions are known as redox initiation, which is also frequently called redox catalysis or redox activation (Odian, 1991).

Redox systems consist of an oxidising agent and a reducing agent. Among the oxisiding and reducing agents which are on top of the list of redox initiators include organic and inorganic peroxides, and either low valency metal ions or non-metallic compounds that are readily oxidised (for example, certain sulphur compounds) respectively. Apart from these initiating agents,

redox systems could also comprise of a mixture of a peroxo compound with metal ions (e.g. Fe^{2+} ions) and a second reducing agent such as a hydrogen sulphite (Braun *et al*., 2005).

Braun and co-workers (2005) commented that the effectiveness of a redox system relies on a number of factors, one being the order of addition of the initiating components. Although it is customary that reducing agent is added before the dropwise addition of the oxidising agent so as to get rid of any molecular oxygen which may be present in the reaction, it should be noted that there are certain cases where the reverse order is required.

Redox polymerisations are hardly ever carried out in organic solvents, but are generally performed in aqueous solution, suspension, or emulsion. They could be completed with relatively low temperatures with high rates and end with the formation of high molecular mass polymers, signifying the uniqueness of redox polymerisations (Braun *et al*., 2005).

It is worth mentioning that Trivedi *et al*. (2005) presented a paper on the results of the evaluation of the optimised reaction conditions of grafting of acrylonitrile (AN) onto the sodium salt of partially carboxymethylated guar gum (Na-PCMGG) by using the tetravalent ceric ammonium nitrate (CAN) as a redox initiator, as well as the characterisation of the graft copolymer by using different techniques. It was found through experiment that there was a marked increase in percentage of grafting (%G) with increase in monomer concentration.

2.4.2.1 Potassium persulphate

Being an inorganic peroxo compound, potassium persulphate (Figure 2.7; $K_2S_2O_8$, common synonyms: potassium peroxodisulphate, potassium peroxydisulphate, potassium perdisulphate, Anthion) used in the initial stage of this study is a thermal initiator that dissociates at a relatively high temperature.

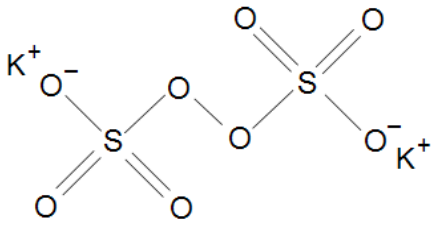

Figure 2.7 Potassium persulphate (KPS)

Although it is widely accepted as an oxidising agent that is mainly used as a component of a redox initiator, KPS is also used regularly without a reducing agent. This is because the initiating agent (concentration 0.1 – 1.0 wt.% with respect to monomer) could decompose thermally into radicals that can initiate polymerisation even at temperature as low as 30 ^{o}C (Braun *et al*., 2005), hence it is generally known as a thermal initiator.

The breakdown of persulphate ions in polymerisation reaction (initiation stage) proceeds according to Equations 2.1 – 2.3 (Braun *et al*., 2005; Rudin, 1999). Each initiator molecule decomposes to yield two types of primary radicals, which are sulphate and hydroxyl radicals. Rudin (1999) proposed that these radicals generally work well in the temperature range of 40

and 90 ^{o}C, while Braun and co-workers (2005) also suggested that the suitable temperature for polymerisation is 40 to 90 ^{o}C for the radicals.

$$S_2O_8^{2-} \longrightarrow 2\ \bullet OSO_3^- \qquad \text{(Eq. 2.1)}$$

$$\bullet OSO_3^- + H_2O \longrightarrow HSO_4^- + \bullet OH \qquad \text{(Eq. 2.2)}$$

$$2\ \bullet OH \longrightarrow H_2O + \frac{1}{2} O_2 \qquad \text{(Eq. 2.3)}$$

2.4.2.2 Tert-butyl hydroperoxide

Peroxides, the organic peroxo compounds, find widespread use as radical sources. There are numerous types of peroxides, which include acyl peroxides such as acetyl and benzoyl peroxides, alkyl peroxides such as cumyl and *t*-butyl peroxides, hydroperoxides such as *t*-butyl and cumyl hydroperoxides, peresters such as t-butyl perbenzoate, and many more (Odian, 1991).

tert-Butyl hydroperoxide (Figure 2.8; $(CH_3)_3COOH$, 1,1-dimethyl ethyl hydroperoxide) is used as an oxidising agent in the initiation of vinyl monomer radical polymerisation reactions and copolymerisation reactions involving vinyl acetate, acrylics, styrene, acrylamide and unsaturated polyesters (Odian, 1991). The dissociation of tBHP proceeds as shown in Equation 2.4.

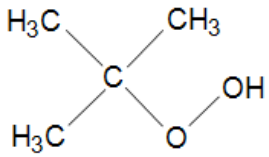

Figure 2.8 Tert-butyl hydroperoxide (tBHP)

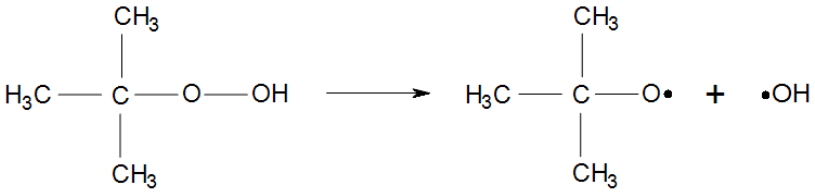

(Eq. 2.4)

2.4.2.3 KPS/SFX and tBHP/SFX

In this study, the oxidising agents KPS and tBHP are respectively paired up with SFX to be the redox initiators.

The efficiency of both the redox pairs had been investigated in emulsion polymerisation. Salomone (1996), using SFX as the reducing agent, evaluated on the effect of three different oxidising agents, including tBHP, KPS and hydrogen peroxide, in reducing the residual styrene monomer in emulsion-based styrene/n-butyl acrylate (40:60) latex. The author concluded that where a redox system is concerned, organic hydroperoxides such as tBHP is more efficient than KPS or hydrogen peroxide in reducing the residual styrene monomer in the styrene/n-butyl acrylate (40:60) latex.

2.5 Crosslinking

Being a reasonably easy method to prepare polysaccharide-based materials, the crosslinking step is a well-known and well-documented reaction. The properties of SAPs are significantly influenced by the nature of the crosslinks. An elastic gel is formed when SAP absorbs liquids. The gel is thus a soft, deformable solid composed of the expanded polymer chains and water (Buchholz and Graham, 1998). Covalent, ionic, and hydrogen bonds are the three major bonding types that join polymer chains together to form covalent, ionic, and physical gels.

There are basically two methods to produce covalent gels. The first type of covalent crosslinks are formed by means of a condensation or addition reaction when a di- or tri-functional reagent reacts with the carboxylic acids (for instance) of the preformed polymer chains. Covalent crosslinks are also introduced via a free-radical initiated addition polymerisation when a di-, tri-, or tetra-vinyl monomer such as *N*,*N*'-methylene bisacrylamide (N-MBA) (Figure 2.9) which is used to copolymerise the major monomer, for instance, AA (Buchholz and Graham, 1998).

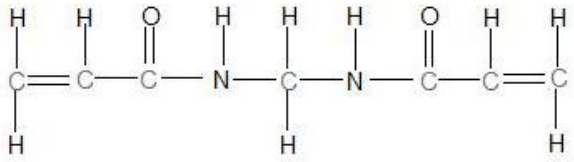

Figure 2.9 *N*,*N*'-Methylene bisacrylamide (N-MBA)

By reacting a polyvalent ion of opposite charge with the charged polymer chains, ionic crosslinks are formed due to association of unlike charges (neutralisation of charges). Compared with covalent crosslinks, the placement of the crosslinks is less influenced by the chemical structure of the crosslinker since the bond is formed by ion association. The major drawback of ionic gels is that ion exchange might occur between the ionic crosslinks and the ionic components present in the liquid, hence changing the nature of the crosslinks and behavior of the SAP. Furthermore, the incorporation of the crosslink and the final structure of the SAP are hard to control because the interionic reaction is very rapid (Buchholz and Graham, 1998).

Generally, physical gel is produced when the segments of one chain form hydrogen bonds with the segments of another chain. The gelling of gelatin solutions, due to the presence of polypeptide chains that allows strong hydrogen bonds between the chains, is a typical example of physical gel. Physical crosslinks have their shortcomings as well. Apart from the reduction of the mass efficiency of the crosslinker due to the extension of the multiple segments of the polymer chains, mere heating of the polymer destroys the crosslinks (Buchholz and Graham, 1998).

2.5.1 Crosslinking of Gels by Copolymerisation

To modify the properties of superabsorbent polymers, small amounts of crosslinkers are inevitably needed. Crosslinking agents introduce intermolecular bridges and/or crosslinks between polymer chains. Unlike

branched polymer in which the side growth of each polymer chain is terminated before the chain has a chance to link up with another chain, in a crosslinked (Figure 2.10) polymer, the growing polymer chains become chemically bonded to each other (Ebewele, 2000).

In superabsorbent polymers, the copolymerisable crosslinkers range widely from difunctional compounds such as *N*,*N*'-methylene bisacrylamide, diacrylate esters and allylmethacrylate, to tri-functional compounds such as 1,1,1-trimethylol-propanetriacrylate and triallylamine, and to tetra-functional compounds such as tetraallyloxyethane (Buchholz and Graham, 1998).

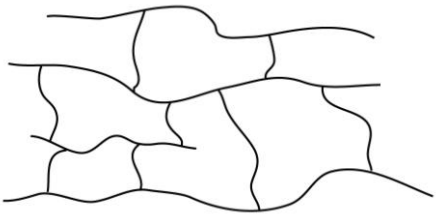

Figure 2.10 Crosslinked polymer

The efficiency of crosslinking agents depends on several factors. Among the variables listed by Buchholz and Graham (1998) are the solubility of the crosslinker in the monomer mixtures, steric hindrance and reduced mobility at the site of pendant double bonds, and the tendency of a given crosslinker to undergo intermolecular addition reactions, i.e. cyclopolymerisation.

2.5.2 Relationship between Crosslinking and Various Properties of SAP

The swelling ratio of the SAPs is affected by the chemical structure of the polymer, whereas the latter is heavily dependent upon the composition of the polymeric matrix, which is the degree of crosslinking. As the amount of crosslinking agent incorporated into the hydrogel matix increases, the degree of crosslinking increases. The more crosslinking agent incorporated into the matrix, the tighter the structure of the crosslinked hydrogel, and the lesser the swelling capacity of the SAP than similar hydrogel prepared with lower degree of crosslinking. The mobility of the polymer chain is hindered by the heavy crosslinking and thus the swelling capacity decreases.

Crini (2005) suggested that in the synthesis of gels by chemical methods, crosslinking density is controlled by the concentration of the crosslinker, reaction time, temperature and other variables. As the chemical structure of the synthesised hydrogel depends on the nature of the crosslinking agent and the degree of crosslinking, there exists a significant influence of the choice of the crosslinking agent on various properties of the SAP, for example, the adsorption property.

In the study of Seidel and co-workers (2001) as cited by Crini (2005), the authors commented that the sturdiness of polymeric material has a close relationship with the choice of crosslinking agent. With crosslinking, both the physical properties and the thermal transition characteristics of the polymer are modified. Ebewele (2000) explained that since crosslinking restricts the

molecular mobility of the macromolecule, it in turn increases the polymer ability to resist deformation under load, that is, increases its modulus. As higher energy is required to induce segmental motion when the crosslink density increases and the restriction on the molecular mobility becomes significant, the thermal transition temperature will increase since thermal transition temperature represents the onset of co-operative segmental motion.

Close to two decades ago, Moe *et al*. (1991) and Skjåk-Bræk and Moe (1992) reported on the new superswelling material with potential biomedical applications based on spherical gel beads of covalently crosslinked sodium alginate. The gel beads which were prepared in the size range of 5 to 4000 μm were characterised by a very rapid swelling in water with an absorbency of 50 to 200 times their dry volume. Swelling of alginate gels could be increased dramatically by a covalent cross-linking of preformed Ca-alginate gels with epichlorohydrin, followed by subsequent removal of Ca^{2+} ions by ethylenediamine tetraacetic acid (EDTA) (Skjåk-Bræk and Moe, 1992). These Na-alginate gels could be dried, and they exhibited unique swelling properties when re-hydrated.

Moe *et al*. (1993) further studied the equilibrium swelling volume of covalently crosslinked sodium alginate (a highly ionised stiff polymer network) gels as a function of electrolyte concentration, pH, and concentration of salts in ethanol-water mixtures. The ionic concentration to swelling was established as the main determining factor for the swelling of the synthesised gels, through the numerical analysis of the Flory theory.

2.5.3 *N,N*'-Methylene Bisacrylamide

The bifunctional compound *N,N*'-methylene bisacrylamide (N-MBA, $C_7H_{10}N_2O_2$, IUPAC name: *N*-[(Prop-2-enoylamino)methyl]prop-2-enamid) is most often used as a water soluble crosslinking agent.

Singh *et al*. (2007) explained that because of the poly-functionality of N-MBA, a new macro-radical that has four reactive sites is formed from crosslinker N-MBA in any polymerisation reaction involving the crosslinking agent (as shown in Figure 2.11).

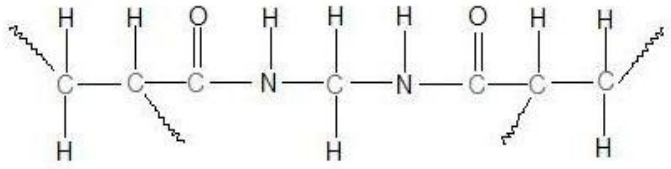

Figure 2.11 Linking sites of N,N'-methylenebisacrylamide

The presence of these reactive sites means that these sites can be linked both with the radicals on the natural polysaccharide (NaAlg) and the synthetic polymers (PAM, PIA and PAA) used in the synthesis of the SAP in the present study. As a result, a three-dimensional network is inevitably formed.

In the article presented by Wang (2007), the author suggested that in the synthesis of cellulose-based SAP, in which N-MBA is employed as the crosslinking agent, the reaction proceeds as proposed in Figure 2.12. With this

knowledge, the mechanism of the crosslinking process between the alginate-based SAP and N-MBA in the current study could well be speculated.

Generally speaking, SAP hydrogels synthesised purely from synthetic polymers without natural polymers have AA as the main component. Kabiri *et al*. (2003) investigated the effect of crosslinker type and concentration on porosity and absorption rate of highly porous SAP hydrogels produced from highly concentrated aqueous solutions of AA/potassium acrylate, in the presence of N-MBA and 1,4-butanedioldiacrylate as the crosslinkers. It was found that both the crosslinkers exhibited similar effects on absorbency behavior in distilled water and saline. The gelation time decreased with increasing crosslinker concentration, especially in the case of N-MBA.

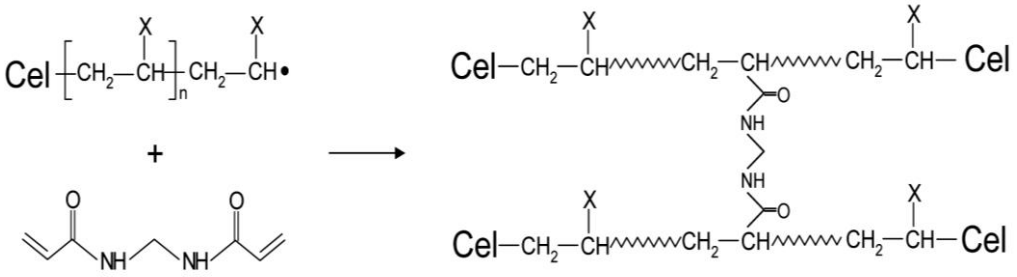

Figure 2.12 Crosslinking mechanism of cellulose-based SAP by N-MBA (Wang, 2007)

Özeroglu and Birdal (2009) employed meso-2,3-dimercaptosuccinic acid-Ce(IV) redox couple for crosslinking polymerisation of AM with N-MBA in acid aqueous medium. The authors observed that the increase concentrations of the acid, initiator and crosslinker led to a decrease in the swelling ratio and rate of swelling of the hydrogels in distilled water.

At the meantime, crosslinking agents such as N-MBA have been popular in the syntheses of SAPs. Graft copolymerisation of AA and AM onto chitosan was carried out by Mahdavinia and co-workers (2004) using KPS as a free radical initiator in the presence of N-MBA as a crosslinker. The effect of reaction variables, such as concentration of N-MBA and ratio of AA/AM, on the water swelling capacity had been investigated. The authors also reported that the hydrogels exhibited salt-sensitivity and cation exchange properties.

Singh *et al*. (2007) prepared psyllium (common name used for several members of the plant genus *Plantago*) and PAM based hydrogel polymeric networks by using N-MBA as crosslinker. The researchers observed that the equilibrium swelling was dependent on both structural aspects of the polymers and swelling environment. Swelling capacity was found to decrease with an increase in the concentration of N-MBA in the polymeric networks.

Yin *et al*. (2008) synthesised a series of hydrogels by graft copolymerisation of NaAlg and AA using N-MBA as a crosslinker. The dynamic swelling experimental results indicated that a remarkable overshooting effect was exhibited in the swelling process of P(NaAlg-*g*-AA) hydrogels in the buffer solutions at pH $\leq$ 4.0. The authors attributed the phenomenon to a cooperative physical crosslink caused by the hydrogen bond formation between the carboxyl groups of the hydrogels. The hydrogen bond crosslinking decreased the swelling capacity and consequently leads to the expulsion of water during the dynamic swelling process.

Wang and Wang (2010) prepared a pH-sensitive semi-interpenetrating network (semi-IPN) SAP composed of NaAlg-*g*-poly(sodium acrylate) (NaA) network and linear polyvinylpyrolidone (PVP) via free-radical solution polymerisation, in the presence of ammonium persulphate and N-MBA as the initiator and crosslinker, respectively. The authors claimed that the introduction of PVP and the formation of the semi-IPN structure enhanced the swelling capacity and rate of swelling of the hydrogel.

2.6 Preparation of Biodegradable SAPs

In an effort to save the environment from synthetic polymers, graft copolymerisation of synthetic polymer on natural polymers such as starch and NaAlg was introduced as an alternative method to produce SAPs. As a result, uncountable research papers on syntheses of such SAPs swarmed the literature world. Basically, these SAPs could be categorised into non-crosslinked and crosslinked-SAPs. There are almost equal amount of literatures found from these two categories, and the following few paragraphs described the first category's SAPs.

In Brazil, Da Silva *et al*. (2007) carried out the synthesis of cashew gum-*g*-PAM at 60 ^{o}C by a radical polymerisation using KPS as the redox initiator under nitrogen atmosphere. By varying the concentration of AM while keeping the concentrations of the initiator and polysaccharide at constant, a series of graft copolymers was prepared. The authors concluded that even with

a low acrylamide/gum ratio, high percentages of AM conversion (%C) and grafting efficiency (%E) were obtained.

Yang and co-workers (2009) carried out the synthesis of carboxymethylcellulose (CMC)-*g*-PAM in an aqueous medium by using ammonium persulphate and sodium sulfite redox system as an initiator. The effects of reaction conditions (such as initiator concentrations, monomer concentrations, initial reaction temperature, and pH value) on the weight-average molecular weight of the copolymers were investigated, and the optimal conditions for the grafting reaction were established.

Pourjavadi *et al*. (2010b) synthesised novel types of highly swelling hydrogels by grafting crosslinked polyacrylamide-*co*-poly-2-acrylamido-2-methylpropane sulfonic acid (PAAm-*co*-PAMPS) chains onto NaAlg through a free radical polymerisation method. The results demonstrated that the biodegradable SAP could successfully deliver a drug to the intestine without losing the drug in the stomach, thus acting as potential candidate as an orally administrated drug delivery system.

There were articles which focused on the syntheses of crosslinked-SAPs as well. Chen and Tan (2006) prepared a novel carboxymethylchitosan-*g*-PAA SAP through graft polymerisation of AA onto the chain of carboxymethylchitosan and subsequent crosslinking, employing ammonium persulphate as the initiator and N-MBA as the crosslinking agent. Optimisation

conditions for SAP with the highest swelling ratio were found by studying the swelling ratio of the polymer synthesised under different conditions.

Lanthong *et al*. (2006) synthesised biodegradable SAPs by graft copolymerisation of AM/IA onto cassava starch via a redox initiator system of ammonium persulfate (APS) and N,N,N',N'-tetramethylethylenediamine (TEMED), in the presence of crosslinking agent (N-MBA), foaming agent (sodium bicarbonate), and a foam stabiliser (a triblock copolymer of polyoxyethylene/polyoxypropylene/polyoxyethylene). In the paper, the authors revealed the results from the investigation of effects of acrylamide-to-itaconic acid ratio, starch-to-monomer ratio, and concentrations of the crosslinking agent and initiator, on the water absorption of the SAPs.

Chang *et al*. (2010), by using epichlorohydrin (ECH) as cross-linker, successfully prepared novel SAPs from carboxymethylcellulose sodium (CMC) and cellulose in the NaOH/urea aqueous system. The results revealed that cellulose behaved as a strong backbone in the hydrogel to support it for keeping its appearance while the CMC contributed to the enhanced size of pores. The maximum swelling ratio in water reached an exciting level of 1000 as the hydrogels keep a steady appearance.

2.7 Swelling capacity of SAPs

The degree of swelling is certainly the most emphasised and significant property measured in a commercial SAP. Swelling not only has direct

influence on the properties of the network, but also is related to the amount of liquid contained per unit cost of the SAP product, e.g. diaper (Buchholz and Graham, 1998).

SAPs take up liquid by a diffusive mechanism. As the activity of water is initially lower in the interior of a SAP particle, water starts diffusing into the particle. As the particle volume increases, the particle chains unavoidably move in the direction opposite to that of the water molecules so as to accommodate the water molecules. Larger sizes of polymer chains compared with the water molecules indicate the slower diffusion of the chains.

The presence of crosslinks ensures that the polymer does not eventually dissolve in the water. However, these crosslinks also force the polymer chains to move cooperatively, hence slowing down the expanding polymer chains. Water stops moving into the particle when the force resulting from the elongation of the polymer chains equals the force resulting from the difference of water concentration between the inside and the outside of the SAP particle (Buchholz and Graham, 1998).

Despite the fact that the swelling capacity of the gel is determined by a difference in chemical potential of the water molecules between the inside and outside of the gel particle, the rate of swelling of the particle is determined by an inward flux of water which is dependent on a gradient in chemical potential, and the size and shape of the swelling particle (Draget *et al.*, 1996).

2.7.1 Various Factors Affecting the Swelling Capacity of SAPs

There are many factors to be considered when measuring the swelling capacity of SAPs. In the context of this study, no matter how precise the swelling capacity method is, certain portions of the alginate may obviously leak out of the gel particle when they become soluble during the swelling process, since alginates are heterogeneous with respect to both chemical composition and molecular mass. In other words, in an invisible and unpredictable way, the swelling capacity and swelling rate of the SAP are bound to be lessened (Draget *et al*., 1996).

The effect of crosslinking on the swelling capacity of SAP has been discussed in considerable detail in Section 2.5.2. However, there are uncountable other variables which are known to have impact on the swelling capacity of SAPs. Among them are particle size, swelling time, inter-particle liquid, swelling liquid, and so on.

It is rather obvious that the swelling capacity is directly affected by the time length allowed for swelling. As the swelling time increased, the swelling capacity will increase until equilibrium is reached. The length of time required for the SAP to reach equilibrium swelling, nonetheless, is determined by the size of the polymer particles (Buchholz and Graham, 1998).

Although the early patent literature showed that the inventors were more interested in the relative end-use performance of the SAPs, in a study by

Sheu (1992) as cited by Buchholz and Graham (1998), the author limited the particle size used for analysis to the particle size distributions useful in diapers, ranging from particle diameters of 100 to 850 µm. The latest editions of industrial swelling methods have the particle diameter distribution narrowed down further to between 300 and 600 µm (Buchholz and Graham, 1998). Meanwhile, Buchholz and Graham (1998) described that swelling to equilibrium is not always the main consideration in industrial swelling methods, and the swelling times could range from as low as 10 minutes or less to 30 minutes or more.

The inter-particle liquid is the swelling liquid which is held between the particles by capillary forces. Inter-particle moisture ought to be excluded when comparing the experiment results to theory, or else the swelling capacity values are bound to be larger than for methods where the inter-particle liquid is accounted for or removed from the swollen gel (Buchholz and Graham, 1998).

The type of liquid used to swell the SAP affects the swelling capacity as well. For example, due to ex-osmosis, hydrogels do not swell significantly in the presence of electrolyte salts – the swelling capacity of SAP decreases with an increase of brine concentration up to a certain concentration of sodium chloride, and even swollen hydrogels shrink dramatically in the presence of salts.

When the hydrogels are subjected to electrolyte salt solutions, the hydrophilic–hydrophobic balance of the networks is lost, hence causing the

pre-swollen gels to de-swell rapidly, thus regaining their original shape and mass (Singh *et al*., 2007). Liu *et al*. (2004) (cited by Singh *et al*., 2007) reported the swelling capacities of the copolymers prepared in an aqueous solution using AM and 2-acrylamido-2-methyl-propanesulfonic acid (AMPS) as monomers, KPS as initiator, and N-MBA as cross-linker to be 2451 and 119 g/g in distilled water and 0.9 % NaCl solution, respectively.

In this study, the SAP is precipitated from the solution with calcium chloride because alginate is able to bind calcium ions selectively and cooperatively. Davidovich-Pinhas and Bianco-Peled (2010) quoted that the swelling behavior of alginate had been experimentally studied by several research groups (Kong *et al*., 2003; Martinsen *et al*., 1989; Pillay and Reza, 1999; Richardson *et al*., 2004; Roger *et al*., 2006). Those studies (Kong *et al*., 2003; Martinsen *et al*., 1989; Roger *et al*., 2006) have proven that an increase in the concentration of calcium decreases the swelling capacity.

2.7.2 Measurement of Swelling Capacity

In general, when the terms ‘swelling’ or ‘absorbency’ are used without the conditions specified, it simply denotes the uptake of distilled water while the sample is freely swollen in the medium, i.e., with no load added on the tested sample. Depending on the amount of the available sample, the sample absorbency level, and the method's precision and accuracy, there are several simple methods for the free-absorbency testing, including sieve, tea-bag,

centrifuge (Zohuriaan and Shokrolahi, 2004), and gravimetric methods (Singh *et al*., 2007).

2.8 Swelling under Load

The ability for SAPs applied in personal care articles to resist de-swelling and deformation under external pressure is necessary since this ability has been identified as a link to improve performance in pad analysis and in diapers. When a swelling polymer particle is under a uniaxial compression, it alters its shape, with the degree of the deformation depending on the modulus which in turn depends on the swelling capacity and initial crosslink density (Buchholz and Graham, 1998).

Buchholz and Graham (1998) described that as early as 1977, Reid, in the author's patent, carried out the analysis for swelling capacity under load from 0.68 to 2.8 kPa for the water-absorbent crosslinked polymers manufactured, although the real loading was undefined.

Polymer area density and particle size distribution are the two variables which affect swelling rate and equilibrium swelling under load since both these variables affect the rate at which the bed porosity and permeability change (Buchholz and Graham, 1998).

In the study of commercial SAPs, an experimental technique named absorbency under load (AUL) has been used to measure the effect of

mechanical compression on the swelling process. Industrial SAP manufacturers usually provide the absorbency under load (AUL) data in patent literature and technical data sheets. The term AUL automatically implies an uptake of 0.9 % sodium chloride solution while pressurising the testing sample with certain amount of loads (often specified to be pressures of 0.3, 0.6, or 0.9 psi, corresponding to 21.1, 42.2, and 63.3 g/cm^2 respectively) (Zohuriaan-Mehr and Kabiri, 2008).

Ramazani-Harandi *et al*. (2006) investigated an experimental method for measuring the swollen gel strength of an acrylic-based SAP. The absorbency under load (AUL) of a SAP sample was first determined followed by the measurement of the mechanical strength of the swollen sample by a rheological method using a controlled strain rheometer. The minimum time required to achieve the highest AUL in each load (0.3, 0.6 and 0.9 psi) was determined to be 60 min. After this time, the AUL values remained unchanged. AUL decreased with increase in loading. The storage modulus (G') of the swollen gel sample (previously absorbed saline solution under pressure of 0.3–0.9 psi) above 1000 Pa at 25 ^oC.

2.9 Thermogravimetric Analysis (TGA)

Under the influence of one or more environmental factors such as heat, light or chemicals, polymer degradation is bound to give rise to a change in the properties of a polymeric product, for example, tensile strength, colour, shape. These changes take place owing to the hydrolysis of the bonds connecting the

polymer chain, which in turn leads to a decrease in the molecular mass of the polymer, hence impinging on the chemical composition of the polymer. Changes brought about by degradation are not necessarily at all undesirable, in biodegradation or cases where deliberate lowering of the molecular mass of a polymer is called for, these changes turned desirable.

Thermal degradation is a process where the deterioration in the properties of the polymer takes place due to thermal factor. Thermal resistance directs the spectral stability, durability, mechanical properties, shelf lives, and life cycles of polymers, whereas thermal degradation prompts the successive deterioration of all the above properties, with the durability of the material becoming restricted and the article becoming brittle. Therefore, Peng and Kong (2007) described that one of the most dominative properties for polymer materials is their thermal resistance.

Nakamura *et al*. (1995) investigated the thermal properties of water insoluble alginate films containing di and trivalent cations, such as Cu^{2+}, Al^{3+}, Fe^{3+}, etc. Changes in the film structure during ionic exchange were studied on the basis of its glass transition temperature (T_g) and heat capacity using differential scanning calorimetry (DSC). The results indicated that the T_g of dry films decreased with increasing ionic radius of cations. The authors further concluded that the alginates form compact crosslinked structures when the ionic radii of the cations were lower.

It is obligatory to learn more about a polymer's thermal stability under inert conditions (for example, dehydration, carbonisation, spontaneous chain degradation, etc.) as well as in the presence of oxygen (oxidation) preceding to any other bulk characterisation. Information on the activity of stabilisers (for instance, against depolymerisation or oxidation), contents of inorganic fillers and reinforcing fibers, and presence of monomer, solvent, or other volatile material could be retrieved and studied by thermogravimetric analysis (TGA) (Braun *et al.*, 2005).

Thermogravimetry (TG) is a well-established experimental technique used in a complete evaluation and interpretation of results when it is known as TGA. The measurement is performed in a defined atmosphere under inert conditions (usually in nitrogen) or oxidising conditions (for example, air or oxygen) while continuously measuring the mass of a sample with a very sensitive electronic balance, under a specific temperature programme (Riesen and Schawe, 2002).

In TG, the temperature programme must be taken to include holding the sample at a constant temperature other than ambient. Mass loss is only seen when there is either a loss of a volatile component or loss of mass due to polymer decomposition (Rudin, 1999). By blank curve subtraction, interfering buoyancy and drag force effects are cancelled off (Riesen and Schawe, 2002).

The method, in which the temperature is programmed to a specific heating rate, is referred to as non-isothermal (dynamic) TGA. Based on

continuous measurement of mass on a sensitive balance (known as thermobalance) as sample temperature is increased in air or in an inert atmosphere, dynamic TGA is the most widely used TGA method (Rudin, 1999). Unlike fundamental isothermal testing which could take up to days, dynamic TGA tests have the edge of being relatively quick, either on the order of minutes or hours.

TGA will provide information on the nature and extent of degradation of the material (Asaletha *et al.*, 1998). The information includes a number of stages of thermal breakdown, mass loss of the material in each stage, threshold temperature, and other data. A schematic TGA curve of a polymer is depicted in Figure 2.13. Compositional analysis (i.e. determination of the content of polymers, carbon black or carbon fibers, ash or fillers, and volatile compounds such as moisture and solvents) could be ideally carried out with TGA. Since decomposition kinetics differ from polymer to polymer, valuable qualitative information could be obtained within the temperature range in which the polymer pyrolyses (Riesen and Schawe, 2002).

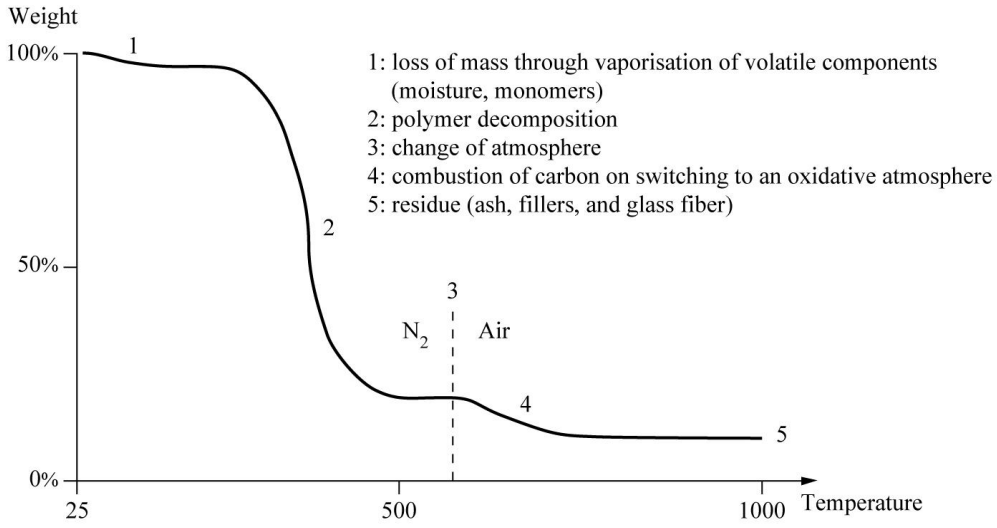

Figure 2.13 Schematic TGA curve of a polymer (Riesen and Schawe, 2002)

The equipment required for TGA comprises a furnace with a recording balance which holds the sample holder, a temperature programmer, an enclosed space for building up the required atmosphere, and a hardware (computer) that records and displays the data. Aluminum, alumina, platinum, and silica are the materials that are frequently used to make the sample holder. The progress of the thermal reaction are affected by the morphology and particle size of the material, and the gas flow rate, while the heating rate and sample size are the key factors which affect the TGA curve (Braun *et al*., 2005).

Holme *et al*. (2003) commented that the depolymerisation of polysaccharides occurs via cleavage of the glycosidic bonds. The glycosidic linkages of alginates are believed to be susceptible to a variety of degradation mechanisms, including oxidative–reductive free radical depolymerisation (ORD-reaction), acid-, alkaline- and enzymatic-catalysed hydrolysis. Smidsrød

et al. (1963), as cited by Holme *et al*. (2003), were mentioned to have proven that the presence of oxygen affects the stability of non-purified alginates due to the presence of phenolic reducing substances which give rise to the ORD-reaction. Meanwhile, Oates and Ledward (1990) reported that alginate undergoes extensive decomposition when it is exposed to temperatures above 250 ^{o}C.

Said *et al*. (1994) investigated the thermal and electrical properties of silver, selenium and uranyl alginates (Ag-alg, Se-alg_4 and UO_2-alg_2) using thermogravimetry, differential thermal analysis (DTA) and electrical conductivity measurements. The authors concluded that metal oxalates were formed as decomposition intermediate.

2.10 Surface Morphology

In order to investigate the physical appearance of a SAP, it is necessary to use SEM for the purpose. There are a few literatures which featured the SEM images of SAPs which were incorporated with NaAlg.

Pourjavadi *et al*. (2006) synthesised a novel SAP hydrogel composed of carboxymethylcellulose (CMC) and NaAlg using N-MBA as a crosslinking agent and ammonium persulphate (APS) as an initiator. The optimum conditions which could provide maximum water swelling capacity was found to be 0.015 mol/L of N-MBA, 0.00486 mol/L of APS, 0.54 weight ratio of NaAlg/CMC, with the reaction temperature fixed at 85 ^{o}C. SEM micrograph

revealed a porous internal structure of the hydrogel. According to the authors, the porosity confirmed the three-dimensional structure of the hydrogel.

Hua and Wang (2009) prepared a novel sodium alginate-*g*-poly(acrylic acid)/sodium humate SAP by graft copolymerisation with sodium alginate, acrylic acid and sodium humate (SH) in aqueous solution, using N-MBA as a crosslinker and ammonium persulfate as an initiator. In their paper, the authors concluded that the surface morphology of NaAlg-*g*-PAA/SH superabsorbent was different from that of NaAlg-*g*-PAA. NaAlg-*g*-PAA has a smooth and tight surface while the sample doped with SH presented an undulant and coarse surface. The authors further concluded that the introduction of SH into the NaAlg-*g*-PAA system could enhance the water absorption capacity. The SAP which contained 10 wt.% sodium humate acquired the highest water absorption capacity, i.e. 1380 g g^{-1} in distilled water and 83 g g^{-1} in 0.9 wt.% NaCl solution.

Gao *et al.* (2009) studied the degradation behavior of hydrogel based on oxidised sodium alginate (OSA) crosslinked with Ca^{2+} in phosphate buffer solution (pH = 7.4) and Tris-(hydroxymethyl) aminomethane–HCl (pH = 7.4) at 37 ^{o}C. In the study, SEM images of sodium alginate and OSA hydrogels were obtained. The SEM images showed that sodium alginate, 10 % OSA and 30 % OSA hydrogels demonstrated laminated structures while 50 % OSA hydrogel showed a different structure from sodium alginate, 10 % OSA and 30 % OSA hydrogels.

In 2010, Işıklan and colleagues reported on the preparation of graft copolymers of NaAlg with IA in aqueous solution using benzoyl peroxide (BPO) as the initiator under nitrogen gas atmosphere. SEM picture exhibited that the surface of the NaAlg-*g*-PIA copolymer was a more spongy structure than that of NaAlg. The results obtained also showed that by varying the reaction conditions such as reaction time, temperature, concentration of monomer and initiator, control of the grafting parameters was possible.

2.11 Biodegradability

Biodegradable polymers are a type of macromolecules which are able to breakdown into smaller compounds or completely degraded in biologically active environments (Baker *et al*., 2009). The breakdown process is normally caused by microorganisms (Cosgrove *et al*., 2007), however biodegradation can also occur through hydrolysis and oxidation processes in biological environment.

Microorganisms of the soil are the main parties which contribute to majority of polymer degradation (Cosgrove *et al*., 2007). Hence, biodegradability of a polymer depends on the types of biological enzymes and microorganisms present in the soil. Nevertheless, the specific populations desirable for a particular degradation are dependent upon numerous environmental factors in the soil, such as soil moisture content, pH, soil organic matter, and etc (Tangjang *et al*., 2009).

For one, Lee and co-workers (2005b) prepared biodegradable SAPs, hydrolysed AN-grafted-NaAlg copolymers by graft copolymerisation of AN on NaAlg, followed by subsequent hydrolysis of the resulting grafted copolymer. The authors concluded that the variables which affected the swelling capacity of the SAPs produced were the percentage add-on, graft copolymerisation conditions and hydrolysis conditions. Furthermore, compared with commercial SAPs, good biodegradability was shown by the SAPs during enzymatic hydrolysis tests.

CHAPTER 3.0

MATERIALS AND METHODS

3.1 Materials

The graft copolymerisation process was carried out by using sodium alginate (NaAlg, R&M, UK) as the backbone polymer and acrylamide (AM, R&M, UK), itaconic acid (IA, Fluka, China), and acrylic acid (AA, R&M, UK) as the monomers. Potassium persulphate (KPS, R&M, UK) and tert-butyl hydroperoxide (tBHP, Merck, Germany), and SFX, R&M, UK were used as the oxidising agents and reducing agent respectively while N,N'-methylenebisacrylamide (N-MBA, R&M, UK) and sodium bicarbonate (SBC, Dulab, Malaysia) were used as the crosslinking agent and neutralising agent respectively. Ethanol (Et-OH, J. Kollin, UK) and calcium chloride dihydrate ($CaCl_2 \cdot 2H_2O$, Systerm, Malaysia) were used as the precipitating agents.

In the test of absorbency under load (AUL), sodium chloride (NaCl, J. Kollin, UK) was used in the swelling medium, whereas potassium bromide (KBr, Merck, Germany) was used as the grinding powder in Infrared (IR) spectroscopy analysis.

All chemical reagents used in the biodegradability test were standard

reagents with analytical grade. The nutrient soil solution was prepared from zinc sulphate ($ZnSO_4$, Systerm, Malaysia), sodium chloride (NaCl, Systerm, Malaysia), iron (II) sulphate ($FeSO_4$, Fisher Scientific, UK), magnesium sulphate ($MgSO_4$, Fisher Scientific, UK), manganese (II) sulphate monohydrate ($MnSO_4 \cdot H_2O$, Ajax Finechem, Australlia) and multivitamins (Sunward Pharmaceutical, Malaysia).

3.2 Methods for Small-scale Synthesis

3.2.1 Gelatinisation of Sodium Alginate

1.0 g of sodium alginate was dispersed with 30 cm^3 of distilled water in a 250 cm^3 beaker. The system was heated to 80 ± 2 ^oC with magnetic stirring at 700 rpm for 30 minutes to form a homogenous, gelatinised sodium alginate paste. Sodium alginate powder was ensured to be properly dispersed with water so that all the powder were wet thoroughly before it was heated at 80 ^oC. This was done through manual stirring using glass rod at the beginning of the gelatinisation process.

3.2.2 Graft Copolymerisation of Poly[acrylamide-*co*-(itaconic acid)] onto Sodium Alginate

After cooling the gelatinised sodium alginate to 45 ^oC, a mixture of distilled water (40 cm^3), AM, IA, and N-MBA was added into it, followed by the initiator pair consisting of SFX and tBHP to initiate the reaction. SBC was

later added into the reaction mixture as a neutralising agent. The system was stirred at 1500 rpm for 30 minutes until completion.

The recipe for the graft copolymerisation of poly[acrylamide-*co*-(itaconic acid)] onto sodium alginate is shown in Table 3.1.

Table 3.1 Recipe for graft copolymerisation of poly[acrylamide-*co*-(itaconic acid)] onto sodium alginate

Ingredient	Quantity
NaAlg Solution	
NaAlg (g)	1.0
Distilled Water (cm^3)	30
Monomer Solution	
N-MBA (x 10^{-3} mole)	0 – 6.2
AM (x 10^{-2} mole)	2.0
IA (x 10^{-3} mole)	2.5
Distilled Water (cm^3)	40
Initiator Solution	
KPS*/ tBHP (× 10^{-4} mole)	0.9 – 9.3
SFX (× 10^{-4} mole)	0.9 – 9.3
Distilled Water (cm^3)	30
Neutralising Agent	
SBC (g)	0.5

Table 3.1 shows that the concentrations of KPS/SFX, tBHP/SFX, $CaCl_2 \cdot 2H_2O$ and N-MBA were varied in four series of reactions, which are as follows:

(i) Series 1 – Varying the number of moles of KPS/SFX used between 0.9 $\times 10^{-4}$ and 9.2 $\times 10^{-4}$ moles,

(ii) Series 2 – Varying the number of moles of tBHP/SFX used between 1.0 $\times 10^{-4}$ and 9.3 $\times 10^{-4}$ moles,

(iii) Series 3 – Varying the concentration of $CaCl_2 \cdot 2H_2O$ between 0.01 M to 0.50 M, and

(iv) Series 4 – Varying the number of moles of N-MBA between 0 and 6.2 $\times 10^{-3}$ moles.

3.2.3 Graft Copolymerisation of Poly(acrylic acid) onto Alginate-*g*-poly[acrylamide-*co*-(itaconic acid)]

The syntheses of SAPs incorporated with AA, Alg-*g*-P(AM-*co*-IA-*co*-AA) and Alg-*g*-P(AM-*co*-IA-*g*-AA), were carried out via two different methods. In the first method, AA was added into the gel mixture obtained in Section 3.2.1 alongside AM and IA at the same time (similar procedures as Section 3.2.2), thus it was specified as one-step synthesis in this study, and hence the product was named Alg-*g*-P(AM-*co*-IA-*co*-AA). In the second method, AA was added at a separate timing (labelled as two-step synthesis) than AM and IA, therefore the SAP is labeled as Alg-*g*-P(AM-*co*-IA-*g*-AA). The second method was described in the following paragraphs.

AA was added into the reaction mixture obtained in Section 3.2.2, followed by the initiator pair – 0.028 g tBHP and 0.048 g of SFX. Addition of the neutralising agent, 0.20 g of SBC, followed almost immediately after that. The system was stirred at 1500 rpm for 30 minutes until completion.

The recipes for the copolymerisation of Alg-*g*-P(AM-*co*-IA-*co*-AA) (Series 1) and Alg-*g*-P(AM-*co*-IA-*g*-AA) (Series 2 to 6) are showed in Table 3.2, in which the molar ratio of AM:IA:AA, and amount of AA, $CaCl_2 \cdot 2H_2O$, N-MBA, volume ratio of $CaCl_2 \cdot 2H_2O$ to SAP solution and the duration of swelling were varied in six series of reactions as follows:

(i) Series 1 – Varying the molar ratio of AM:IA:AA between 1:1:8 to 9:1:0 in one-step synthesis,

(ii) Series 2 – Varying the number of moles of AA between 0 and 8.8×10^{-2} moles in two-step synthesis,

(iii) Series 3 – Varying the concentration of $CaCl_2 \cdot 2H_2O$ between 0.01 M to 0.50 M in two-step synthesis,

(iv) Series 4 – Varying the number of moles of N-MBA between 0 and 1.0×10^{-2} moles in two-step synthesis,

(v) Series 5 – Varying the volume ratio of $CaCl_2 \cdot 2H_2O$ to SAP solution from 1:1 to 5:1 in two-step synthesis, and

(vi) Series 6 – Varying the duration of swelling between 4 and 72 hours in two-step synthesis.

Table 3.2 Recipes for small-scale graft copolymerisation of poly(acrylic acid) onto alginate-*g*-poly[acrylamide-*co*-(itaconic acid)]

Synthesis	**1-step**	**2-step**
Ingredient	**Quantity**	
NaAlg Solution		
NaAlg (g)	4.0	1.0
Distilled water (cm^3)	50	30
Monomer Solution (First Charge)		
N-MBA ($\times 10^{-2}$ mole)	-	0 – 1.0
AM ($\times 10^{-2}$ mole)	1.0 – 9.0	2.0
IA ($\times 10^{-3}$ mole)	10	2.5
AA ($\times 10^{-2}$ mole)	8.0 – 0	-
Distilled water (cm^3)	80	40
Initiator Solution (First Charge)		
tBHP ($\times 10^{-4}$ mole)	8.3 (1.0 wt.% monomer)	3.1
SFX ($\times 10^{-4}$ mole)	8.5 – 8.6	3.1
Distilled water (cm^3)	-	30
Neutralising Agent (First Charge)		
SBC (g)	2.0 – 8.0	0.2 – 6.0
Monomer Solution (Second Charge)		
AA ($\times 10^{-2}$ mole)	-	0 – 8.8
Distilled water (cm^3)	-	20
Initiator Solution (Second Charge)		
tBHP ($\times 10^{-4}$ mole)	-	3.1
SFX ($\times 10^{-4}$ mole)	-	3.1
Distilled water (cm^3)	-	30
Neutralising Agent (Second Charge)		
SBC (g)	-	0.2 – 6.0

3.2.4 Precipitation of Product Solution

The product appeared as a semi-viscous solution. At the initial stage, the solution was precipitated by pouring the solution into ethanol. Another precipitating agent, $CaCl_2 \cdot 2H_2O$, was utilised instead when the dry product obtained via ethanol precipitating method was found to be soluble in water.

In the second method, the solution was precipitated by dripping the solution dropwise from a separatory funnel into a $CaCl_2$ solution under stirring to form the final product, which was dried overnight in an oven at 55 ^oC.

3.3 Methods for Bigger-scale Synthesis

3.3.1 Gelatinisation of Sodium Alginate

18.0 g of sodium alginate was dispersed in distilled water in a 1000 cm^3 beaker. The system was heated at 80 ± 2 ^oC with mechanical stirring, using a metal stirrer, at 1600 rpm for 30 minutes to form a homogenous, gelatinised sodium alginate paste.

3.3.2 Graft Copolymerisation of Poly[acrylamide-*co*-(itaconic acid)] onto Sodium Alginate

After cooling the gelatinised sodium alginate to 45^oC, a mixture of distilled water with AM, IA, and N-MBA was added into it, followed by the initiator pair consisting of SFX and tBHP to initiate the reaction. SBC was

later added into the reaction mixture as a neutralising agent (Table 3.3). The system was stirred at 1600 rpm for 30 minutes until completion.

When adding in the redox initiators, it should be noted that the reducing agent was added before the addition of the oxidising agent so as to get rid of any molecular oxygen which may be present in the reaction.

3.3.3 Graft Copolymerisation of Poly(acrylic acid) onto Alginate-*g*-poly[acrylamide-*co*-(itaconic acid)]

A mixture of distilled water and AA was poured into the reaction mixture obtained in Section 3.3.2, followed by the addition of the initiator pair. Addition of the neutralising agent, SBC, followed almost immediately after that (Table 3.3). The system was stirred at 1600 rpm for 30 minutes until completion.

The water level of the water bath should be higher or at least equal to the gel inside the beaker so that the gel was thermally stable. To achieve better heat stability of the gel and to avoid water evaporation, a piece of aluminium foil was used to cover the mouth of the beaker .

The complete recipe for the graft copolymerisation of poly(acrylic acid) onto alginate-*g*-poly[acrylamide-*co*-(itaconic acid)] is shown in Table 3.3.

Table 3.3 Recipe for bigger-scale graft copolymerisation of poly(acrylic acid) onto alginate-*g*-poly[acrylamide-*co*-(itaconic acid)]

Ingredient	Quantity
NaAlg Solution	
NaAlg (g)	18.0
Distilled water (cm^3)	250
Monomer Solution (First Charge)	
N-MBA ($\times 10^{-4}$ mole)	4.44
AM ($\times 10^{-1}$ mole)	4.05
IA ($\times 10^{-2}$ mole)	4.50
Distilled water (cm^3)	250
Initiator Solution (First Charge)	
tBHP ($\times 10^{-3}$ mole)	5.57
SFX ($\times 10^{-3}$ mole)	5.57
Distilled water (cm^3)	100
Neutralising Agent (First Charge)	
SBC (g)	9.00
Monomer Solution (Second Charge)	
AA ($\times 10^{-2}$ mole)	5.25
Distilled water (cm^3)	150
Initiator Solution (Second Charge)	
tBHP ($\times 10^{-3}$ mole)	5.57
SFX ($\times 10^{-3}$ mole)	5.57
Distilled water (cm^3)	150
Neutralising Agent (Second Charge)	
SBC (g)	3.60

The parameters which might affect the swelling capacities of the synthesised product, crosslinked-alginate-*g*-poly[acrylamide-*co*-(itaconic acid) -*g*-(acrylic acid)], including the concentration of $CaCl_2 \cdot 2H_2O$, dilution of gel and particle size of dry beads, were investigated in three series of reactions, as follows:

(i) Series 1 – Varying the concentration of $CaCl_2 \cdot 2H_2O$ between 0.0125 M and 0.20 M,

(ii) Series 2 – Varying the ratio of SAP solution to water between 1:0 to 1:4

(iii) Series 3 – Varying the particle size of the dry beads of crosslinked-Alg-*g*-P(AM-*co*-IA-*g*-AA) between 0.074–0.149 mm (200–100 mesh size) and 4.000 – 4.760 mm (5 – 4 mesh size).

3.3.4 Precipitation of Product Solution

The product was precipitated using the precipitating agent, $CaCl_2 \cdot 2H_2O$, as described in Section 3.2.4.

3.3.5 Preparation of SAP Beads with Different Sizes

To prepare SAP beads of different sizes, the dry 0.05 M $CaCl_2$-precipitated SAP beads were ground to smaller sizes and categorised into different groups of sizes using screen of different mesh sizes.

Mesh size is the number of openings per (linear) inch of mesh. The beads were divided according to mesh sizes which were divided into four categories – from 4.760 – 4.000 mm (4.0 – 5.0 mesh), 4.000 – 1.000 mm (5.0 – 18.0 mesh), 1.000 – 0.149 mm (18.0 – 100.0 mesh) to 0.149 – 0.074 mm (100 – 200.0 mesh).

3.4 Characterisation

3.4.1 Swelling Capacity of Superabsorbent Polymer

90 cm^3 of distilled water was added to 0.1 g of the dry final product in a 100 cm^3 Petri dish with a glass cover. The polymer was allowed to swell for 72 hours (unless specified otherwise) at room temperature. The swollen gel was then removed from the water by filtering through a 100-mesh sieve and drained for 5 minutes at room temperature.

The gel obtained was weighed for its wet mass and then dried overnight in a conventional oven at 55 ^oC. Swelling capacity of the sample was calculated using Equation 3.1,

$$\text{Swelling capacity} = (W_1 - W_0) / W_0 \qquad \text{(Eq. 3.1)}$$

where W_0 is the mass of the dry sample and W_1 is the mass of the water swollen gel.

3.4.2 Absorbency under Load (AUL)

With a screen fabric made of nylon placed on top, a glass filter plate was placed in a tray. A fixed amount of dried SAP sample (i.e. 0.23 g, corresponding to a 0.0325 g/cm^2 coverage) was distributed uniformly on the screen fabric with a surface area of 7.069 cm^2. The tray was then filled with 0.9 % sodium chloride solution up to the edge of the filter plate. A cylindrical solid load (variable weight), which could slip freely in a glass cylinder with an external diameter of 30 mm, was used to apply the desired load (applied pressure 20 – 40 g/cm^2) on the sample. The dish and its contents were covered to prevent evaporation of water.

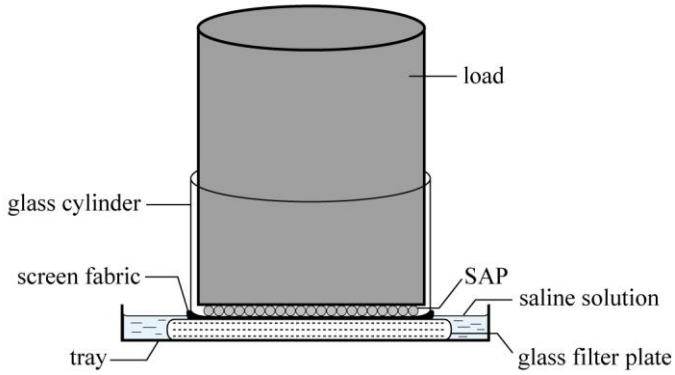

Figure 3.1 Absorbency under load (AUL) tester

The SAP was allowed to soak in the solution for a defined duration (1 to 8 hours), at room temperature. After the required duration, the swollen particles were weighed again and AUL was calculated using equation 3.2.

$$\mathrm{AUL} = \frac{W_2 - W_1}{W_1} \qquad \text{(Eq. 3.2)}$$

where W_1 and W_2 denote the masses of dry SAP and swollen hydrogel, respectively.

3.4.3 Infrared Spectroscopy

Infrared spectra of the SAPs in KBr pellets were obtained from 4000 – 400 cm^{-1} using PerkinElmer FTIR spectrometer Spectrum RX1.

The SAP sample and KBr powder in the mass ratio of 1:10 was transferred into an agate mortar with a spatula. Using an agate pestle, the mixture was ground together until it gave a consistency of fine flour.

After assembling the die with the lower pellet polished facing upward in the cylinder bore, the ground mixture was transferred into the cylinder bore so that it was evenly distributed across the polished face of the lower pellet. Gently inserting the plunger and lightly swivelling the mixture achieved a flat, even surface of mixture. With the polished face towards the mixture, the second pellet was inserted into the bore, followed by the plunger.

The die assembly was pressed between the ram and the piston of a hydraulic press to obtain a translucent and homogeneous KBr disk. After dismantling the die, the disk was transferred to the disk holder, which in turn, was mounted in the spectrometer. The IR spectrum was then obtained.

There are a few precaution steps when carrying out Infrared Spectroscopy analysis. First, the potassium bromide (KBr) powder must be of spectroscopic grade purity, and be spectroscopically dry. The combination of sample and KBr must be ground into homogenous powder so that the scattering effects from large crystals are prevented (Pavia *et al*., 2005).

Secondly, moisture-free samples should be used for IR analysis so that the spectra would not be influenced by peaks of water or carbon dioxide.

Thirdly, in order to obtain a translucent disk, the ground powder (mixture of KBr and sample) should be distributed evenly on top of the lower pellet in the cylinder bore. We should avoid from putting too much sample on top of the pellet so that the disk obtained was translucent.

Lastly, correct pressure should be used to press the mixture of KBr and sample. Too high pressure would cause the disk to break on removal from the pellets; too low pressure would cause the disk to be non-translucent. Fingers should not come in contact with the surfaces of pellets, disks or any of the optical surfaces so that the disk obtained would be free from contaminants.

3.4.4 Thermogravimetric Analysis (TGA)

The thermogravimetric analyser used in this study was Mettler Toledo TGA SDTA851e. The SAP sample prepared in Section 3.2.4 with an amount around 5.0 mg was weighed into a standard 70 µL alumina crucible. The

crucible containing the SAP sample was then placed into the furnace of thermogravimetric analyser. The sample was heated at a heating rate of 20 ^{o}C/min in nitrogen atmosphere. The thermal decomposition temperatures, T_d, of the samples were determined from the inflection points of the transitions. The temperature programme, heating rate, purge gas, gas flow rate, sample size, and sample holder are summarised in Table 3.4.

Table 3.4 Process conditions of thermogravimetric analysis

Temperature programme	Dynamic (Non-isothermal)
Start temperature, ^{o}C	25
End temperature, ^{o}C	900
Heating rate, ^{o}C/min	20
Purge gas	Nitrogen
Gas flow rate, mL/min	20
Sample size, mg	± 5.0
Sample holder, μL	Standard alumina 150

3.4.5 Determination of Total Solids Content (TSC) and Conversion of Monomer

For each SAP sample, three replicas were weighed using a four-decimal analytical balance. Around 1.0 g of SAP gel obtained from Section 3.3.3 was transferred to an aluminium dish and weighed accurately. The exact masses of the empty and gel-containing aluminium dishes were recorded. The samples were then dried in an oven at 105 – 110 ^{o}C for an hour. After that, the dishes were taken out and cooled down in a desiccator. The dishes were

weighed again to find the masses of the SAP residues. The processes of drying and cooling were repeated until a constant mass of SAP residue was obtained.

An advantage of cooling down the aluminium dish in a desiccator is that this act could deter dusts or other contaminants from staining in the aluminium dish before reading had been recorded down. Moisture in the air could also affect the results if the dish was left in the air for relatively long before being weighed.

For each SAP sample, the mean actual total solids content (TSC) was taken as the average of three replicates. The detailed calculations of actual TSC, mean actual TSC, theoretical TSC, percentage error and monomer conversion for each SAP sample are shown in Appendix D. The equations for the calculations of theoretical TSC and percentage monomer conversion are shown in Equations 3.3 and 3.4, respectively.

$$\text{Theoretical TSC} = \frac{\text{Mass of solid in gel}}{\text{Total mass of gel}} \times 100\% \qquad \text{(Eq. 3.3)}$$

$$\text{Percentage monomer conversion} = \frac{\text{Mean actual TSC} - (\text{Mass fraction of non-polymer solid} \times 100\%)}{\text{Mass fraction of monomer}} \qquad \text{(Eq. 3.4)}$$

3.4.6 Study of Surface Morphology

The morphology of the SAP, synthesised using the method described in Section 3.3 and precipitated by ethanol, was examined using scanning electron microscope (JSM-6701F, JEOL Limited, Japan) at an accelerating voltage of 2.0 kV.

3.4.7 Microbial Degradation

3.4.7.1 Collection of soil sample

The vegetable farm soil is a type of loose, loamy soil which contains a combination of microorganisms and some organic materials (compost, rotted leaves or wood chips, old manure and etc.) which help in the growth of vegetable plants. The soil was found to be of pH 7.97 and possessed a moisture percentage of 11.30 %. Generally, the type of bacteria community present in the soil depends on the characteristics (moisture, pH and reaction) of the soil (Tangjang *et al*., 2009).

By employing random sampling method, two sub-samples were collected at a vegetable farm which is located in Perak, Malaysia. Upon obtaining the upper soil layer to a depth of about 3 inches below surface by using a shovel, a plastic container was used to enclose the soil samples up to two third of its volume. The container was loosely capped in order to allow gas exchange; the soil samples were kept at room temperature for one day.

3.4.7.2 Preparation of soil supernatant with nutrient

In order to prepare the nutrient-supplemented soil solution, 100 g of the soil was mixed with 200 mL of sterile minimum mineral (MM) culture medium in laminar air flow. The composition of the medium is as follows (per litre): 0.7 g of $MgSO_4$, 0.005 g of NaCl, 0.002 g of $FeSO_4$, 0.002 g of $ZnSO_4$, 0.001 g of $MnSO_4$ and 1 tablet of multivitamin (0.4435 g). In order to prevent denaturation of vitamins under high temperature, the vitamins were added only after the mineral solution was autoclaved (120 ^{o}C for 15 minutes).

The mixture was centrifuged at 6500 rcf for 15 minutes. Subsequently, the supernatant was filtered and transferred to a 250 mL Erlenmeyer flask. Lastly, the solution was topped up with deionised water to a total volume of 200 mL before use.

3.4.7.3 Weight loss test

This test was performed by measuring the weight loss of the SAP which was immersed in the soil supernatant as a function of duration of incubation. The SAP sample which was employed in this test was Alg-*g*-P(AM-*co*-IA-*g*-AA) which was crosslinked with 2.5×10^{-5} moles of N-MBA (similar synthesis method as Section 4.3.1.7). The percentage loss was calculated according to Equation 3.5.

$$\text{Percentage loss} = \frac{M_0 - M_t}{M_0} \times 100\% \qquad \text{(Eq. 3.5)}$$

where M_0 is the initial mass; M_t is the final mass (after dried) at a predetermined time t. An average of two measurements was taken (Franco *et al.*, 2004).

At different time intervals (10, 20, 30 and 40 days), approximately 0.1 g of the SAP was collected and transferred into a 15 mL tube and was repeatedly washed in order to remove all the debris and planktonic microorganisms. The SAP was then dried overnight in an oven at 60 ^{o}C, and the dried SAP sample was cooled in a desiccator before taking its dry mass.

CHAPTER 4.0

RESULTS AND DISCUSSION

4.1 Syntheses of Alginate Graft Copolymers

Upon addition into water, alginates lump with water. Using glass rod, alginate was dispersed in cold water first before heating so as to obtain a properly dispersed and hydrated mixture. With rapid dispersion in cold water, the powder particles were completely dispersed before the beginning of the increase in viscosity (Hunik, 2001).

Although alginate is easily dispersed in cold water, the dissolution of alginate in cold water was sufficiently slow. Once the powder was well-dispersed in cold water, the mixture was heated with stirring to about 80 ^{o}C for faster dissolution.

In small-scale polymerisation, magnetic stirring was employed since the reaction vessel used was a small beaker. The stirring effect brought about by the magnetic stirrer bar was sufficient to create effective mixing of the alginate and water. Oppositely, mechanical stirring was used for bigger-scale polymerisation so that ideal and thorough mixing of the contents in the big reactor flask could be attained. Furthermore, high speed stirring increased the rate of dissolution.

Air bubbles were trapped during the gelatinisation of sodium alginate due to the stirring effect. It is therefore necessary to allow the product mixture to cool down after gelatinisation. Upon cooling, the mixture could settle properly into a clear gel. Moreover, the polymerisation reaction of AM, IA and/or AA onto the NaAlg backbone was carried out at 45 ^{o}C in this study. The alginate gel produced was henceforth cooled down to 45 ^{o}C before the polymerisation step.

As discussed in Section 2.4.2, the reducing agent, SFX, was added before the dropwise addition of the oxidising agent, tBHP, so as to cautiously exclude any molecular oxygen which may be present in the reaction medium. Atmospheric oxygen reacts very rapidly with hydrocarbon radicals to form peroxy radicals during radical polymerisations, as shown in Equation 4.1.

$$R\bullet + \bullet O\text{-}O\bullet \longrightarrow R\text{-}O\text{-}O\bullet \qquad \text{(Eq. 4.1)}$$

Even though peroxy radicals are known to be less reactive than most alkyl or aryl radicals, they may well add a further monomer molecule and regenerate an alkyl radical which is capable of reacting again with oxygen, hence significantly reducing the rate of consumption of monomer (Braun *et al.*, 2005).

As discussed in Section 2.3.2, there are altogether three categories of methods to prepare graft copolymers. Combining all the facts, it is most probably that the graft copolymerisation in this study proceeds via both the

second and third methods, which are “grafting from” and “grafting onto”. In “grafting from”, the redox initiator first attacked the sodium alginate (polymer backbone), generating active sites bearing radical centers. The polymerisation of monomers that consist of AM, IA and/or AA is then initiated when these monomer units are grafted from the radical centers found on the alginate backbone.

On the other hand, in “grafting onto”, the monomer units are initiated by the redox initiator and polymerisation begins with the monomer. The growing chains attacks the alginate backbone and this is where the “grafting onto” happens – the polymerising chains are grafted onto the alginate backbone.

These two methods are speculated to occur simultaneously as the aqueous system is added with both the sodium alginate and monomers before adding in the redox initiator. When the initiators are added in, the initiator radicals are most likely to attack both the alginate chains and monomer units, hence forming the phenomena of “grafting from” and “grafting onto” at the same time.

However, taking the work done by Da Silva *et al*. (2007) as a reference, it is most likely that the graft copolymerisation in this study proceeds via the “grafting from” method, although the “grafting onto” method is not at all impossible. In their study, the researchers proposed that a hydrogen radical is abstracted from the hydroxyl group of the polysaccharide to form

alkoxy radicals on the substrate, upon the generation of sulphate ion radicals from the decomposition of persulphate initiator, and results in active centres on the substrate, which in turn initiates a radical polymerisation of AM and leads to a graft copolymer.

At the beginning stage, small-scale synthesis was carried out before bigger-scale synthesis. This was to cut cost and save materials, since there were a lot of parameters to be ascertained in different series of tests. From an economical point of view, running the syntheses at a large scale before the verification of the ratio of constituting materials is not cost-effective. However, the disadvantages of running the syntheses at a small scale included inaccuracy in the weighing of raw materials which in turn would lead to low consistency and reproducibility in some of the results obtained.

Figure 4.1 depicts the product of the polymerisation, the semi-viscous SAP solution.

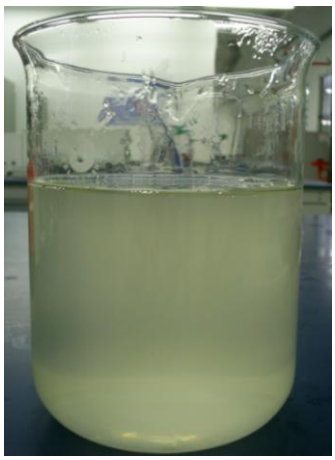

Figure 4.1 Semi-viscous SAP solution

4.2 Precipitation of Product Solution

Ethanol could well precipitate the SAP solution formed. By pouring the SAP solution into ethanol, a lump of SAP sample was obtained. The dry sample looked uneven on the surface, with both white-shaded and translucent patches as the outer appearance. This phenomenon could be contributed by heterogeneous distribution of ethanol solution in the wet gel. Areas which were swarmed with ethanol molecules would tend to look translucent while areas which were not thoroughly surrounded by the ethanol molecules would be inclined to appear white. Figures 4.2 and 4.3 illustrate the wet and dry Alg-*g*-P(AM-*co*-IA-*g*-AA) samples obtained via precipitation with ethanol.

Figure 4.2 Wet ethanol-precipitated Alg-*g*-P(AM-*co*-IA-*g*-AA)

Figure 4.3 Dry ethanol-precipitated Alg-*g*-P(AM-*co*-IA-*g*-AA)

Although ethanol could precipitate the SAP solution and recover the SAP in solid form, the SAP samples obtained were soluble in water. In applications which require the SAPs to be water-insoluble, for example, in diapers, the SAP produced would be rendered useless. Therefore, an alternative precipitating agent, $CaCl_2 \cdot 2H_2O$, was utilised instead when it was proven to produce SAP samples which would not dissolve in water.

The SAP samples obtained via the precipitation with $CaCl_2$ for both small-scale and bigger-scale syntheses differed slightly in terms of gel strength. For samples synthesised using the similar recipe and precipitated using $CaCl_2$ of similar concentration, wet precipitated SAP samples from the small-scale synthesis looked weaker and had a non-uniform rounded shape, while the wet precipitated samples from the bigger-scale synthesis looked stronger and took after a round shape. This resulted in a non-uniform shape with translucent appearance in the dry samples for the small-scale synthesis, and a more unison shape with transparent appearance in the dry samples for the bigger-scale synthesis.

The contributing factor of this phenomenon could be the difference in the extent of stirring processes in both the small-scale and bigger-scale syntheses. In the small-scale synthesis, the stirring brought about by the magnetic stirring bar was far too gentle if compared with the stirring done by the mechanical stirrer in the bigger-scale synthesis. In the latter, the whole mixture was thoroughly and homogeneously stirred throughout the synthesis process. Whereas in the former, the stirring force produced by the magnetic

bar might not be strong enough to mix and stir the whole gel efficiently and homogenously as the latter.

The possible consequences of this difference in stirring efficiency were that higher total solids content were obtained for the SAP of the latter than in the former – the overall structure of the polymer particles formed in the bigger-scale synthesis was more compact due to the higher concentration of polymer in the SAP. Therefore, when $CaCl_2$ was used to precipitate the respective gels, the compact structure in the latter would give the SAP better strength, tougher look, and hence rounded shape. Figures 4.4 and 4.5 show the $CaCl_2$-precipitated wet and dry crosslinked-Alg-*g*-P(AM-*co*-IA-*g*-AA) samples, respectively.

The dry SAP samples precipitated with $CaCl_2$ had a milky white appearance (Figure 4.5). The presence of calcium in the SAP led to more brittle sample, this being more accentuated by increasing calcium concentration.

Figure 4.4 Wet $CaCl_2$-precipitated crosslinked-Alg-*g*-P(AM-*co*-IA-*g*-AA)

Figure 4.5 Dry $CaCl_2$-precipitated crosslinked-Alg-*g*-P(AM-*co*-IA-*g*-AA)

4.3 Measurement of Swelling Capacity of Superabsorbent Polymer

In this study, swelling studies of the polymeric networks were carried out in aqueous medium by gravimetric method. To attain equilibrium swelling, known mass of polymer product was taken and immersed in excess amount of solvent (i.e. ethanol and distilled water, respectively) for a known period of time (e.g. 8 hours) at a fixed temperature.

The Petri dish used to soak the dry SAP sample was covered with a glass cover. Apart from avoiding contamination from the surroundings, this precaution step could prevent water from evaporating from the surface and causing a change in the swelling process.

After the swollen gel beads were removed of the unabsorbed water by filtering through a 100-mesh screen, they were allowed to be drained in the

screen for 5 minutes at room temperature. Only after ensuring that there was no water leaching out from the swollen gel sample, the sample was weighed for its wet mass and dried overnight in a conventional oven at 55°C.

4.3.1 Swelling Capacity of Superabsorbent Polymer Obtained via Small-scale Synthesis

4.3.1.1 Effect of molar ratio of AM:IA:AA on the swelling capacity of alginate graft copolymers

In order to obtain the optimum molar ratio of AM, IA and AA which would give the highest swelling capacity to the polymer, the molar ratio of AM to AA was varied from 1:8 to 9:0 while holding the molar ratio of IA constant at 1 in the one-step synthesis. Each IA molecule bears two carboxylic (–COOH) groups which enables the respective polymer to pack orderly in a crystalline structure. An increase in crystallinity would limit the swelling capacity of the SAP. Thus the molar ratio of IA in the SAP was fixed at 1. Figure 4.6 depicts the graph of swelling capacity of sodium alginate graft copolymers in ethanol against the molar ratio of AM:IA:AA.

As the molar ratio of AM:IA:AA increased from 1:1:8 to 9:1:0, the swelling capacity of Alg-*g*-P(AM-*co*-IA-*co*-AA) in ethanol increased. Furthermore, when no AA was added into the synthesis, the SAP absorbed ethanol to its fullest. This finding suggests that the presence of AA in the one-step synthesis of Alg-*g*-P(AM-*co*-IA-*co*-AA) did not improve the swelling capacity of the SAP. In other words, in one-step synthesis, AM and IA (9:1

molar ratio) alone are adequate to cause the SAP, Alg-*g*-P(AM-*co*-IA), to swell to its maximum. Henceforth, only AM and IA were added as the first charge in subsequent syntheses.

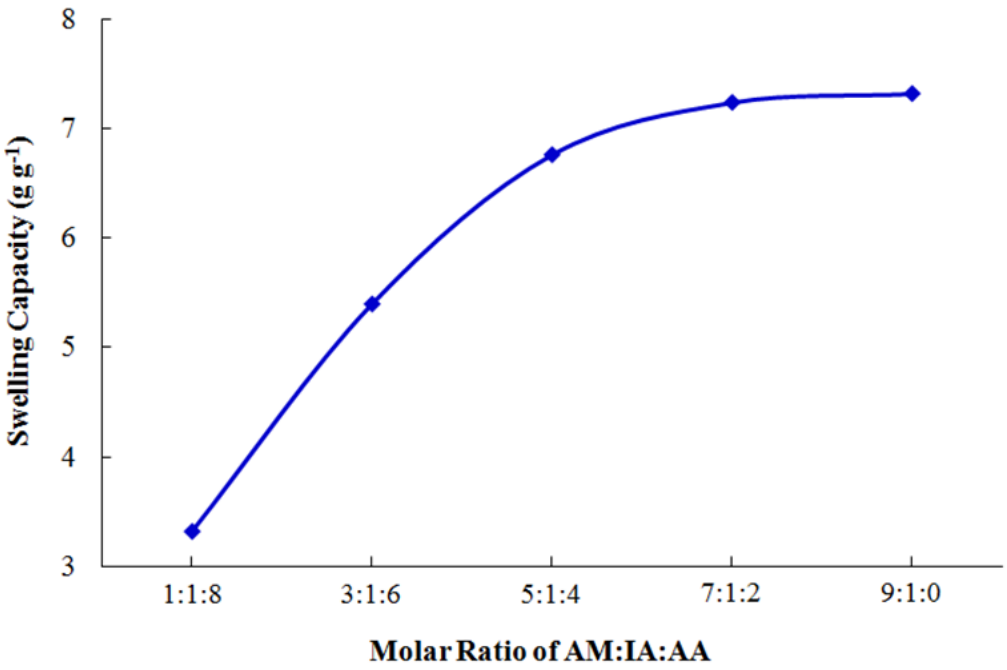

Figure 4.6 Swelling capacity of alginate graft copolymers against molar ratio of AM:IA:AA

4.3.1.2 Effect of initiator concentration on the swelling capacity of Alg-*g*-P(AM-*co*-IA)

To determine the type of initiator and amount of initiator needed to obtain maximum swelling capacity of the SAP synthesised, two types of oxidising agents, KPS and tBHP, were paired up with the reducing agent, SFX, in two different tests.

For a start, 0.9 – 9.2 × 10^{-4} moles of KPS and SFX were employed to initiate the synthesis of Alg-*g*-P(AM-*co*-IA). Figure 4.7 shows the graph of swelling capacity of Alg-*g*-P(AM-*co*-IA) in ethanol, plotted against the number of moles of KPS. As shown, the swelling capacity of the SAP increased from 6.29 to 7.12 g g^{-1} when the number of moles of KPS increased from 0.9 to 1.9 × 10^{-4} moles. As the amount of initiator increased further from 1.9 to 9.2 × 10^{-4} moles, the swelling capacity of the SAP decreased gradually to 5.62 g g^{-1}.

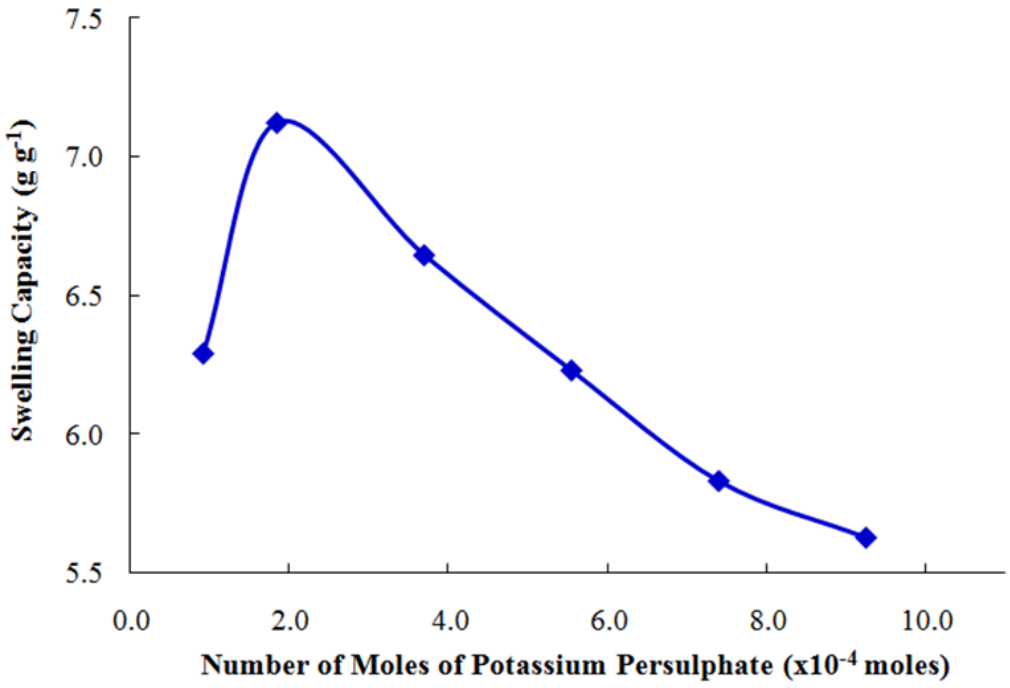

Figure 4.7 Swelling capacity of Alg-*g*-P(AM-*co*-IA) against number of moles of KPS

On the other hand, the numbers of moles of another initiator pair, tBHP and SFX, were each varied from 1.0 to 9.3 × 10^{-4} moles. Figure 4.8 refers to the plot of swelling capacity of Alg-*g*-P(AM-*co*-IA) in ethanol with respect to the number of moles of tBHP.

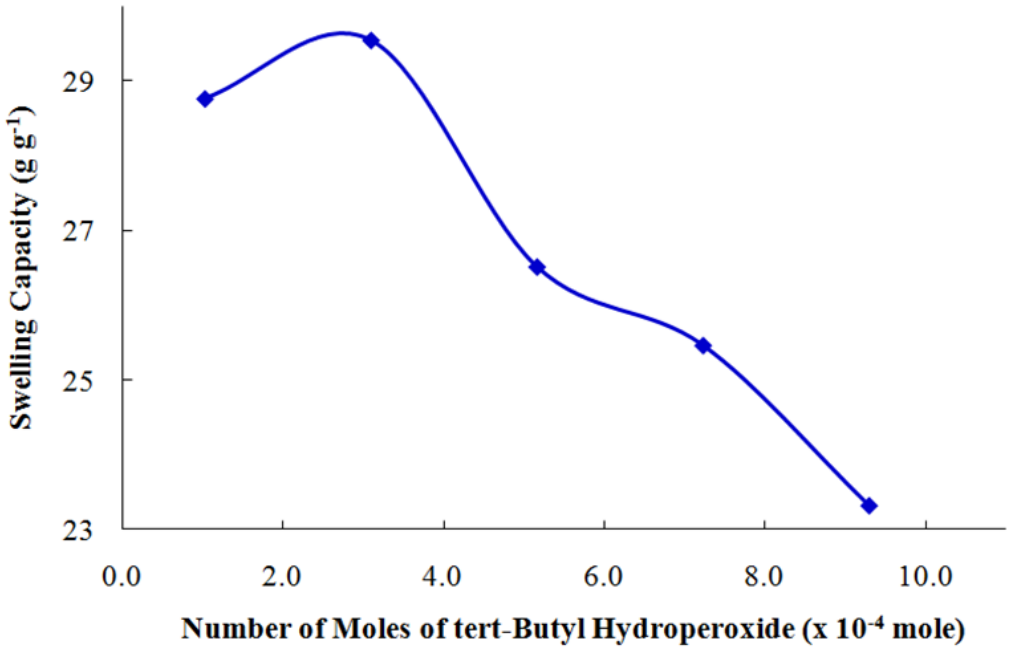

Figure 4.8 Swelling capacity of Alg-*g*-P(AM-*co*-IA) against number of moles of tBHP

From Figure 4.8, it can be clearly perceived that the overall swelling capacity of the polymer in ethanol had improved enormously if compared to the polymer initiated by the KPS/SFX pair, with the highest swelling capacity of the polymer recorded at 29.6 g g^{-1}, in which the polymer was synthesised by the initiation of 3.1×10^{-4} moles of tBHP and SFX each. It is thus logical to conclude that tBHP is a more efficient oxidising agent than KPS in carrying out the synthesis of the polymer. Hence, the initiator pair of KPS/SFX would not be implemented further in this study.

Since as mentioned above, the polymer swelled best in ethanol when the initiator was 3.1×10^{-4} moles in amount, the succeeding syntheses were all initiated with 3.1×10^{-4} moles of tBHP and SFX each.

Both Figures 4.7 and 4.8 revealed that when the maximum swelling capacity had been achieved, a further increase in the amount of the initiator led to a decrease in the swelling capacity of Alg-*g*-P(AM-*co*-IA) in ethanol. The maximum swelling capacities obtained were 7.12 g g^{-1} and 29.6 g g^{-1} when KPS/SFX and tBHP/SFX were at 1.85×10^{-4} and 3.1×10^{-4} moles respectively. An increase in the concentration of initiator resulted in an increase in the number of free radicals on the substrates, which would lead to the increase in branching and crosslinking density in the network. Chen and Zhao (2000) referred this phenomenon as "self-crosslinking". As the crosslinking density increased, the swelling capacity would drop as the flow of water molecules into the SAP particles was restricted by the denser particle. This explained why an increase in the amount of initiating agents retarded the swelling capacity of the SAP.

4.3.1.3 Effect of AA grafting on the swelling capacity of Alg-*g*-P(AM-*co*-IA-*g*-AA)

Section 4.3.1.1 illustrated that the addition of AA alongside AM and IA in the one-step synthesis was redundant, since in one-step synthesis, AM and IA (9:1 molar ratio) alone could cause the SAP Alg-*g*-P(AM-*co*-IA) to swell to its utmost. This phenomenon, however, did not denote that AA is an unnecessary ingredient in the synthesis of a superabsorbent.

Although merely AM and IA were added as the first and only charge in the above syntheses, the idea that adding AA in the subsequent charge to

enhance the swelling capacity of the SAP synthesised was not ruled out. Consequently, AA was again introduced into the synthesis, but this time, as a second charge. Together with the initiator pair, 0.3 to 8.8 × 10^{-2} moles of AA was added in the second charge.

Figure 4.9 shows the swelling capacity of Alg-*g*-P(AM-*co*-IA-*g*-AA) in ethanol plotted against the number of moles of AA. The finding indicated that adding AA at a separate timing than AM and IA could well swell the polymer, unlike when all three monomers were added in the similar charge. From less than 10 g g^{-1} of ethanol absorbed (cf Figure 4.6), the swelling capacity had expanded greatly to as high as 42.3 g g^{-1} when 0.3× 10^{-2} moles of AA was added. As the amount of AA increased from 0.3 to 8.8 × 10^{-2} moles, the swelling capacity of Alg-*g*-P(AM-*co*-IA-*g*-AA) decreased from 42.3 to 2.63 g g^{-1}. This observation was supported by the fact that incorporation of higher amount of monomer brings about self-crosslinking, hence, accessibility of more solvent into the SAP matrix is prevented (Singh *et al*., 2007).

Apart from the above, the finding in this section proves that this technique of dwi-charge grafting is a better choice as it provides better swelling capacity to the SAP. Therefore, the following syntheses which involved AA were all carried out using this two-step technique.

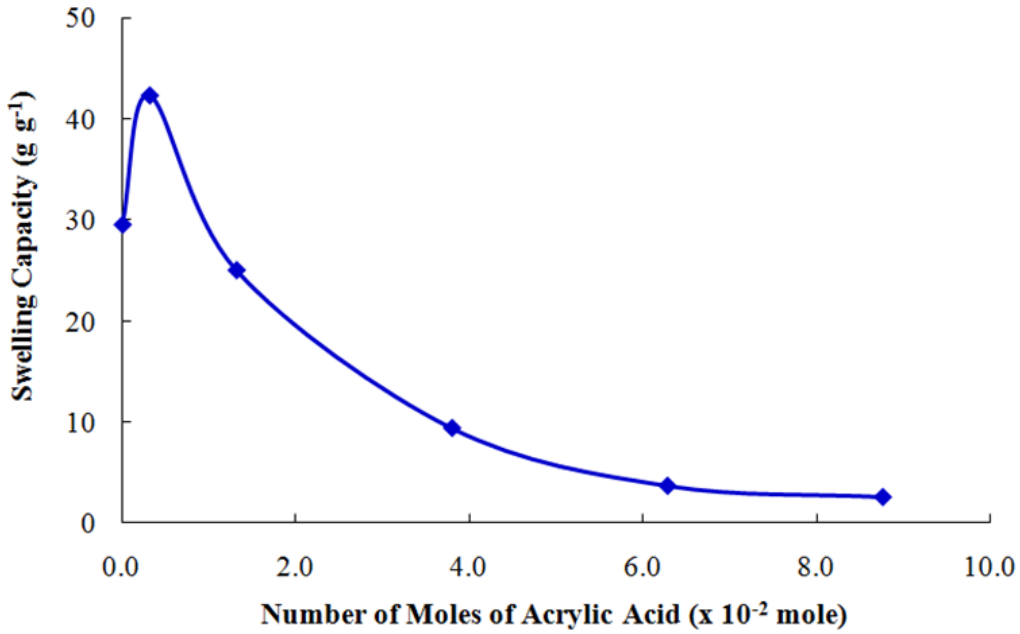

Figure 4.9 Swelling capacity of Alg-*g*-P(AM-*co*-IA-*g*-AA) against number of moles of AA

4.3.1.4 Effect of $CaCl_2$ concentration on the swelling capacity of Alg-*g*-P(AM-*co*-IA) and Alg-*g*-P(AM-*co*-IA-*g*-AA)

Ethanol, which was used as the precipitating agent in the preliminary tests, could not be considered as a good precipitating agent. This is because the SAP samples obtained via the precipitation not only would not swell in water, the samples dissolved in water instead. Therefore, a second alternative, $CaCl_2 \cdot 2H_2O$, was utilised as the precipitating agent. The concentration of $CaCl_2$ was varied from 0.01 to 0.50 M (0.09 to 4.5 × 10^{-2} moles) to determine a maximum swelling capacity in Alg-*g*-P(AM-*co*-IA).

Figure 4.10 shows that as the concentration of $CaCl_2$ used to precipitate the SAP solution increased from 0.01 to 0.50 M, the swelling capacity of the water-swollen Alg-*g*-P(AM-*co*-IA) decreased from 155 to 7.50 g g^{-1}. This

indicated that 0.01 M of $CaCl_2$ was sufficient to result in maximum water absorbency of the SAP synthesised. This is most probably that at low concentration of $CaCl_2$, there was less restriction of the entry of water molecules into the polymer core as the calcium ions accumulated at the surface of the polymer was less. Once the water molecules had entered the core, they would form interactions with the functional groups such as carboxylic and alcohol groups, and therefore, held the water and caused the polymer to swell. However, the drawback of less calcium ions on the outer surface of the SAP is that the SAP gel obtained was not strong enough and could be burst easily.

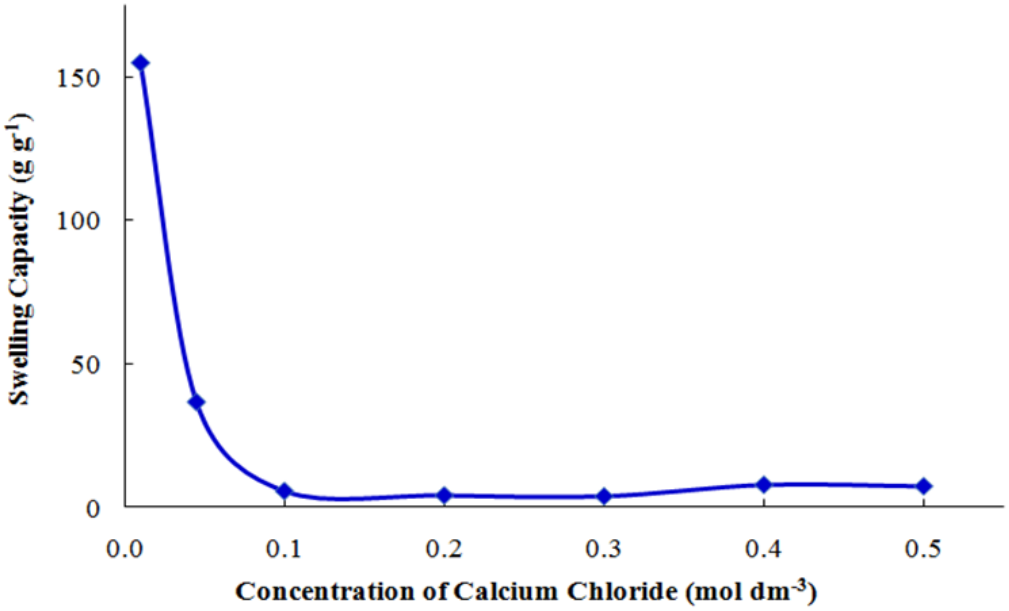

Figure 4.10 Swelling capacity of Alg-*g*-P(AM-*co*-IA) against the concentration of $CaCl_2$

Similarly, $CaCl_2$ was varied from 0.01 to 0.50 M to assess the concentration of $CaCl_2$ required to precipitate the gel to lead to a maximum water absorbency in Alg-*g*-P(AM-*co*-IA-*g*-AA). The SAP was swollen in

water for 72 hours, and Figure 4.11 portrays the graph of swelling capacity of the SAP with respect to the concentration of $CaCl_2$.

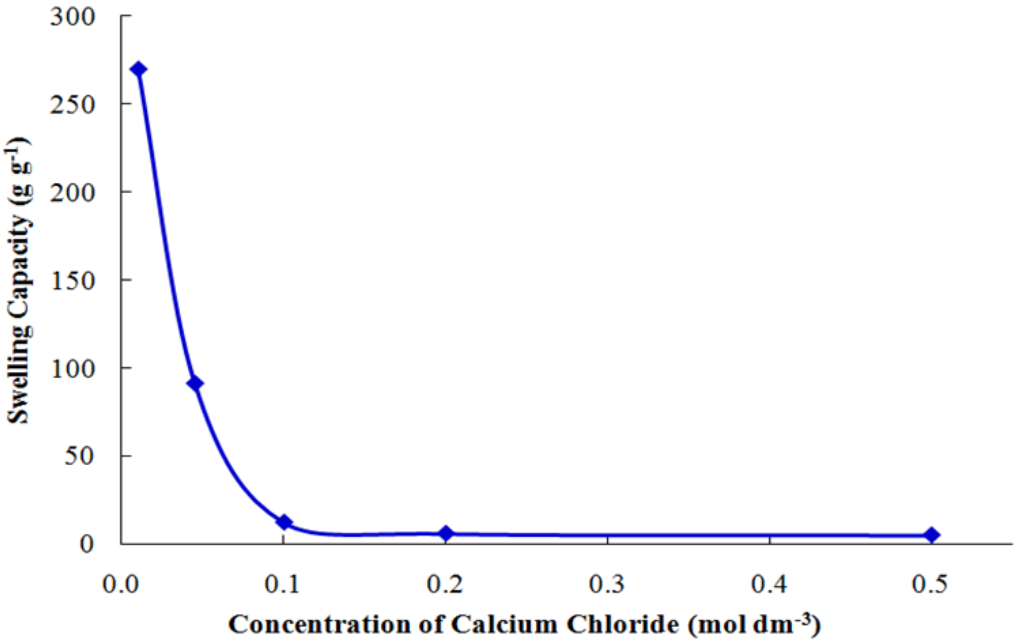

Figure 4.11 Swelling capacity of Alg-*g*-P(AM-*co*-IA-*g*-AA) against the concentration of $CaCl_2$

Identical to the trend found in Alg-*g*-P(AM-*co*-IA) (Figure 4.10), the swelling capacity of Alg-*g*-P(AM-*co*-IA-*g*-AA) decreased from 270 to 5 g g^{-1} with an increase in the amount of $CaCl_2$ from 0.01 to 0.50 M. The reason behind this finding is similar to the explanation above.

For the SAP beads, gel density was high in the outer shell but low in the core. This was because dense alginate gel matrix was rapidly formed in the outer layer of the bead as alginate droplets came into contact with the divalent calcium ions, thus significantly hindered the diffusion of water molecules into the core of the beads during the swelling process. This restriction became more prominent when the concentration of $CaCl_2$ increased, hence explaining the

decrease in the swelling capacity of the synthesised SAP with increasing amount of $CaCl_2$.

Although it is obvious that 0.01 M $CaCl_2$ would best precipitate the SAP solution (in terms of water absorbency of the SAP), the gel strength of the SAP obtained via the precipitation of lower concentration of $CaCl_2$ could not match that of the SAP precipitated by higher concentration of $CaCl_2$. This phenomenon was most suitably explained by the fact that increasing the concentration of $CaCl_2$ strengthened the gel surface, and hence caused the gel to be tougher in terms of gel strength.

4.3.1.5 Effect of N-MBA concentration on the swelling capacity of crosslinked-Alg-*g*-P(AM-*co*-IA) and crosslinked-Alg-*g*-P(AM-*co*-IA- *g*-AA)

In an attempt to increase the gel strength of the polymer synthesised, a crosslinking agent, N-MBA, was added. The crosslinker was varied from 0.1 to 6.24×10^{-3} moles. The crosslinked-Alg-*g*-P(AM-*co*-IA) SAP solution was precipitated using 0.01 M $CaCl_2$ and the dry sample was then reswollen in distilled water for 72 hours. Figure 4.12 shows the plot of swelling capacity of crosslinked-Alg-*g*-P(AM-*co*-IA) against the number of moles of N-MBA.

Compared with the SAP not added with any N-MBA, the swelling capacity of crosslinked-Alg-*g*-P(AM-*co*-IA) had improved significantly from 222 to 654 g g^{-1} with the addition of a minor 0.10×10^{-3} moles of N-MBA.

Nevertheless, there was a steady decrease in the swelling capacity of the polymer from 654 to 55.7 g g^{-1} with the gradual increase in the amount of the crosslinking agent from 0.10 to 6.24 × 10^{-3} moles.

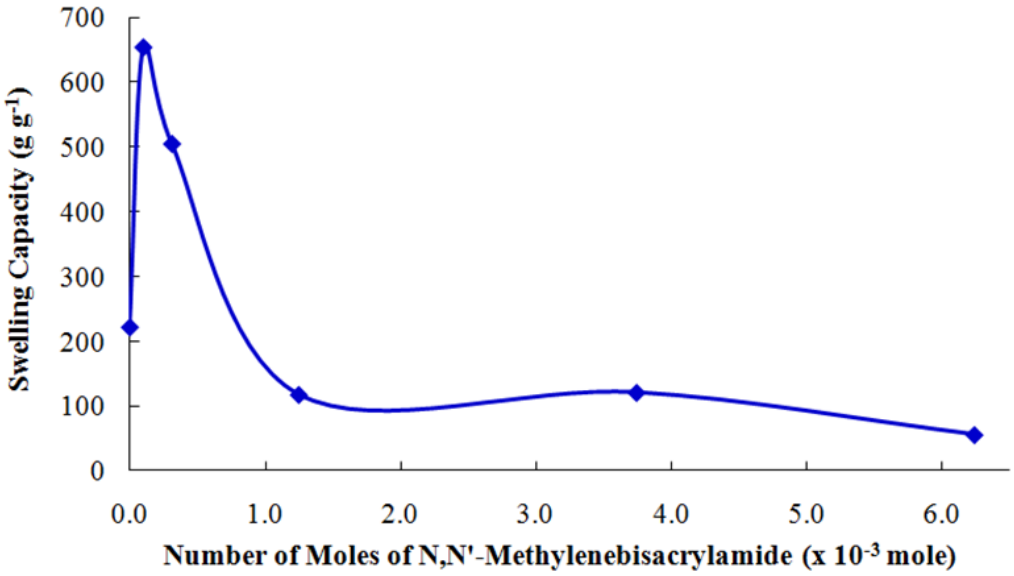

Figure 4.12 Swelling capacity of crosslinked-Alg-*g*-P(AM-*co*-IA) against number of moles of N-MBA

This trend signified that an adequate amount of N-MBA would improve the water uptake of the SAP as mild crosslinking could retain water within the three-dimensional structure but further addition of N-MBA would retard the water absorbency of the polymer. This is in coherence with the general understanding about crosslinker – increasing of crosslinker concentration results in an increase of crosslinking density, leading to a decreased swelling capacity (Gao *et al.*, 2009; Hua and Wang, 2009; Li and Wang, 2005; Singh *et al.*, 2007).

Likewise, to observe the effect of crosslinking agent on the swelling capacity of crosslinked-Alg-*g*-P(AM-*co*-IA-*g*-AA), N-MBA was varied from 0.0025 to 1.0 × 10^{-2} moles while precipitating the SAP solution with 0.01 M $CaCl_2$. The SAP was swollen in water for 72 hours, and Figure 4.13 shows the graph of swelling capacity of crosslinked-Alg-*g*-P(AM-*co*-IA-*g*-AA) against the number of moles of N-MBA.

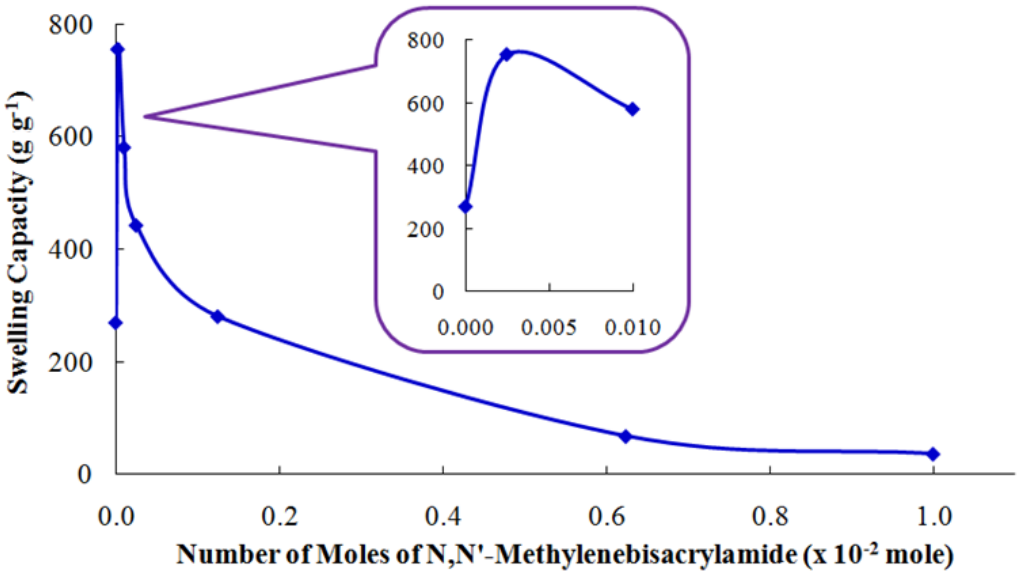

Figure 4.13 Swelling capacity of crosslinked-Alg-*g*-P(AM-*co*-IA-*g*-AA) against number of moles of N-MBA

The SAP not added with any N-MBA had a swelling capacity of 270 g g^{-1} upon precipitation by 0.01 M of $CaCl_2$. Nonetheless, upon addition of a negligible amount of 0.0025 × 10^{-2} moles of N-MBA, the swelling capacity of crosslinked-Alg-*g*-P(AM-*co*-IA-*g*-AA) shot up to 754 g g^{-1}. Further addition of N-MBA from 0.0025 to 1.0 × 10^{-2} moles witnessed a decline in the swelling capacity of the SAP from 754 to 36.8 g g^{-1}.

The conclusion drawn from this finding is that a sufficient amount of N-MBA is necessary to improve the swelling capacity of the SAP, but further increase in the amount of N-MBA would create higher density of crosslink junctions. Without N-MBA, water tends to sip out as there is limited extent of entanglement which can hold the water. A small extent of crosslinking network could thus maintain the absorbed water within the entangled structure.

However, an increase in the crosslinking density would decrease the pore size of the crosslinked network, which would hinder the polymer network from growing in size by confining the amount of water entering the matrix, thus results in a decrease in swelling capacity (Gao *et al*., 2009; Singh *et al*., 2007). In other words, both the spaces among the SAP chains (Li and Wang, 2005) and elasticity of the polymeric network (Hua and Wang, 2009) decrease when the crosslinking density increases, thus leading to a drop in swelling capacity. Chen and Tan (2006) regarded this phenomenon as the decrease in the molar mass between crosslink points (M_c) with the increase in crosslinker concentration, which inhibits the stretching of the polymer chains.

4.3.1.6 Effect of volume ratio of $CaCl_2$ to SAP solution on the swelling capacity of crosslinked-Alg-*g*-P(AM-*co*-IA-*g*-AA)

While the effect of the concentration of $CaCl_2$ on the swelling capacity of Alg-*g*-P(AM-*co*-IA-*g*-AA) was discussed in Section 4.3.1.4, swelling capacity of the crosslinked-Alg-*g*-P(AM-*co*-IA-*g*-AA) with different volume ratio of $CaCl_2$ to the SAP solution is focused in this section. Section 4.3.1.5

revealed that the addition of 0.0025×10^{-2} moles of N-MBA to the synthesis would bring about the highest swelling capacity in the SAP, thus the SAP in this section was synthesised by this particular amount of crosslinking agent.

The volume ratio of 0.05 M $CaCl_2$ to SAP solution was varied from 1:1 to 5:1. Although earlier finding (Section 4.3.1.4) indicated that lower concentration of $CaCl_2$ would lead to higher water absorbency in the SAP, the concentration of $CaCl_2$ was not fixed at lower values than 0.05 M because the gel strength of the polymer would suffer from a plunge when the amount of calcium ions available for surface crosslinking was too low. Hence 0.05 M of $CaCl_2$ preferred in this section served as a compromise between gel strength and water absorbency of the SAP.

Unlike all other sections in which the SAP beads were recovered by dripping 45 cm^3 of the gel into 90 cm^3 of $CaCl_2$ solution, the polymer in this section was obtained by randomly pouring a fixed volume of the gel into different volume of 0.05 M $CaCl_2$ solution. This was to evaluate the effect of different volume of $CaCl_2$ solution towards the swelling capacity of the polymer.

Figure 4.14 represents the plot of swelling capacity of crosslinked-Alg-*g*-P(AM-*co*-IA-*g*-AA) with respect to the volume ratio of $CaCl_2$ to SAP solution.

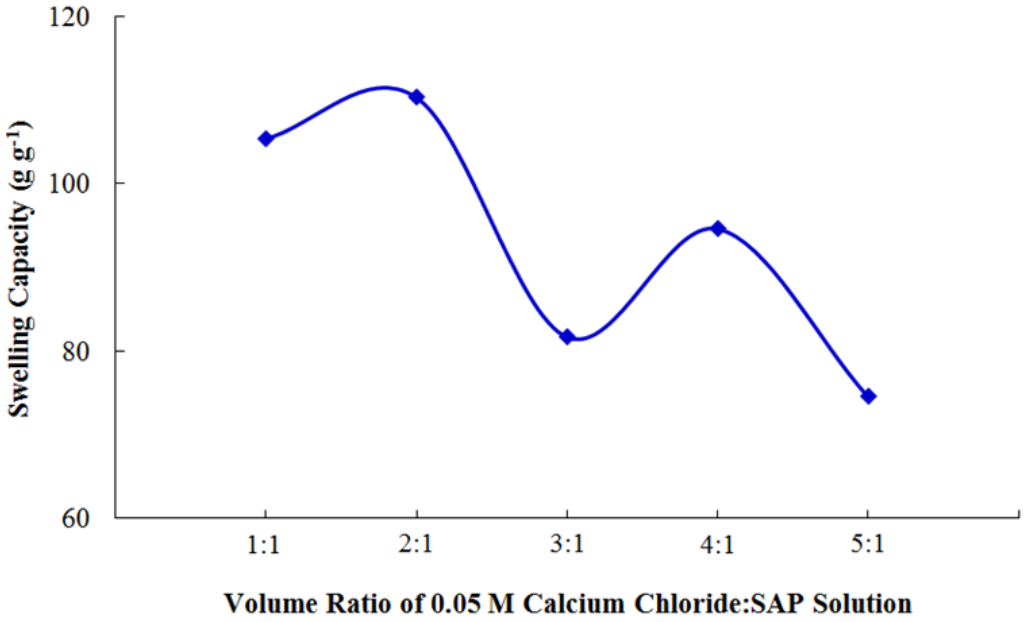

Figure 4.14 Swelling capacity of crosslinked Alg-*g*-P(AM-*co*-IA-*g*-AA) against volume ratio of 0.05 M $CaCl_2$ to SAP solution

Generally, the swelling capacity of the SAP dropped as the volume ratio of $CaCl_2$ increased. The highest water absorbency was recorded in the SAP precipitated with the volume ratio of 0.05 M $CaCl_2$:SAP solution being 2:1, with swelling capacity of 110 g g^{-1}. Thus, it could be concluded that this volume ratio of 0.05 M $CaCl_2$ to SAP solution was the most appropriate that should be used as the standard for precipitating the gel.

4.3.1.7 Effect of duration of swelling on the swelling capacity of crosslinked-Alg-*g*-P(AM-*co*-IA-*g*-AA)

Whenever the swelling of SAP was mentioned before this section, the swelling period should be noted as 72 hours. In this section, the duration of swelling of the SAP was varied from 4 to 72 hours to determine the SAP's ability to absorb water over time. The SAP was crosslinked with 2.5 × 10^{-5}

moles of N-MBA and precipitated by 0.05 M $CaCl_2$. Figure 4.15 explains the swelling capacity of crosslinked-Alg-*g*-P(AM-*co*-IA-*g*-AA) with respect to the duration of swelling.

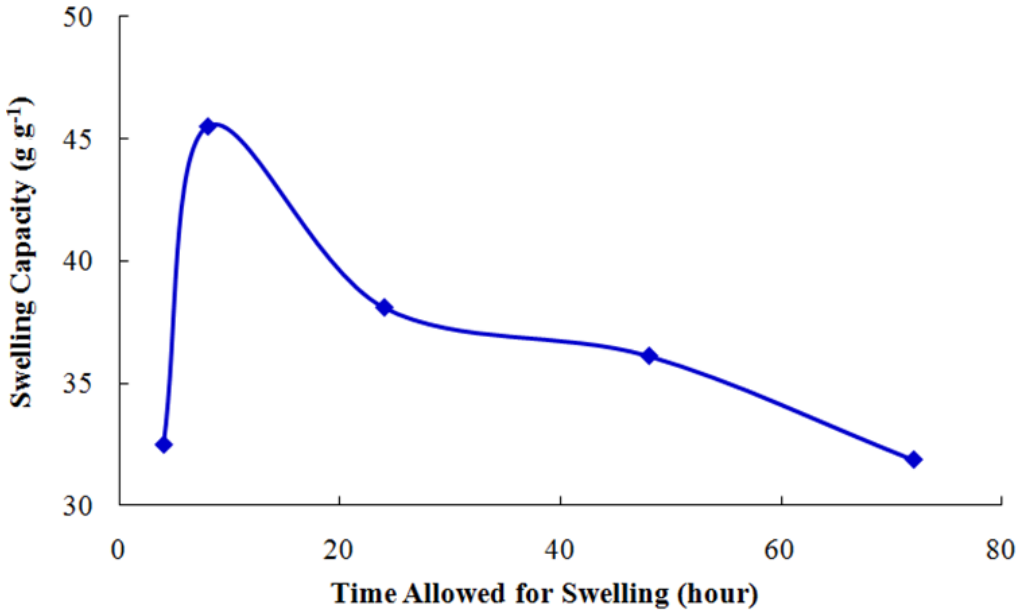

Figure 4.15 Swelling capacity of crosslinked-Alg-*g*-P(AM-*co*-IA-*g*-AA) against the time allowed for swelling

The swelling capacity of the SAP was at its highest at 46 g g^{-1} when the SAP was left to swell for 8 hours. Further increase in the time span of swelling, however, impeded the water absorbency of the SAP. Since the result showed that the swelling of the SAP would be at its maximum by 8 hours, it indicated that the SAP could absorb water at a reasonable rate during this period of time.

In Section 4.3.1.6, the highest swelling capacity in distilled water for a time span of 72 hours of the SAP precipitated with a volume ratio of 2:1 of 0.05 M $CaCl_2$ to SAP solution was recorded as 110 g g^{-1}, while in this section,

it is obvious that the similar SAP only showed a swelling capacity as low as 32 $g\ g^{-1}$.

The reason for the difference in the swelling capacities of the two is that the SAP product mentioned in Section 4.3.1.6 was obtained by randomly pouring 45 cm^3 of the SAP solution into 90 cm^3 of 0.05 M $CaCl_2$ solution; while in this section, the SAP was obtained as gel beads by dripping 45 cm^3 of the gel into 90 cm^3 of $CaCl_2$ solution. Hence, it is most probably that the method of precipitation had affected the swelling capacity of the product.

While pouring the SAP solution into the precipitating agent decreased the surface area of the SAP (because a lump sample of the SAP was obtained), SAP beads with higher surface area were formed when dripping the SAP solution dropwise into the precipitating agent. Higher volume of water was held by SAP particles with lower surface area, and vice versa. Therefore, beads of SAP held less water compared to a big lump of SAP, and thus the swelling capacity of SAP obtained via dropwise precipitation was lower than those obtained via pouring precipitation.

4.3.2 Swelling Capacity of Superabsorbent Polymer Obtained via Bigger-scale Synthesis

4.3.2.1 Effect of $CaCl_2$ concentration on the swelling capacity of crosslinked-Alg-*g*-P(AM-*co*-IA-*g*-AA)

The effect of the concentration of $CaCl_2$ on the water swelling capacities of the SAPs produced via small-scale syntheses had been discussed in much detail in Section 4.3.1.4. It is therefore not difficult to predict the outcome of the investigation in this section, in which the concentration of $CaCl_2$ was varied in order to investigate its effect on the swelling capacity of the SAP, crosslinked-Alg-*g*-P(AM-*co*-IA-*g*-AA), produced via bigger-scale synthesis.

In this section of the study, $CaCl_2$ was varied from 0.0125 to 0.20 M. Since the result of Section 4.3.1.7 showed that the SAP would swell to its maximum by 8 hours, the samples were swollen in water for 8 hours in this section. Figure 4.16 illustrates the graph of swelling capacity of crosslinked-Alg-*g*-P(AM-*co*-IA-*g*-AA) with respect to the concentration of $CaCl_2$.

The swelling capacity of the SAP decreased gradually from 363 to 8 g g^{-1} when the concentration of $CaCl_2$ increased from 0.01 to 0.20 M. This trend was exactly as expected, since there would be a restriction for the entry of water molecules into the polymer matrix when the gel density on the outer layer of the polymer beads increased with increasing calcium ions concentration, thus causing the swelling capacity of the SAP to dive.

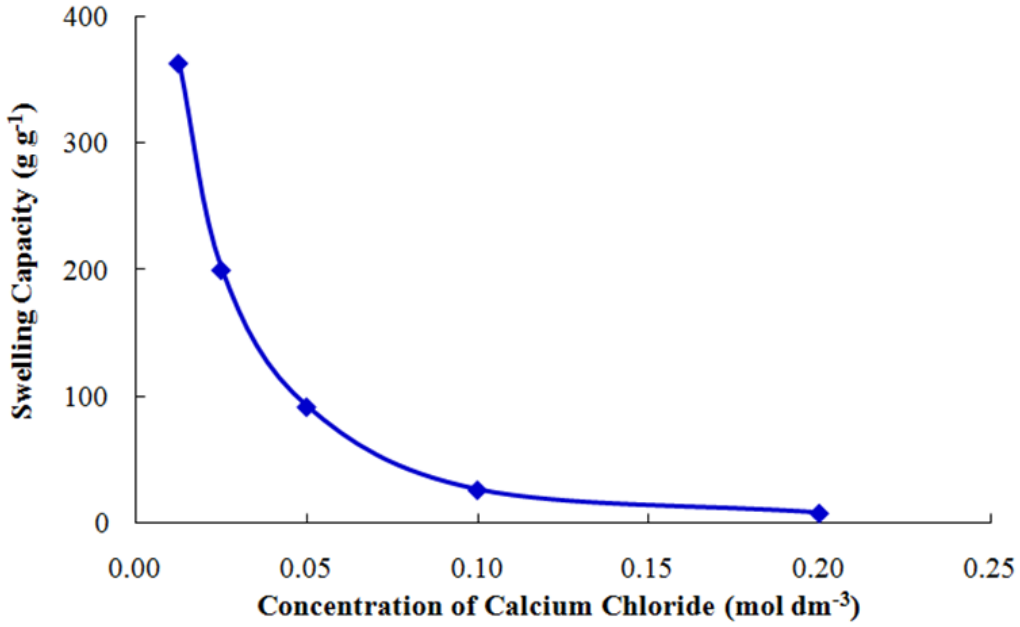

Figure 4.16 Swelling capacity of crosslinked-Alg-*g*-P(AM-*co*-IA-*g*-AA) (bigger-scale synthesis) against the concentration of $CaCl_2$

It is worthwhile to highlight that compared to the SAP produced via small-scale synthesis, the respective swelling capacities of the bigger-scale samples precipitated with similar concentration of $CaCl_2$ had improved. Comparing Figure 4.16 with Figure 4.15, the swelling capacities for crosslinked-Alg-*g*-P(AM-*co*-IA-*g*-AA) precipitated with 0.05 M $CaCl_2$ and swelled for 8 hours, were 46 and 92 g g^{-1}, for small-scale and bigger-scale syntheses, respectively.

The factor which contributes to this phenomenon is most probably due to the stirring efficiency of the SAP solution in both the small-scale and bigger-scale syntheses. Gentler stirring was applied by magnetic stirring in small-scale synthesis compared to the more intensive stirring displayed by mechanical stirring in bigger-scale synthesis. Furthermore, better temperature

control for the bigger-scale synthesis could be another factor why a more homogenous SAP solution was obtained for the latter.

The SAP particles synthesised in the latter were henceforth predicted to be of higher and more consistent molecular masses, since the rate of collision among the monomers in the gel was deemed to be higher. With longer or more polymer chains formed, the functional groups such as hydroxyl and carboxylic groups would increase in amount, and hence more water molecules could be held within the matrix during the swelling process. This could well-explain why the SAP produced in bigger-scale synthesis swelled better than that of small-scale synthesis, although all other parameters were held constant.

The standard errors for the swelling capacities obtained for the SAP samples precipitated with 0.0125, 0.025, 0.05, 0.1 and 0.2 M $CaCl_2$ were 4.3, 3.2, 2.3, 10 and 3.5 % respectively. Gravimetric method is subjected to systematic errors. In the current study, the sources of errors included presence of contaminants in the samples, and the absorption of water in the air by the SAPs during the weighing process due to the hygroscopic nature of the SAPs.

4.3.2.2 Effect of dilution of SAP solution on the swelling capacity of crosslinked-Alg-*g*-P(AM-*co*-IA-*g*-AA)

In this section, the synthesised SAP solution was diluted with distilled water in the volume ratio of SAP solution to water being 1:0 to 1:4, followed by precipitation of each of the diluted SAP solution with 0.05 M of $CaCl_2$ and

subsequently swelling the dry samples for 8 hours in distilled water, in order to observe the effect of dilution of the SAP solution on the swelling capacity of the SAP.

As shown in Figure 4.17, the original SAP solution (volume ratio of SAP solution to water = 1:0) swelled as much as 140 g g^{-1}. When the volume ratio of SAP solution to water was 1:1, the swelling capacity of the SAP dropped drastically to 34 g g^{-1}. Further dilution had shown to reduce the swelling capacity of the SAP to as low as 7 g g^{-1}.

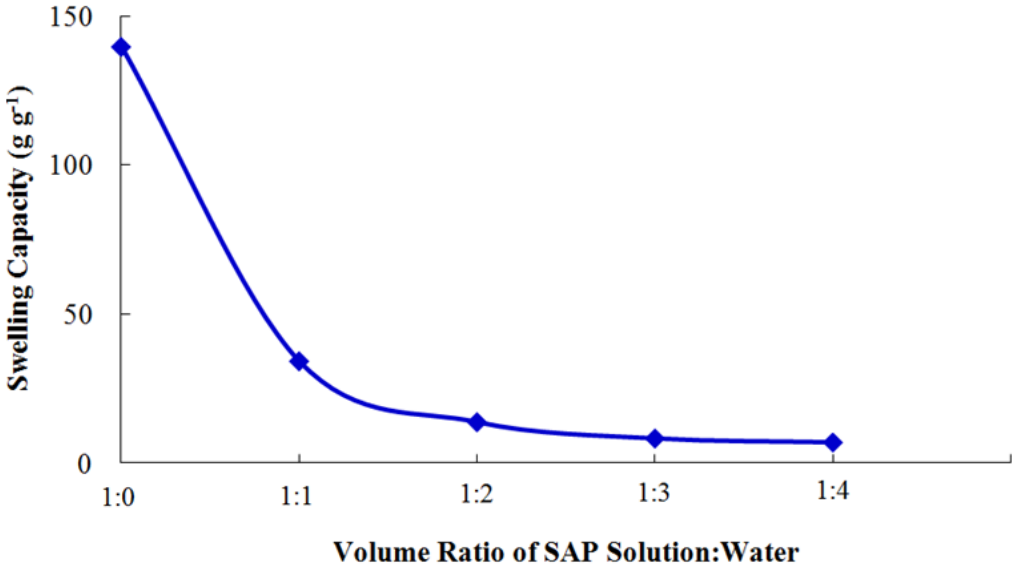

Figure 4.17 Swelling capacity of crosslinked-Alg-*g*-P(AM-*co*-IA-*g*-AA) against the volume ratio of SAP solution to water

The results showed that as the SAP solution became more diluted, the swelling capacity of the precipitated SAP sample would be lower. This phenomenon is not hard to be understood, since a more diluted SAP solution would lead to less SAP macromolecules in every litre of the SAP solution. Therefore, when the SAP solution was later precipitated using calcium ions,

the number of SAP molecules in each bead became less with fewer molecules available for enclosure into the bead matrix. With fewer polymer chains entrapped in each bead, the trapping of water molecules in the matrix became less efficient since there were fewer functional groups available in the matrix to bind to the water molecules. Hence, the swelling capacity of the SAP will decrease with increasing number of dilution of the SAP solution.

4.3.2.3 Effect of particle size of dry polymer on the swelling capacity of crosslinked-Alg-*g*-P(AM-*co*-IA-*g*-AA)

In order to investigate the effect of particle size on the swelling capacity of the SAP, the dry 0.05 M $CaCl_2$-precipitated SAP beads of different sizes were soaked in distilled water for 8 hours. Figure 4.18 shows the swelling capacity of the SAP plotted against the diameter of the dry SAP bead.

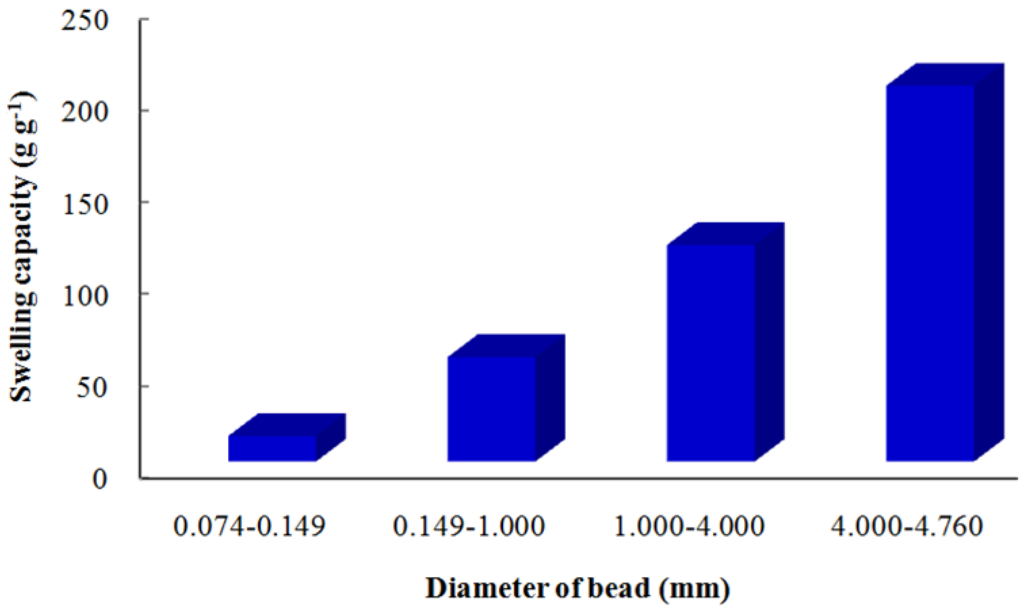

Figure 4.18 Swelling capacity of crosslinked-Alg-*g*-P(AM-*co*-IA-*g*-AA) against diameter of dry bead

As the particle size of the SAP increased from 0.074 – 0.149 mm to 4.000 – 4.760 mm, the swelling capacity of the SAP sample raised from 14 to 205 g g^{-1}. As the surface area of the sample particles decreased with increasing particle size, higher volume of water could be retained by the bead particles (cf Section 4.3.1.7). This was why the swelling capacity of the SAP increased with increasing particle size, and vice versa.

4.4 Measurement of Absorbency under Load (AUL)

The AUL test measured the SAP's ability to absorb 0.9 wt.% NaCl solution against a pressure of 20 – 40 g/cm². As a precaution, the Petri dish with its content was covered to prevent surface evaporation and probable change in the saline concentration.

The AUL test was carried out by varying the mass of the load in order to obtain varying applied pressures from 0 to 40 g/cm^2. The SAP sample used in this test was the SAP produced via small-scale synthesis, crosslinked-Alg-*g*-P(AM-*co*-IA-*g*-AA), which had been crosslinked with 0.0025×10^{-2} moles of N-MBA, and further precipitated using 0.05 M $CaCl_2$. Figure 4.19 shows the swelling capacity of the SAP under different applied pressure (i.e. AUL), as a function of the duration of swelling.

In general, for all the SAP samples, the AUL increased when the time allowed for swelling increased. Compared to the SAPs which were applied with pressures of 20, 30 or 40 g/cm^2, the absorbency of the control SAP

sample (i.e. the applied pressure = 0 g/cm^2) was the highest, in which the AUL raised 130 %, from 10 to 23 g g^{-1}, when the time allowed for swelling increased from 1 to 8 hours. As the applied pressure increased from 0 to 40 g/cm^2, the AUL of the SAP sample declined with the time allowed for swelling being held constant. For example, when the SAP was allowed to swell for 8 hours, the AUL decreased by more than half (56.5 %), from 23 to 10 g g^{-1}, as the applied pressure increased from 0 to 40 g/cm^2.

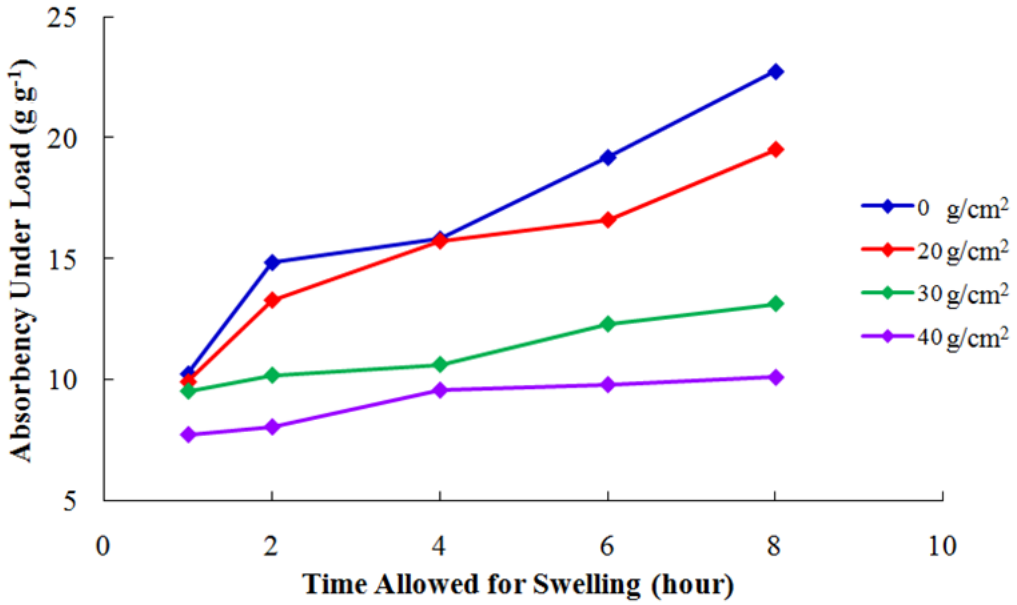

Figure 4.19 Absorbency under load of crosslinked-Alg-*g*-P(AM-*co*-IA-*g*-AA) against time allowed for swelling

When the pressure applied to the SAP increased, the ability for the sample to take up solvent in the gel matrix decreased. This inefficiency of solvent uptake was basically due to the external pressure exerted upon the sample, which restricted the increase in volume of the sample bead. The higher the applied pressure, the higher will be the forces to restrict the increase in volume, hence lower the solvent uptake and resulting in lower AUL.

The indication of this test was that the SAP synthesised in this research could reasonably absorb saline solution under applied pressure, even at pressure of at least up to 40 g/cm^2. This information might come handy in applications which require the SAP to absorb water or saline solution under load.

Apart from studying the trend in the changes of AUL with respect to time and applied pressure, the rates of solvent uptake could also be deduced from Figure 4.19. Regardless of the applied pressure, the rate of solvent uptake was higher in the first hour of swelling, i.e. between Hour 1 and 2, compared to the last two hours of swelling, i.e. between Hour 6 and 8. Taking the load of 20 g/cm^2 as an example, the rate of solvent uptake was 5.6×10^{-2} g/min in between Hour 1 and 2. However, the rate of solvent uptake was 2.4×10^{-2} g/min in between Hour 6 and 8.

During the first hour of the AUL test, water diffused into the SAP sample due to the high difference in osmotic pressure between the gel and solvent phases. The presence of the pressure difference provided the driving force for the diffusion of solvent into the gel phase, which was the SAP sample. Towards the sixth hour, the diffusion process slowed down because the difference in osmotic pressure had narrowed down. The rate of solvent uptake was therefore lower at the later stage compared to earlier stage.

Compared to the swelling capacity of the SAP in distilled water, the SAP obviously exhibited lower absorbency in saline solution. This is due to

the decrease in the difference of osmotic pressure between the gel and solvent phase (Ramazani-Harandi *et al*., 2006).

4.5 Infrared Spectroscopy

The samples used in IR analysis include NaAlg, Alg-*g*-PAM, Alg-*g*-PIA, Alg-*g*-PAA, Alg-*g*-P(AM-*co*-IA), Alg-*g*-P(AM-*co*-IA-*g*-AA) and crosslinked-Alg-*g*-P(AM-*co*-IA-*g*-AA). The second to second last samples were synthesised without incorporating the crosslinking agent, N-MBA, while the last sample was crosslinked with N-MBA. All these samples were precipitated using 0.05 M $CaCl_2$.

IR spectra were obtained for the starting material and products synthesised in the 4000 – 400 cm^{-1} range. Figure 4.20 illustrates the IR spectra of NaAlg, Alg-*g*-PAM and Alg-*g*-PIA (from top to bottom) while Figure 4.21 depicts the IR spectra of Alg-*g*-PAA, Alg-*g*-P(AM-*co*-IA), Alg-*g*-P(AM-*co*-IA-*g*-AA) and crosslinked-Alg-*g*-P(AM-*co*-IA-*g*-AA) (from top to bottom), respectively. Table 4.1 specifies the assignments of IR absorption bands for all the SAPs.

In the IR spectrum of NaAlg, the broad absorbing peak which is present at 3432 cm^{-1} is characterised as the H-bonded O–H stretching frequency (Xu *et al*., 2006). The band at approximately 2900 cm^{-1} is assigned to C–H stretching. Although the fingerprint region (1000 – 750 cm^{-1}) is seldom looked into in detail by researchers, it is the most discussed region in

carbohydrates (Leal *et al.*, 2008). The weak peaks at 1300, 1090 and 947 cm^{-1} are all due to stretching vibrations of C–O from glycosidic bonds, with the stretching vibration of C–O–C from glycosidic bonds contributes to the peak at 947 cm^{-1} as well.

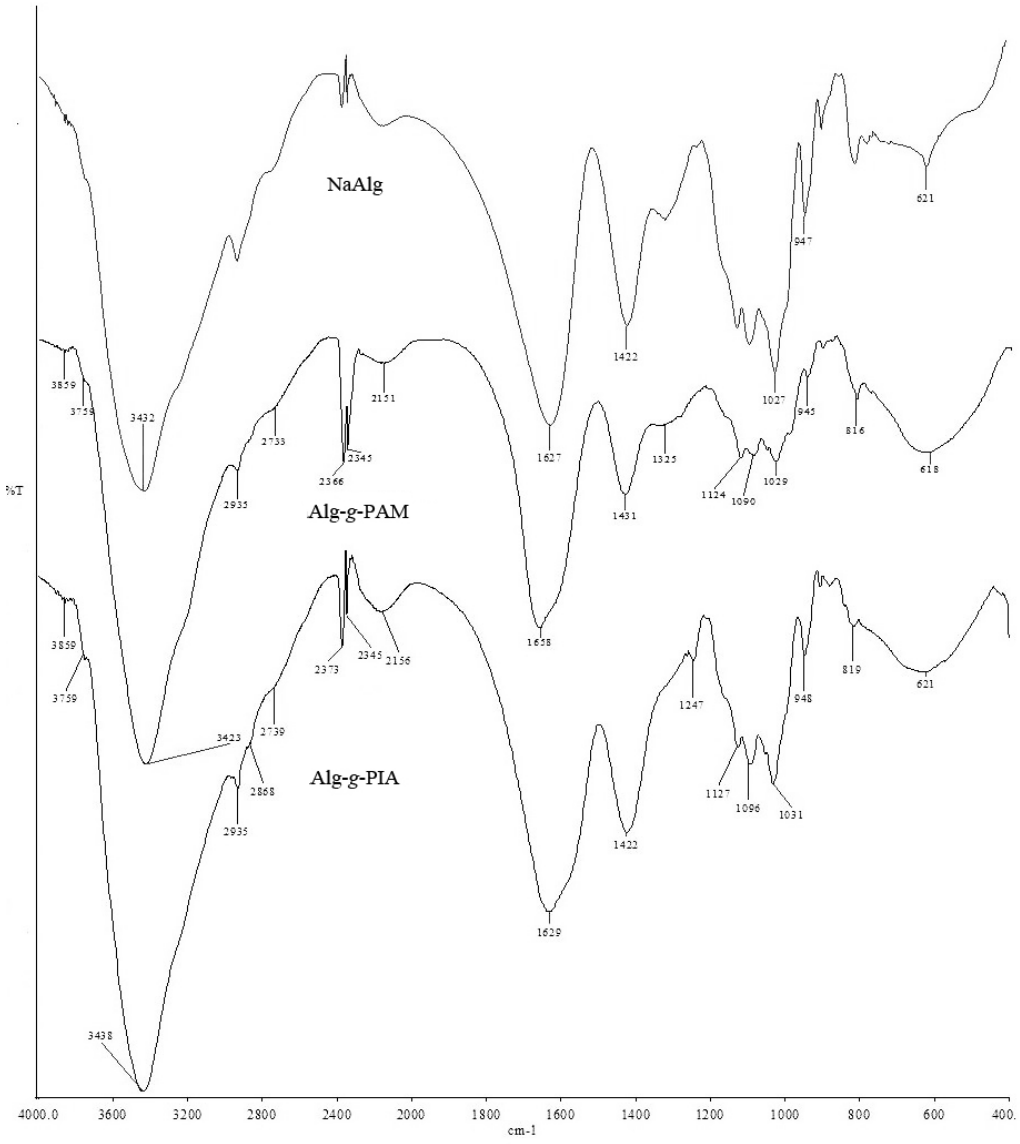

Figure 4.20 IR spectra of NaAlg, Alg-*g*-PAM and Alg-*g*-PIA (from top to bottom)

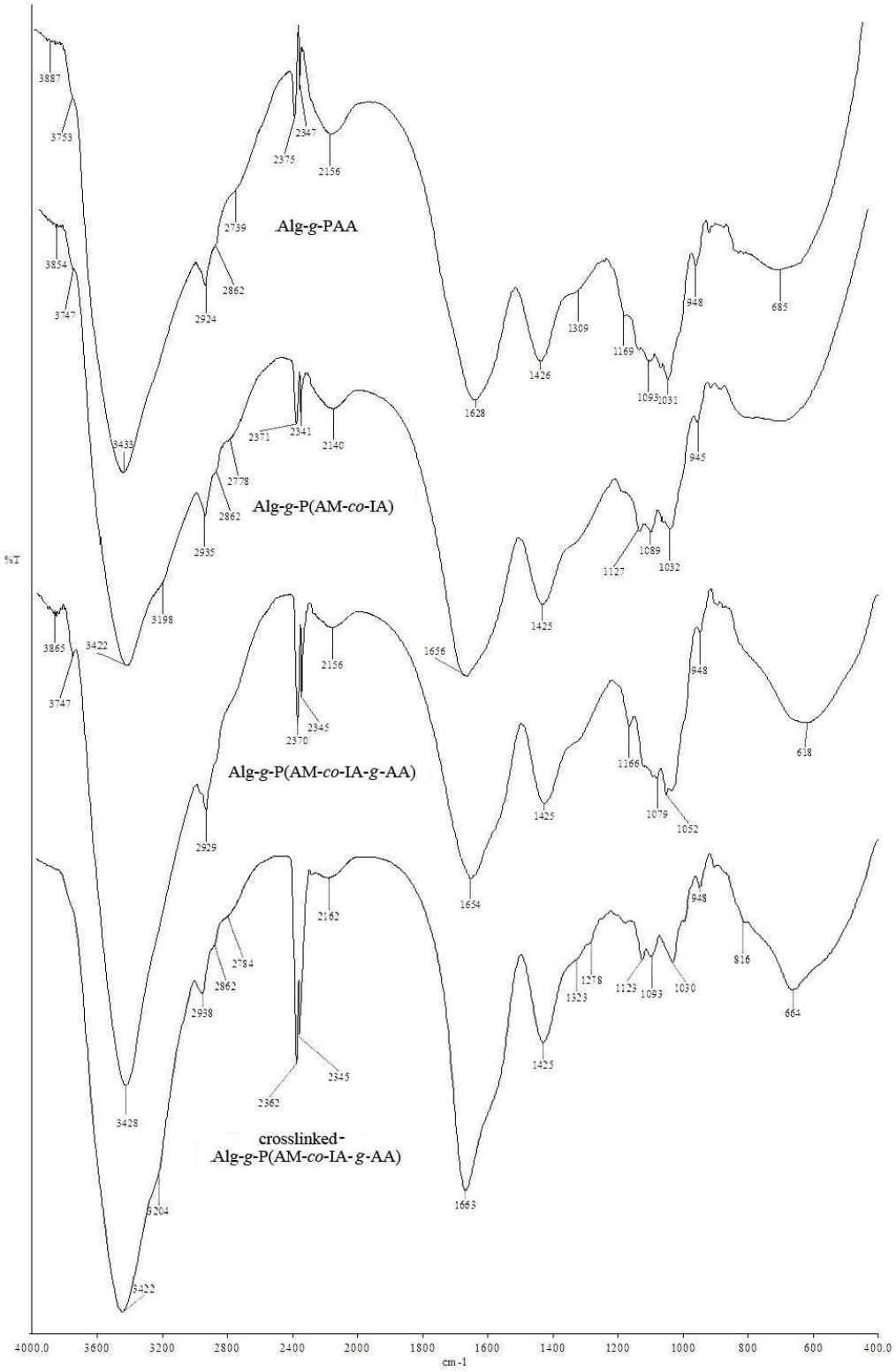

Figure 4.21 IR spectra of Alg-*g*-PAA, Alg-*g*-P(AM-*co*-IA), Alg-*g*-P(AM-*co*-IA-*g*-AA) and crosslinked-Alg-*g*-P(AM-*co*-IA-*g*-AA) (from top to bottom)

Table 4.1 Assignments of IR absorption bands

Intensity/ shape	**Assignment**	**NaAlg (cm^{-1})**	**Alg-*g*-PIA, Alg-*g*-PAA (cm^{-1})**	**Alg-*g*-PAM, Alg-*g*-P(AM-*co*-IA), Alg-*g*-P(AM-*co*-IA-*g*-AA), crosslinked-Alg-*g*-P(AM-*co*-IA-*g*-AA) (cm^{-1})**
Strong/ Broad	O–H stretching	3432	3438, 3433	3422 – 3428
Weak/ Sharp	C–H stretching		2938 – 2924	
Strong/ Sharp	Asymmetric stretching of carboxylate COO^-	1627	1629, 1628	1654 – 1663
Medium/ Sharp	C–OH deformation + symmetric stretching of carboxylate COO^-	1422	1422, 1426	1425 – 1431
Weak/ Broad	C–O stretching		1300 – 1325	
Medium/ Sharp	C–O and C–O–C stretching		1079 – 1093	
Weak/ Sharp	C–O stretching		945 – 948	

Two obvious peaks could be observed for the carboxylate group. For NaAlg, the stretching of the COO^- group which is attached to the sodium ion

shows two distinct peaks, which are observed at 1627 and 1422 cm^{-1}. The former is caused by the asymmetric stretching vibration of the carboxylate COO^- while the latter is deduced to be due to C–OH deformation vibration with contribution of COO^- symmetric stretching vibration of the carboxylate group (Soares *et al*., 2004; Wang and Wang, 2010; Xu *et al*., 2006).

Generally, all the IR spectra of the synthesised polymers looked similar in terms of presence of peaks. The spectra exhibit a strong, broad absorbing peak in between 3423 and 3438 cm^{-1}. These peaks correspond to the H-bonded O–H stretching vibrations of each of the polymer. Similarly, the weak signals in between 2935 and 2924 cm^{-1} are contributed by the C–H stretching vibrations of the respective compounds.

In the IR spectrum of Alg-*g*-PAM, the medium absorption band of COO^- symmetric stretching vibration (detected at 1422 cm^{-1} for NaAlg) has shifted to the left to 1431 cm^{-1}, most likely due to the presence of C–N group in $–CONH_2$ (Wang and Wang, 2010). This is a proof of the presence of PAM. For Alg-*g*-PIA and Alg-*g*-PAA, the similar band is found at 1422 cm^{-1} (two –COOH groups in PIA made no obvious change to the wavenumber) and 1426 cm^{-1} (–COOH group in PAA shifted the band to the left) respectively since C–N group is absent in these SAPs. Thus the IR spectra for Alg-*g*-P(AM-*co*-IA), Alg-*g*-P(AM-*co*-IA-*g*-AA) and crosslinked-Alg-*g*-P(AM-*co*-IA-*g*-AA) exhibit that the band lied at 1425 cm^{-1}, which is in between 1431 and 1422 cm^{-1}.

There is another obvious difference between the IR spectra of NaAlg, and Alg-*g*-PAM, Alg-*g*-P(AM-*co*-IA), Alg-*g*-P(AM-*co*-IA-*g*-AA) and crosslinked-Alg-*g*-P(AM-*co*-IA-*g*-AA). Compared with the peak for the asymmetric stretching of the COO^- group attached to the sodium ion in NaAlg which is observed at 1627 cm^{-1}, the peak at 1627 cm^{-1} has been shifted to the left to the range of 1654 and 1663 cm^{-1} for Alg-*g*-PAM, Alg-*g*-P(AM-*co*-IA), Alg-*g*-P(AM-*co*-IA-*g*-AA) and crosslinked-Alg-*g*-P(AM-*co*-IA-*g*-AA).

This shift in wavenumber served as a proof to the formation of SAPs, most probably due to the existence of strong hydrogen-bonding interaction between the –COOH and –C=O groups (Lin *et al*., 2009, as cited by Wang and Wang, 2010), which is even more accentuated by the existence of C–N group found in $–C(=O)NH_2$ of PAM. This hydrogen bonding interaction is most prominent in the crosslinked-Alg-*g*-P(AM-*co*-IA-*g*-AA), owing to the presence of two additional –C(=O)NH– groups contributed by the crosslinking agent. This explained why the IR spectrum for this particular SAP witnesses the largest shift in the asymmetric stretching of the COO^- group, which is 1663 cm^{-1}.

For IR spectra of Alg-*g*-PAM, Alg-*g*-P(AM-*co*-IA), Alg-*g*-P(AM-*co*-IA-*g*-AA) and crosslinked-Alg-*g*-P(AM-*co*-IA-*g*-AA), both the peaks for –NH stretching vibration (commonly found at approximately 3330 and 3190 cm^{-1}) in NH-group of N-MBA or $–CONH_2$ groups of PAM are thought to be shielded by the broad –OH stretching frequency which happened to overlap the peaks, which occurred in the range of 3438 and 3423 cm^{-1}.

4.6 Thermogravimetric Analysis (TGA)

While running TGA, the key point to note is the contact surface between the sample and the alumina crucible. The contact surface of the sample must be flat and touching the crucible's inner surface, and then only is the crucible inserted into the thermogravimetric analyser's furnace. This is to ensure that the thermal contact is optimised, hence achieving complete thermal decomposition of the sample.

In this study, the sample was heated from 25 to 900 ^{o}C at a rate of 20 ^{o}C/min, with nitrogen gas purging at a rate of 20 mL/min. The heating rate is a factor which determines the thermal decomposition temperature, T_d. Increasing heating rates would increase the T_d since as the degradation time is reduced with higher heating rates, the sample would have less exposure to heat (Ahmad *et al.*, 2007). A reasonable heating rate of 20 ^{o}C/min was chosen in this study.

4.6.1 TGA Thermogram of Sodium Alginate

The samples used in TGA were similar with those used in Section 4.5.1. Studies showed the onset of weight loss in NaAlg and samples containing the polysaccharide occurred near 60 °C which is due to the loss of water present in the sample. In other words, in an initial stage of the thermogram, the weight loss in the temperature range of ambient temperature to about 150 ^{o}C is a result of the dehydration process of the water contained in

the SAP sample. Therefore the temperature shown in the TGA curves below begins from 140 instead of 25 ^{o}C.

The thermal stability of NaAlg was assessed by TGA. The TGA curve of NaAlg (Figure 4.22) shows two-steps of degradation. The first degradation of sample occurred at an inflection point of 244.28 ^{o}C, followed by gradual decomposition with an inflection point at 445.89 °C.

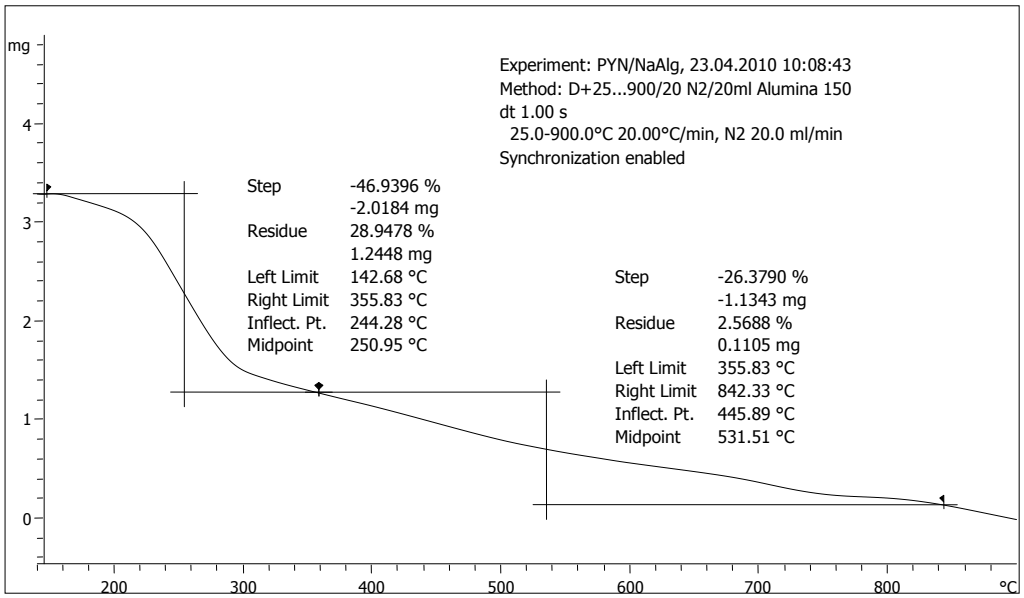

Figure 4.22 TGA thermogram of NaAlg

The first decomposition shows the decomposition of NaAlg in nitrogen atmosphere by the dehydration of the saccharide rings, breaking up of C-H bonds and breaking of the C–O–C glycosidic bonds in the main chain of the polysaccharides. In the second degradation process, Na_2CO_3 and other carbonaceous materials were formed (Soares *et al.*, 2004). The decomposition product of the second degradation is characterised as the residue of Na_2CO_3,

which is a carbonaceous material. 28.9 % by weight of the sample remained at 355.83 °C and 2.6 % was left in the sample at 842.33 °C.

4.6.2 TGA Thermograms of Various Alginate Graft Copolymers

For discussion purpose, only the thermograms of Alg-*g*-PAM, Alg-*g*-PIA, Alg-*g*-PAA, and SAP sample crosslinked-Alg-*g*-P(AM-*co*-IA-*g*-AA) are shown, from Figures 4.23 to 4.26.

In general, the thermograms obtained for the samples Alg-*g*-PAM, Alg-*g*-PIA, Alg-*g*-PAA, Alg-*g*-P(AM-*co*-IA), and Alg-*g*-P(AM-*co*-IA-*g*-AA) had similar trend with that of crosslinked-Alg-*g*-(AM-*co*-IA-*g*-AA), except that the thermal degradation points occurred at different temperatures. To evaluate the degradation characteristics, the thermal decomposition points (T_d) based on the inflection points of all the above-mentioned samples were compared with those of NaAlg in Table 4.2.

Generally speaking, the thermograms of Alg-*g*-PAM and Alg-*g*-PAA are divided into two steps. The first degradation step which happened at the inflection point of 258 – 259 ^{o}C corresponded to the decomposition of the functional groups of PAM and PAA, combined with the thermal degradation of NaAlg (Lanthong *et al*., 2006; Yang *et al*., 2009), which is associated with a complex process, including dehydration of the saccharide rings and breaking of the C–O–C glycosidic bonds in the main chain of the polysaccharide (Chen and Tan, 2006). The second step which happened at around the inflection point

of 415 and 437 ^{o}C for the respective graft copolymers was believed to be associated with the breakage of the C–C bonds in the PAM or PAA chain (Chen and Tan, 2006).

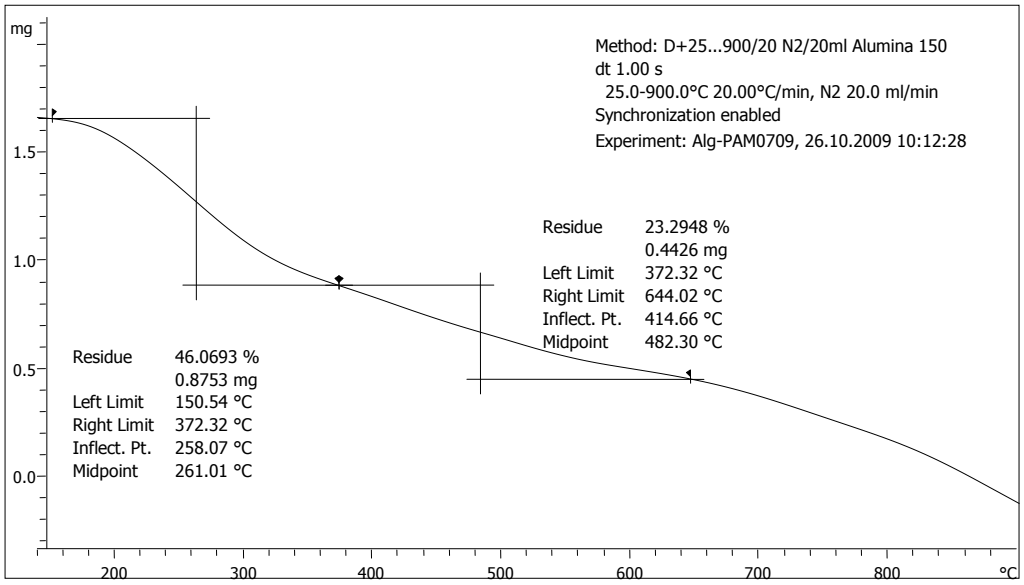

Figure 4.23 TGA thermogram of Alg-*g*-PAM

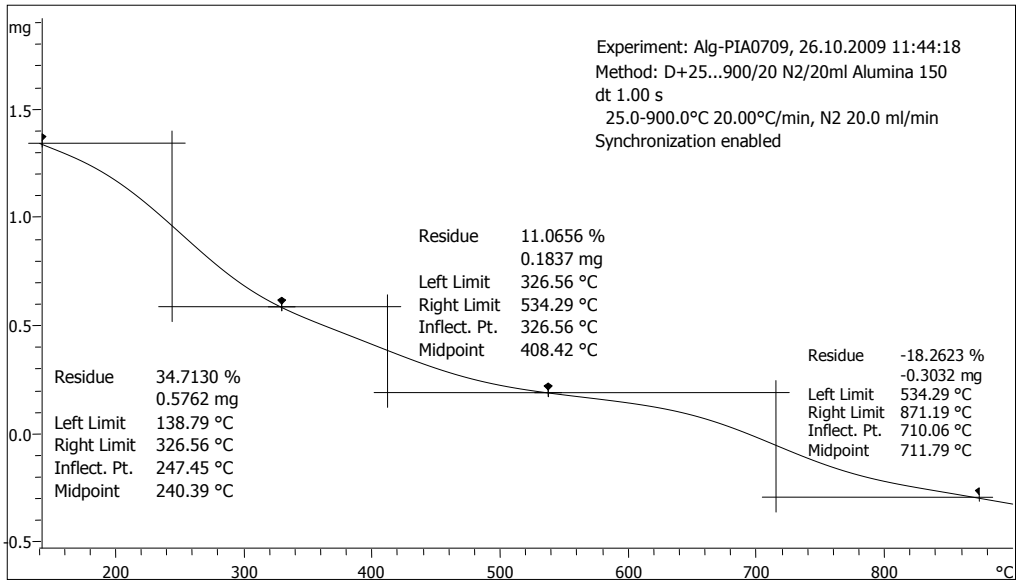

Figure 4.24 TGA thermogram of Alg-*g*-PIA

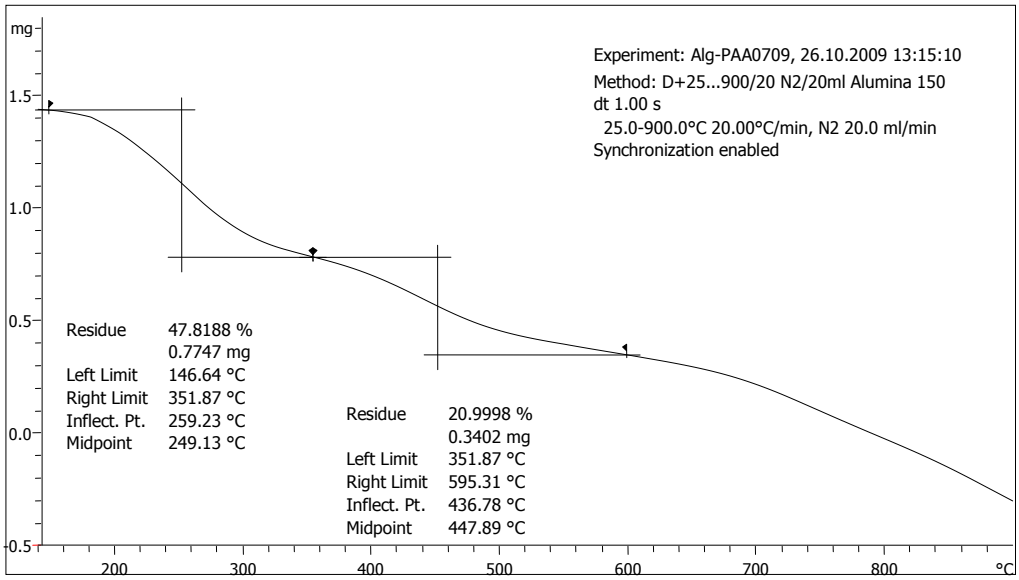

Figure 4.25 TGA thermogram of Alg-*g*-PAA

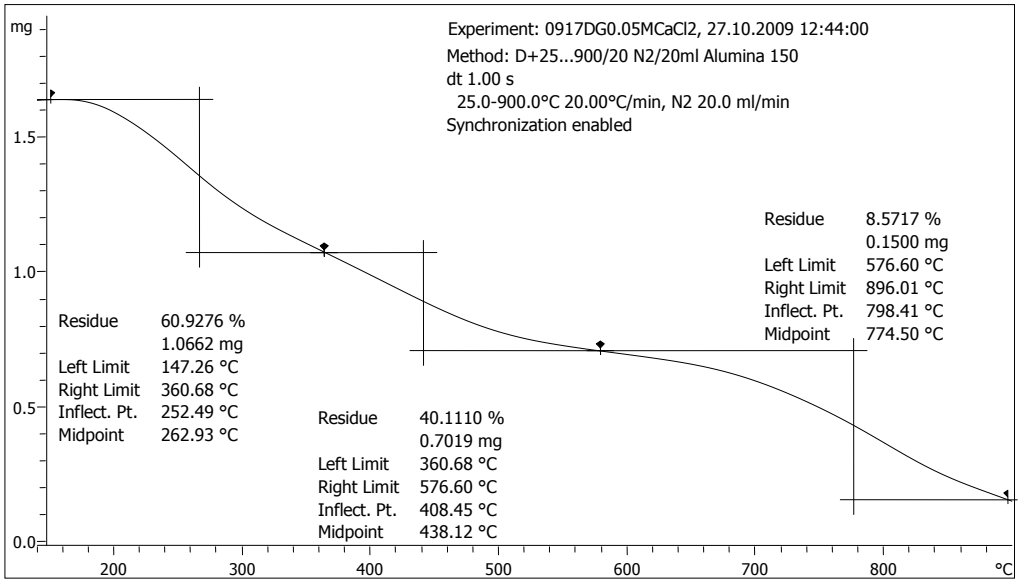

Figure 4.26 TGA thermogram of crosslinked-Alg-*g*-(AM-*co*-IA-*g*-AA)

The thermograms of Alg-*g*-PIA, Alg-*g*-P(AM-*co*-IA), Alg-*g*-P(AM-*co*-IA-*g*-AA) and crosslinked-Alg-*g*-P(AM-*co*-IA-*g*-AA) show three degradation steps. Apart from the thermal degradation of NaAlg, the first degradation step (inflection points in between 247 and 260 ^{o}C) is also deduced to be the result

of the decomposition of the functional groups of PAM (if any), PAA (if any) or PIA (Lanthong *et al*., 2006).

Table 4.2 Thermal decomposition temperatures (based on inflection points), T_d, of NaAlg and other samples

Sample	Inflection Point 1	Inflection Point 2	Inflection Point 3
NaAlg	244.28	445.89	
Alg-*g*-PAM	258.07	414.66	
Alg-*g*-PIA	247.45	326.56	710.06
Alg-*g*-PAA	259.23	436.78	
Alg-*g*-P(AM-*co*-IA)	260.82	401.04	838.08
Alg-*g*-P(AM-*co*-IA-*g*-AA)	256.94	402.07	774.37
Crosslinked-Alg-*g*-P(AM-*co*-IA-*g*-AA)	252.49	408.45	798.41

The second degradation step for Alg-*g*-PIA, Alg-*g*-P(AM-*co*-IA), Alg-*g*-P(AM-*co*-IA-*g*-AA) and crosslinked-Alg-*g*-P(AM-*co*-IA-*g*-AA) occurred at an inflection point lower than those of NaAlg, Alg-*g*-PAM and Alg-*g*-PAA. They are 327 ^{o}C for Alg-*g*-PIA and 401 – 408 ^{o}C for the other three samples (Table 4.2). This degradation step is believed to be caused by the degradation of the polymer side chain and matrices through the decomposition of the C–C chains of PIA, combined with the degradation of C–C bonds in PAM and/or PAA portion(s) (if any). Table 4.2 shows that this degradation step occurred at a lower temperature for Alg-*g*-PIA. When the graft copolymer samples were also grafted with PAM or both PAM and PAA in addition to PIA, this degradation step occurred at a higher temperature.

The third degradation step for Alg-*g*-PIA, Alg-*g*-P(AM-*co*-IA), Alg-*g*-P(AM-*co*-IA-*g*-AA) and crosslinked-Alg-*g*-P(AM-*co*-IA-*g*-AA) was found at inflection points of more than 700 ^{o}C. Since this degradation step is not found in the thermograms of the samples without PIA, this step is most probably the contribution from the further degradation of PIA. The occurrence of this degradation step is consistent with the presence of PIA in these samples.

The presence of crosslinking agent (N-MBA) in crosslinked-Alg-*g*-P(AM-*co*-IA-*g*-AA) show slight increase in second and third inflection points compared to the sample without crosslinking agent. The thermal stability of the crosslinked copolymer was slightly higher due to the degradation of the additional C–C bonds contributed by the crosslinker.

There is an obvious discrepancy between the thermograms of NaAlg and crosslinked-Alg-*g*-P(AM-*co*-IA-*g*-AA). From Figure 4.22, 28.9 wt.% of the NaAlg sample remained at 355.83 °C; whereas only 2.6 wt.% of it was left at 842.33 °C. However, Figure 4.26 shows that at 360.68 °C, the residue of crosslinked-Alg-*g*-P(AM-*co*-IA-*g*-AA) sample was as high as 60.9 wt.%, with 8.6 wt.% of it left at 896.01 °C. A conclusion can thus be drawn – the incorporation of PAM, PAA and PIA into the SAP had obviously increased the thermal stability of the SAP. From merely less than 30 wt.% left-over in NaAlg sample at around 360 ^{o}C, the residue had increased to more than 60 wt.% for the SAP sample at the same temperature. The thermal stability of the NaAlg-based SAP was thus enhanced by the synthetic portion, hence decreasing the thermal degradability of the SAP.

4.7 Total Solids Content (TSC) and Percentage of Monomer Conversion

The mathematical formula to derive the total solids content (TSC) and percentage monomer conversion are shown in Appendix D. The calculations for the theoretical and mean actual TSC are illustrated in Appendices E and F respectively, while the calculations on the percentage monomer conversion and percentage error of TSC are tabulated in Appendix G. The theoretical TSC, mean actual TSC and percentage monomer conversion are summarised in Table 4.3.

Table 4.3 Theoretical total solids content, mean actual total solids content and percentage monomer conversion

Description	Value
Theoretical TSC (%)	7.39
Mean actual TSC (%)	7.20
Percentage monomer conversion (%)	96.7

The theoretical TSC was found to be 7.39 % while the mean actual TSC was determined as 7.20 %. The percentage error obtained for TSC was therefore 2.57 %. The low deviation between the values of theoretical and mean actual TSC gave rise to a low percentage error in TSC. The results indicated that the total solids collected at the end of the polymerisation were close to the expected total solids. Given that "total solids" referred not only to the SAP (crosslinked-Alg-*g*-P(AM-*co*-IA-*g*-AA)), but also the initiators (tBHP and SFX) and neutralising agent (SBC), there could be a likelihood that a large

portion of the initiators and neutralising agent were lost during the reaction, hence causing the mean actual TSC to be slightly lower than expected.

The percentage monomer conversion was as high as 96.7 %. The high percentage of monomer conversion indicated that the conversion from NaAlg, AM, IA, AA and N-MBA to the SAP, crosslinked-Alg-*g*-P(AM-*co*-IA-*g*-AA), was nearly complete at the end of the polymerisation process. This showed that the time allowed for polymerisation of the SAP was sufficient and adequate, even though a slightly longer time of polymerisation would have resulted in a 100 % monomer conversion.

4.8 Morphology Observation by Scanning Electron Microscopy (SEM)

The SAP sample used in SEM was crosslinked-Alg-*g*-P(AM-*co*-IA-*g*-AA) which was synthesised via the method described in Section 3.3. The morphology of the SAP was examined using the scanning electron microscope of JEOL at an accelerating voltage of 2.0 kV. Figure 4.27 shows the SEM micrographs of the SAP at different magnifications.

The morphology of crosslinked-Alg-*g*-P(AM-*co*-IA-*g*-AA) was unique in the sense that the sample is uneven and slightly porous. The folds found on the SAP signified that the SAP has a high surface area; hence higher rate of water transfer is expected to occur for the SAP.

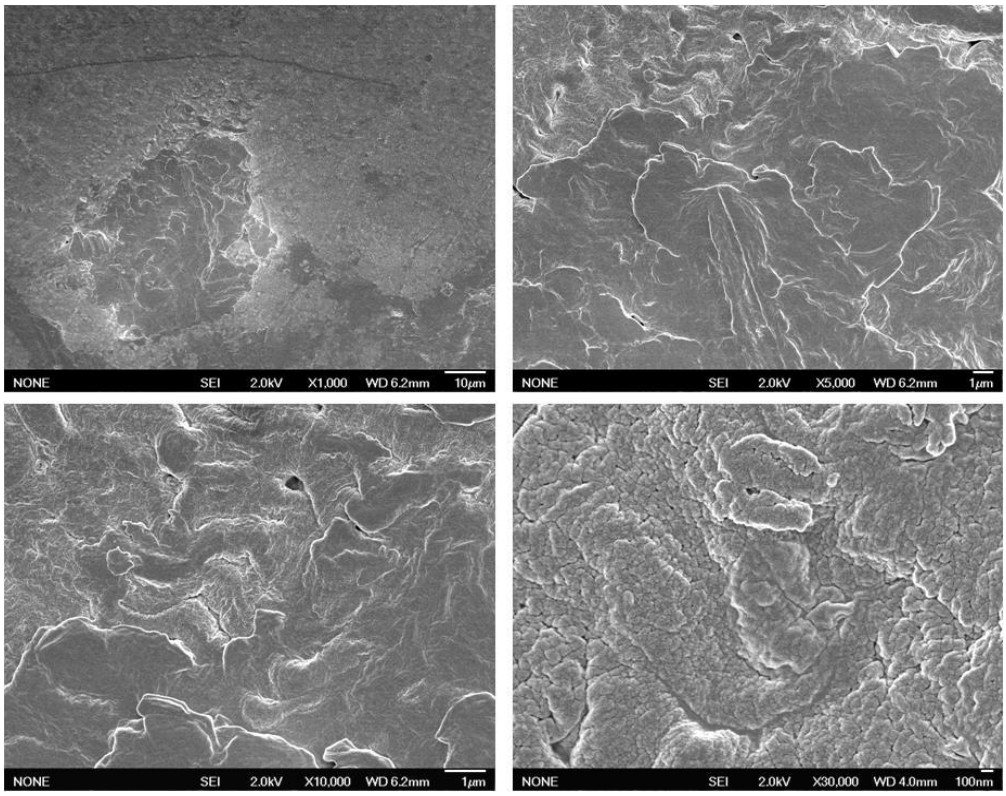

Figure 4.27 SEM micrographs of crosslinked-Alg-*g*-P(AM-*co*-IA-*g*-AA) at different magnifications

4.9 Weight Loss Test Using Soil Supernatant

Figure 4.28 shows the percentage weight loss of the SAP sample, crosslinked-Alg-*g*-P(AM-*co*-IA-*g*-AA), in the soil solution of organic vegetable farm soil which had been added with nutrients (sterile minimum mineral). During the first 20 days of incubation, the SAP sample showed a rapid decline in weight, in which the weight loss was as high as 72.2 % by day 20.

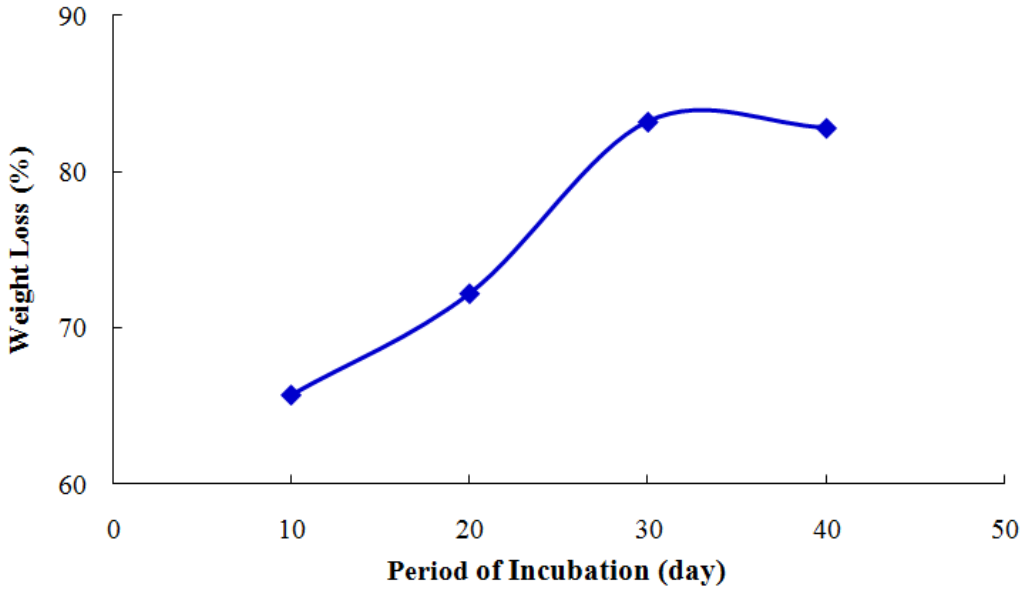

Figure 4.28 Percentage weight loss of SAP against period of incubation in soil supernatant

However, from day 20 onwards, the weight loss persisted with a slightly slower rate, with the weight loss recorded as 82.8 % by day 40. This could be due to the depletion of nutrients that support the microbial growth, thereby slowing down the rate of polymer degradation.

In conclusion, the SAP evaluated is biodegradable, although the incorporation of PAM, PAA and PIA into the SAP had increased the thermal stability of the SAP. It has shown excellent biodegradability in indigenous microorganism soil sample from an organic vegetable farm within a short period of time, i.e. up to 83 % of weight loss in 40 days.

CHAPTER 5.0

CONCLUSIONS

Owing to the rapid growth in both population and economy, many countries are faced with environmental problems such as that related to waste. Two of the items that are contributing further to this problem would be the baby diapers and sanitary napkins. One of the serious problems that is being faced by the diapers and napkins industry is the biodegradability of the products. The development of biodegradable baby diapers and napkins would thus be a step forward in the right direction for the aforementioned industry. The biodegradable SAP synthesised in this study might therefore be a good constituent of the baby diapers and napkins in the market.

Sodium alginate-derived products are currently used as additives to alter and stabilise the texture of food, a scaffold for the encapsulation and immunoprotection of transplanted cells, and in the treatment of exuding wounds. Currently, utilisation of the renewable sodium alginate as the alternatives for synthetic, petroleum-based polymer is an active area of research in the polymer industry.

Use of polysaccharides such as sodium alginate in polymers, specifically SAPs, not only reduces our dependence on petrochemical-derived

monomers, but the polysaccharide portion will also biodegrade, causing the finished polymer article to lose its integrity and be reduced to small particles.

In this study, Alg-*g*-P(AM-*co*-IA), Alg-*g*-P(AM-*co*-IA-*co*-AA) (with or without crosslinking) and Alg-*g*-P(AM-*co*-IA-*g*-AA) (with or without crosslinking) were synthesised via graft copolymerisation of AM, IA and AA (where applicable) onto sodium alginate. The first and second SAPs were produced via small-scale syntheses, while crosslinked-Alg-*g*-P(AM-*co*-IA-*g*-AA was produced in both small-scale and bigger-scale syntheses.

With similar recipe and precipitated using $CaCl_2$ of similar concentration, the wet SAP samples synthesised from the small-scale synthesis looked weaker and took after a non-uniform round shape, whereas the wet precipitated samples from the bigger-scale synthesis looked stronger on the exterior and had a rounded shape.

In the small-scale synthesis, the swelling capacity of Alg-*g*-P(AM-*co*-IA-*co*-AA) in ethanol increased as the molar ratio of AM:AA increased from 1:8 to 9:0. The SAP absorbed ethanol to its fullest when there was no AA added into the synthesis reaction. In view of this fact, only AM and IA were added as the first charge in the succeeding syntheses.

Between KPS/SFX and tBHP/SFX, the swelling capacity of Alg-*g*-P(AM-*co*-IA) was higher when initiated by the latter initiating agents. The overall swelling capacity of the SAP synthesised via the initiation of

tBHP/SFX pair recorded the highest swelling capacity of 29.6 g g^{-1}, when 3.1 × 10^{-4} moles of tBHP and SFX each was used. KPS was therefore dropped as the oxidising agent whilst tBHP was implemented further in this study.

When 3.0 × 10^{-3} to 8.8 × 10^{-2} moles of AA was introduced into the SAP synthesis as a second charge, the swelling capacity of the Alg-*g*-P(AM-*co*-IA-*g*-AA) in ethanol decreased from 42.3 to 2.63 g g^{-1}, with the SAP incorporated with 3.0 × 10^{-3} moles of AA recording the highest swelling capacity. Accessibility of more solvent into the SAP matrix was prevented since higher amount of AA monomer would lead to self-crosslinking.

0.01 M of $CaCl_2$ was adequate to bring about maximum swelling capacity of Alg-*g*-P(AM-*co*-IA). This was because when the concentration of $CaCl_2$ used to precipitate the SAP increased from 0.01 to 0.50 M, the swelling capacity of the water-swollen SAP decreased from 155 to 7.50 g g^{-1}.

Similar to the trend of Alg-*g*-P(AM-*co*-IA), the swelling capacity of Alg-*g*-P(AM-*co*-IA-*g*-AA) decreased from 270 to 5 g g^{-1} when the amount of $CaCl_2$ increased from 0.01 to 0.50 M. An increase in the amount of calcium ions would form alginate gel matrix with higher density in the outer sphere of the bead, therefore restricting the entry of water molecules, thus decreasing the swelling capacity of the SAP.

The swelling capacity of Alg-*g*-P(AM-*co*-IA) improved drastically to 654 g g^{-1} when 1.0 × 10^{-4} moles of N-MBA was added to the SAP, thus

forming crosslinked-Alg-*g*-P(AM-*co*-IA). However, the swelling capacity of the SAP decreased gradually from 654 to 55.7 g g^{-1} when the amount of the crosslinking agent increased from 1.0×10^{-4} moles to 6.24×10^{-3} moles. An increase in the concentration of crosslinker results in an increase in crosslinking density, thus leading to a decreased swelling capacity.

When the number of moles of N-MBA increased from 0 to 2.5×10^{-5} moles of N-MBA, the swelling capacity of crosslinked-Alg-*g*-P(AM-*co*-IA-*g*-AA) shot up from 270 to 754 g g^{-1}, upon precipitation by 0.01 M of $CaCl_2$. However, the swelling capacity of the SAP declined from 754 to 36.8 g g^{-1} when the number of moles of N-MBA increased from 2.5×10^{-5} to 1.0×10^{-2} moles.

In general, as the volume ratio of 0.05 M $CaCl_2$:SAP solution increased from 1:1 to 5:1, the swelling capacity of crosslinked-Alg-*g*-P(AM-*co*-IA-*g*-AA) decreased. The highest swelling capacity was recorded as 110 g g^{-1}, in which the SAP was precipitated with 0.05 M $CaCl_2$:SAP solution being 2:1. As a result, double the amount of 0.05 M $CaCl_2$ to SAP solution was the most suitable volume used for precipitating the SAP solution.

When the duration of swelling of crosslinked-Alg-*g*-P(AM-*co*-IA-*g*-AA) was varied from 4 to 72 hours, the highest swelling capacity was recorded as 46 g g^{-1}, in which the SAP was swelled in water for 8 hours. This outcome showed that the SAP could absorb water at a reasonable rate and 8 hours were sufficient for optimum swelling of the SAP.

Meanwhile, in the bigger-scale synthesis, when the concentration of $CaCl_2$ increased from 0.0125 to 0.20 M, the swelling capacity of crosslinked-Alg-*g*-P(AM-*co*-IA-*g*-AA) decreased gradually from 363 to 8 g g^{-1}. This trend was foreseen, since the swelling capacity of the SAP was supposed to decrease when water molecules were restricted from entering the polymer matrix, as the gel density on the outer sphere of the polymer beads increased with increasing calcium ions.

To observe the effect of dilution on the swelling capacity of crosslinked-Alg-*g*-P(AM-*co*-IA-*g*-AA), the synthesised SAP solution was diluted up to five times using water, followed by precipitation of each of the diluted gel with 0.05 M of $CaCl_2$ and then swelled the dry samples for 8 hours in distilled water. When the volume ratio of SAP solution:water was adjusted from 1:0 to 1:4, the swelling capacity of the SAP reduced from 140 g g^{-1} to as low as 7 g g^{-1}.

The swelling capacity of crosslinked-Alg-*g*-P(AM-*co*-IA-*g*-AA) raised from 14 to 205 g g^{-1} when the particle size of the SAP beads increased from 0.074 – 0.149 to 4.000 – 4.760 mm. A higher volume of water could be retained by the bead particles when the surface area of the sample particles decreased with increasing particle size, thus increasing the swelling capacity of the SAP.

In the AUL test, crosslinked-Alg-*g*-P(AM-*co*-IA-*g*-AA) increased in AUL when the time allowed for swelling under load increased. The AUL

obtained by the SAP without any load (the applied pressure was 0 g/cm^2) was the highest compared to the SAPs which were applied with pressures of 20, 30 or 40 g/cm^2, in which the AUL raised from 10 to 23 g g^{-1} when the time allowed for swelling increased from 1 to 8 hours. In other words, the AUL throughout all the different durations of swelling decreased as the applied pressure increased from 0 to 40 g/cm^2.

Among the peaks found in the IR spectrum of NaAlg was the broad absorbing peak at 3432 cm^{-1} which was characterised as the H-bonded O–H stretching frequency. The band at approximately 2900 cm^{-1} was assigned to C–H stretching. The respective weak and medium peaks at 1627 and 1422 cm^{-1} were characterised as the asymmetric stretching vibration of the carboxylate COO^-, and C–OH deformation vibration with contribution of COO^- symmetric stretching vibration. The weak peaks at 1300, 1090 and 947 cm^{-1} were all attributed to the stretching vibrations of C–O from glycosidic bonds, with 947 cm^{-1} contributed by the stretching vibration of C–O–C as well.

Generally, all the IR spectra of the synthesised SAPs looked similar in terms of the presence of peaks. The spectra exhibited a strong, broad absorbing peak in between 3423 and 3438 cm^{-1} which was attributed to the H-bonded O–H stretching vibrations of each of the SAP and a weak peak in between 2935 and 2924 cm^{-1} were contributed by the C–H stretching vibrations of the respective compounds.

Most likely due to the presence of C–N group in $–CONH_2$, the shift to the left to 1431 cm^{-1} for the band of COO^- symmetric stretching vibration for Alg-*g*-PAM served as a proof of AM grafted onto NaAlg. Meanwhile, the shift in the peak of asymmetric stretching of the COO^- to the range of 1654 and 1663 cm^{-1} for Alg-*g*-PAM, Alg-*g*-P(AM-*co*-IA), Alg-*g*-P(AM-*co*-IA-*g*-AA) and crosslinked-Alg-*g*-P(AM-*co*-IA-*g*-AA), probably due to the existence of strong hydrogen-bonding interaction between the –COOH and –C=O groups, ascertained the formation of the SAPs.

In the thermogram of NaAlg, the decomposition of NaAlg in nitrogen atmosphere occurred in the first degradation step, followed by the formation of Na_2CO_3 and other carbonaceous materials in the second degradation step. The TGA thermograms of Alg-*g*-PIA, Alg-*g*-P(AM-*co*-IA), Alg-*g*-P(AM-*co*-IA-*g*-AA) and crosslinked-Alg-*g*-P(AM-*co*-IA-*g*-AA) showed three degradation steps. The first degradation step (inflection points in between 247 and 260 ^oC) was speculated to be the thermal degradation of NaAlg and decomposition of the functional groups of the PAM(if any), PAA(if any) and PIA.

Meanwhile, the second degradation step occurred at an inflection point which was lower than those of Alg-*g*-PAM (415 ^oC) and Alg-*g*-PAA (437 ^oC), which were 327 ^oC for Alg-*g*-PIA and 401 – 408 ^oC for the other three SAPs. Degradation of the polymer side chain and matrices of PIA, combined with the degradation of C–C bonds in PAM and/or PAA portion(s) (if any) were believed to have caused this degradation step. The third degradation step was found at inflection points of more than 700 ^oC when IA was introduced in the

polymerisation. This was speculated to be contributed by further decomposition of PIA.

In the test for TSC and percentage monomer conversion using SAP solution of crosslinked-Alg-*g*-P(AM-*co*-IA-*g*-AA), the mean actual TSC was determined as 7.20 % while the theoretical TSC was found to be 7.39 %. Hence, the percentage error obtained for TSC was 2.57 %. The percentage monomer conversion obtained was as high as 96.7 %, which showed that the monomer conversion was near to completion in the polymerisation process.

The SEM micrographs of crosslinked-Alg-*g*-P(AM-*co*-IA-*g*-AA) showed that the sample was uneven and slightly porous, suggesting that the SAP has a high surface area, and thus higher rate of water transfer is anticipated for the SAP.

In the microbial degradation test done via weight loss test using soil supernatant, the speedy loss in weight of crosslinked-Alg-*g*-P(AM-*co*-IA-*g*-AA) was significant, in which the weight loss of the SAP was as high as 72.2 % by day 20. By day 40, the SAP experienced a total weight loss of 83 %. These figures showed that the SAP synthesised in the current study exhibited excellent biodegradability.

Further study could be carried out by determining the grafting efficiency of AM/IA/AA onto the sodium alginate backbone. The composition of the elements found in the SAP could be verified via Elemental Analysis.

Other than these, the effect of polymerisation time on the swelling capacity of the SAP could be examined by varying the length of time of polymerisation.

Differential Scanning Calorimetry (DSC) and TGA analyses could be carried out to observe the effect of molar ratio of AM:IA:AA, and concentrations of initiator, crosslinking agent and precipitating agent on the thermal behaviour, i.e. glass transition temperature (T_g) and T_d values, of the SAP synthesised. Last but not least, the biodegradability of the SAP could be further established through different methods, for example, the Biochemical Oxygen Demand (BOD) test.

REFERENCES

Ahmad, Z., Al-Awadi, N. A. and Al-Sagheer, F. (2007). Morphology, thermal stability and visco-elastic properties of polystyrene-poly(vinyl chloride) blends. *Polymer Degradation and Stability*, 92, 1025 – 1033.

Alger, M. (1997). *Polymer science dictionary* (pp. 526). 2nd Ed. London: Chapman & Hall, London.

Asaletha, R., Kumaran, M. G. and Thomas, S. (1998). Thermal behaviour of natural rubber/polystyrene blends: thermogravimetric and differential scanning calorimetric analysis. *Polymer Degradation and Stability*, 61, 431 – 439.

Baker, K. L., Langenhede, S., Nicol, G. W., Ricketts, D., Killham, K., Campbell, C. D. and James, I. P. (2009). Environmental and spatial characterisation of bacterial community composition in soil to inform sampling strategies. *Soil Biology & Biochemistry*, 41, 2292–2298.

Biswal, D. R. and Singh, R. P. (2004). Characterisation of carboxymethyl cellulose and polyacrylamide graft copolymer. *Carbohydrate Polymers*, 57, 379–387.

Braun, D., Cherdron, H., Rehahn, M., Ritter, H. and Voit, B. (2005). *Polymer synthesis: theory and practice* (pp. 5; 123; 149–150; 164; 166; 175–176; 257–259). 4th Ed. Germany: Springer-Verlag.

Buchholz, F. L. and Graham A. T. (Eds.). (1998). *Modern superabsorbent polymer technology* (pp. 7–8; 20–21; 30–31; 55–58; 147; 158–159; 187). New York: Wiley-VCH.

Chandia, N. P., Matsuhiro, B., Ortiz, J. S. and Mansilla, A. (2005). Carbohydrates from the sequential extraction of Lessonia vadosa (phaeophyta). *Journal of the Chilean Chemical Society*, 50, 501–504.

Chang, C. Y., Duan, B., Cai, J. and Zhang, L. N. (2010). Superabsorbent hydrogels based on cellulose for smart swelling and controllable delivery. *European Polymer Journal*, 46, 92–100.

Chen, J., and Zhao, Y. (2000). Relationship between water absorbency and reaction conditions in aqueous solution polymerization of polyacrylate superabsorbents. *Journal of Applied Polymer Science*, 75(6), 808–814.

Chen, Y. and Tan, H. (2006). Crosslinked carboxymethylchitosan-*g*-poly(acrylic acid) copolymer as a novel superabsorbent polymer. *Carbohydrate Research*, 341, 887–896.

Cosgrove, L., McGeechan, P. L., Robson, G. D. and Handley, P. S. (2007). Fungal communities associated with degradation of polyester polyurethane in soil. *Applied and Enviromental Microbiology*, 73, 5817–5824.

Crini, G. (2005). Recent developments in polysaccharide-based materials used as adsorbents in wastewater treatment. *Progress in Polymer Science*, 30, 38–70.

Cui, S. W. and Wang, Q. (2006). Functional properties of carbohydrates: polysaccharide gums. In H. H. Yiu (Ed.), *Handbook of food science, technology, and engineering* (pp. 4–11). UK: CRC Press.

Da Silva, D. A., de Paula, R. C. M. and Feitosa, J. P. A. (2007). Graft copolymerisation of acrylamide onto cashew gum. *European Polymer Journal*, 43, 2620–2629.

Danjaji, I. D., Nawang, R., Ishiaku, U. S., Ismail, H. and Mohd Ishak, Z. A. M. (2002). Degradation studies and moisture uptake of sago-starch-filled linear low-density polyethylene composites. *Polymer Testing*, 21, 75–81.

Davidovich-Pinhas, M. and Bianco-Peled, H. (2010). A quantitative analysis of alginate swelling. *Carbohydrate Polymers*, 79, 1020–1027.

Davis, T. A., Volesky, B. and Mucci, A. (2003). A review of the biochemistry of heavy metal biosorption by brown algae. *Water Research*, 37, 4311–4330.

Draget, K. I. (2009). Alginates. In G. O. Phillips and P. A. Williams (Eds.), *Handbook of hydrocolloids* (pp. 380). 2nd Ed. UK: CRC Woodhead Publishing Limited.

Draget, K. I., Skjik-Braek, G., Christensen, B. E., Gåserød, O. and Smidsrød, O. (1996). Swelling and partial solubilization of alginic acid gel beads in acidic buffer. *Carbohydrate Polymers*, 29, 209–215.

Draget, K. I., Smidsrød, O. and Skjåk-Bræk, G. (2005). *Alginates from algae*. In Steinbuchel, A. and Rhee, S. K. (Eds), *Polysaccharides and polyamides in the food industry*: *properties, production, and patents* (pp.1 – 30). Weinheim: Wiley-VCH.

Ebewele, R. O. (2000). *Polymer science and technology* (pp. 8; 182; 363; 431–432). Boca Raton: CRC Press.

Elliott, J. E., Macdonald, M., Nie, J., and Bowman, C. N. (2004). Structure and swelling of poly(acrylic acid) hydrogels: effect of pH, ionic strength, and dilution on the crosslinked polymer structure. *Polymer*, 45(5), 1503–1510.

FMC Biopolymer (2010), "Alginates/PGA/Chemistry," FMC Corporation. [Online]. Available: http://www.fmcbiopolymer.com/Food/Ingredients/AlginatesPGA/Chemistry.aspx. Accessed on 7th July 2011.

Franco, C. R. D., Cyras, V. P., Busalmen, J. P. and Ruseckaite, R. A. (2004). Degradation of polycaprolactone/starch blends and composites with sisal fibre. *Polymer Degradation and Stability*, 86, 95–103.

Gao, C. M., Liu, M. Z., Chen, J. and Zhang, X. (2009). Preparation and controlled degradation of oxidized sodium alginate hydrogel. *Polymer Degradation and Stability*, 94, 1405–1410.

Glicksman, M. (1953). Natural polysaccharide gums in the food industry. In E. M. Mrak and G. F. Stewart (Eds.), *Advances in food research* (pp. 138). US: Academic Press.

Han, T. L., Kumar, R. N., Rozman, H. D. and Noor, M. A. M. (2003). GMA grafted sago starch as a reactive component in ultra violet radiation curable coatings. *Carbohydrate Polymers*, 54, 509–516.

Holme, H. K., Lindmo, K., Kristiansen, A. and Smidsrød, O. (2003). Thermal depolymerization of alginate in the solid state. *Carbohydrate Polymers*, 54, 431–438.

Hua, S. B. and Wang, A. Q. (2009). Synthesis, characterization and swelling behaviors of sodium alginate-*g*-poly(acrylic acid)/sodium humate superabsorbent. *Carbohydrate Polymers*, 75, 79–84.

Huang, Y. H., Yu, H. Q. and Xiao, C. B. (2007). pH-sensitive cationic guar gum/poly (acrylic acid) polyelectrolyte hydrogels: Swelling and in vitro drug release. *Carbohydrate Polymers*, 69, 774–783.

Hunik, J. H. (2001). Immobilization at large scale with the resonance nozzle technique. In Wijffels, R. H. (Ed.), *Immobilized cells* (pp. 152). Germany: Springer-Verlag.

Işıklan, N., Kurşun, F. and İnal, M. (2010). Graft copolymerization of itaconic acid onto sodium alginate using benzoyl peroxide. *Carbohydrate Polymers*, 79, 665–672.

Kabiri, K., Omidian, H., Hashemi, S. A. and Zohuriaan-Mehr, M. J. (2003). Synthesis of fast-swelling superabsorbent hydrogels: effect of crosslinker type and concentration on porosity and absorption rate. *European Polymer Journal*, 39, 1341–1348.

Karadag, E. and Saraydin, D. (2002). Swelling of superabsorbent acrylamide/sodium acrylate hydrogels prepared using multifunctional crosslinkers. *Turkish Journal of Chemistry*, 26, 863–875.

Kong, H. J., Lee, K. Y. and Mooney, D. J. (2003). Nondestructively probing the cross-linking density of polymeric hydrogels. *Macromolecules*, 36, 7887–7890.

Krusic, K. M., Dzunuzovic, E., Trifunovic, S., and Filipovic, J. (2004). Polyacrylamide and poly(itaconic acid) complexes. *European Polymer Journal*, 40, 793–798.

Lanthong, P., Nuisin, R. and Kiatkamjornwong, S. (2006). Graft copolymerization, characterization, and degradation of cassava starch-*g*-acrylamide/itaconic acid superabsorbents. *Carbohydrate Polymers*, 66, 229–245.

Larsen, B., Smidsrød, O., Painter, T. J. and Haug, A. (1970). Calculation of the nearest-neighbour frequencies in fragments of alginate from the yields of free monomers after partial hydrolysis. *Acta Chemica Scandinavica*, 24, 726–728.

Leal, D., Matsuhiro, B., Rossi, M. and Caruso, F. (2008). FT-IR spectra of alginic acid block fractions in three species of brown seaweeds. *Carbohydrate Research*, 343, 308–316.

Lee, J. S., Kumar, R. N., Rozman, H. D. and Azemi, B. M. N. (2005a). Pasting, swelling and solubility properties of UV initiated starch-graft-poly(AA). *Food Chemistry*, 91, 203–211.

Lee, Y. H., Kim, J. S. and Kim, H. D. (2005b). A study of biodegradable superabsorbent materials based on acrylonitrile grafted sodium alginate. *Key Engineering Materials*, 277–279, 450–454.

Lewis, J. G., Stanley, N. F. and Guist, G. G. (1988). Commercial production and applications of algal hydrocolloids. In C. A. Lembi and J. R. Waaland, *Algae and human affairs* (pp. 206). UK: Cambridge University Press.

Li, A. and Wang, A. (2005). Synthesis and properties of clay-based superabsorbent composite. *European Polymer Journal*, 41, 1630–1637.

Lin, W., Guan, Y., Zhang, Y. J., Xu, J. and Zhu, X. X. (2009). Salt-induced erosion of hydrogen-bonded layer-by-layer assembled films. *Soft Matter*, 5, 860–867.

Liu, Y., Xie, J. J., Zhu, M. F. and Zhang, X. Y. (2004). A study of the synthesis and properties of AM/AMPS copolymer as superabsorbent. *Macromolecular Materials and Engineering*, 289, 1074–1078.

Mahdavinia, G. R., Pourjavadi, A., Hosseinzadeh, H. and Zohuriaan, M. J. (2004). Modified chitosan. 4. Superabsorbent hydrogels from poly(acrylic acid-co-acrylamide) grafted chitosan with salt- and pH-responsiveness properties. *European Polymer Journal*, 40, 1399–1407.

Martinsen, A., Skjåk-Bræk, G. and Smidsrød, O. (1989). Alginate as immobilization material: I. Correlation between chemical and physical properties of alginate gel beads. *Biotechnology and Bioengineerin*g, 33, 79–89.

Mishra, A., Yadav, A., Pal, S. and Singh, A. (2006). Biodegradable graft copolymers of fenugreek mucilage and polyacrylamide: A renewable reservoir to biomaterials. *Carbohydrate Polymers*, 65, 58–63.

Moe, S. T., Draget, K. I., Skjåk-Braek, G. and Smidsrød, O. (1995). Alginates. In A. M. Stephen (Ed.), *Food polysaccharides and their applications* (pp. 245–286). New York: Marcel Dekker.

Moe, S. T., Skjåk-Bræk, G., Elgsaeter, A. and Smidsrød, O. (1993). Swelling of covalently crosslinked alginate gels: influence of ionic solutes and nonpolar solvents. *Macromolecules*, 26, 3589–3597.

Moe, S. T., Skjåk-Bræk, G., Smidsrød, O. (1991). Covalently cross-linked sodium alginate beads. *Food Hydrocolloids*, 5, 119–123.

Murray, P. R. S. (1977). *Principles of organic chemistry*. 2nd Edition. (pp. 297 – 306). London: Heinemann Educational Books.

Nakamura, K., Nishimura, Y., Hatakeyama, H. and Hatakeyama, T. (1995). Thermal properties of water insoluble alginate films containing di- and trivalent cations. *Thermochimica Acta*, 267, 343–353.

Oates, C. G. and Ledward, D. A. (1990). Studies on the effect of heat on alginates. *Food Hydrocolloids*, 4, 215–220.

Odian, G. (1991). *Principles of polymerization* (pp. 143; 212–213; 219; 311; 313; 454). 3rd Ed. US: John Wiley & Sons Inc.

Omidian, H., Hashemi, S. A., Sammes, P. G. and Meldrum, I. G. (1998). Modified acrylic-based superabsorbent polymers. Effect of temperature and initiator concentration. *Polymer*, 39, 3459–3466.

Omidian, H., Rocca, J. G. and Park, K. (2005). Advances in superporous hydrogels. *Journal of Controlled Release*, 102, 3–12.

Orive, G., Hernández, R. M., Gascón, A. R. and Pedraz, J. L. (2006). Encapsulation of cells in alginate gels. In J. M. Guisan, *Immobilization of enzymes and cells* (pp. 345–348). US: Humana Press.

Özeroglu, C. and Birdal, A. (2009). Swelling properties of acrylamide-N,N′ ′-methylene bis(acrylamide) hydrogels synthesized by using meso-2,3-dimercaptosuccinic acid-cerium(IV) redox couple. *eXPRESS Polymer Letters*, 3, 168–176.

Painter, T. J., Smidsrød, O. and Haug, A. (1968). A computer study of the changes in composition-distribution occurring during random depolymerisation of a binary linear heteropolysaccharide. *Acta Chemica Scandinavica*, 22, 1637–1648.

Patel, G. M., Patel, C. P. and Trivedi, H. C. (1999). Ceric-induced grafting of methyl acrylate onto sodium salt of partially carboxymethylated sodium alginate. *European Polymer Journal*, 35, 201–208.

Pavia, D. L., Lampman, G. M. and Kriz, G. S. (2005). *Introduction to spectroscopy: a guide for students of organic chemistry* (pp. 13–48). 3rd Ed. USA: Brooks/Cole Thomson Learning.

Peng, Z. and Kong, L. X. (2007). A thermal degradation mechanism of polyvinyl alcohol/silica nanocomposites. *Polymer Degradation and Stability*, 92, 1061–1071.

Pillay, V. and Reza, F. (1999). In vitro release modulation from crosslinked pellets for site-specific drug delivery to the gastrointestinal tract I. Comparison of pH-responsive drug release and associated kinetics. *Journal Controlled Release*, 59, 229–242.

Pourjavadi, A. and Zohuriaan-Mehr, M. J. (2002). Modification of carbohydrate polymers via grafting in air. 2. Ceric-initiated graft copolymerization of acrylonitrile onto natural and modified polysaccharides. *Starch*, 54, 482–488.

Pourjavadi, A., Barzegar, S. and Mahdavinia, G. R. (2006). MBA-crosslinked Na-Alg/CMC as a smart full-polysaccharide superabsorbent hydrogels. *Carbohydrate Polymers*, 66, 386–395.

Pourjavadi, A., Eftekhar, J. P., Seidi, F. and Salimi, H. (2010a). Synthesis and swelling behavior of acrylated starch-g-poly(acrylic acid) and acrylated starch-g-poly(acrylic amide) hydrogels. *Carbohydrate Polymers*, 79, 933–940.

Pourjavadi, A., Zeidabadi, F. and Barzegar, S. (2010b). Alginate-based biodegradable superabsorbents as candidates for diclofenac sodium delivery systems. *Journal of Applied Polymer Science*, 118, 2015–2023.

Preechawong, D., Peesan, M., Supaphol, P. and Rujiravanit, R. (2004). Characterization of starch/poly(e-caprolactone) hybrid foams. *Polymer Testing*, 23, 651–657.

Ramazani-Harandi, M. J., Zohuriaan-Mehr, M. J., Yousefi, A. A., Ershad-Langroudi, A. and Kabiri, K. (2006). Rheological determination of the swollen gel strength of superabsorbent polymer hydrogels. *Polymer Testing*, 25, 470–474.

Reid, A. R. (1977). Absorption rate of absorbent polymers by treating with glyoxal, US Patent 4,051,086.

Richardson, J. C., Dettmar, P. W., Hampson, F. C. and Melia, C. D. (2004). Oesophageal bioadhesion of sodium alginate suspensions: Particle swelling and mucosal retention. *European Journal of Pharmaceutical Sciences*, 23, 49–56.

Riesen, R. and Schawe, J. (Eds.). (2002). *Collected applications thermal analysis: thermoplastics* (pp. 12–13). 2nd Ed. Schwerzenbach: Mettler-Toledo GmbH.

Rioux, L.-E., Turgeon, S .L. and Beaulieu, M. (2007). Characterization of polysaccharides extracted from brown seaweeds. *Carbohydrate Polymers*, 69, 530–537.

Robyt, J. F. (1998). *Essentials of carbohydrates chemistry: With 370 Illustrations* (pp. 180–183). US: Springer.

Roger, S., Talbot, D. and Bee, A. (2006). Preparation and effect of Ca^{2+} on water solubility, particle release and swelling properties of magnetic alginate films. *Journal of Magnetism and Magnetic Materials*, 305, 221–227.

Rosa, D. S., Lopes, D. R. and Calil, M. R. (2005). Thermal properties and enzymatic degradation of blends of poly(3-caprolactone) with starches. *Polymer Testing*, 24, 756–761.

Rudin, A. (1999). *The elements of polymer science and engineering: an introductory text and reference for engineers and chemists* (pp. 90–102, 277–297). 2nd Ed. US: Academic Press.

Saboktakin, M. R., Maharramov, A. and Ramazanov, M. A. (2009). pH-sensitive starch hydrogels via free radical graft copolymerization, synthesis and properties. *Carbohydrate Polymers*, 77, 634–638.

Sabra, W. and Deckwer, W.D. (2004). Alginate – a polysaccharide of industrial interest and diverse biological functions. In S. Dumitriu, *Polysaccharides: structural diversity and functional versatility* (pp. 515–529). UK: CRC Press.

Said, A. A., Abd El-Wahab, M. M. M. and Hassan, R. M. (1994). *Thermochimica Acta*, 233, 13– 24.

Salomone, J. C. (Ed.). (1996). Alphabet "P". In *Polymeric materials encyclopedia* (Vol. 7, pp. 4947–4950). US: CRC Press.

Sannino, A. and Nicolais, L. (2005). Concurrent effect of microporosity and chemical structure on the equilibrium sorption properties of cellulose-based hydrogels. *Polymer*, 46, 4676–4685.

Seidel, C., Kulicke, W. M., Heb, C., Hartmann, B., Lechner, M. D. and Lazik, W. (2001). Influence of the cross-linking agent on the gel structure of starch derivatives. *Starch*, 53, 305–310.

Sheu (1992). Cables such as optical fiber cables including superabsorbent polymeric materials which are temperature and salt tolerant, US Patent 5,163,115.

Singh, B., Chauhan, G. S., Kumar, S. and Chauhan, N. (2007). Synthesis, characterization and swelling responses of pH sensitive psyllium and polyacrylamide based hydrogels for the use in drug delivery (I). *Carbohydrate Polymers*, 67, 190–200.

Skjåk-Bræk, G. and Moe, S. T. (1992). Alginate gels, US Patent 5,144,016.

Skjåk-Bræk, G., Larsen, B. and Grasdalen, H. (1986). Monomer sequence and acetylation pattern in some bacterial alginates. *Carbohydrate Research*, 154, 239–250.

Smidsrød, O. and Whittington, S. G. (1969). Monte Carlo investigation of chemical inhomogeneity in copolymers. *Macromolecules*, 2, 42–44.

Smidsrød, O., Haug, A., and Larsen, B. (1963). Degradation of alginate in the presence of reducing compounds. *Acta Chimica Scandinavica*, 17, 2628–2637.

Soares, J. P., Santos, J. E., Chierice, G. O. and Cavalheiro, E. T. G. (2004). Thermal behavior of alginic acid and its sodium salt. *Ecletica Quimica*, 29, 53–56.

Tangjang, S., Arunachalam, K., Arunachalam, A. and Shukla, A. K. (2009). Microbial population dynamics of soil under traditional Agroforestry systems in Northeast India. *Research Journal of Soil Biology*, 1, 1–7.

Thomas, S. (2004). Wound dressings. In D. T. Rovee and H. I. Maibach, *The epidermis in wound healing* (pp. 219–220). UK: CRC Press.

Torres, M. R., Sousa, A. P. A., Filho, E. T. A. S., Melo, D. F., Feitosa, J. P. A., de Paulab, R. C. M. and Lima, M. G. S (2007). Extraction and physicochemical characterization of Sargassum vulgare alginate from Brazil. *Carbohydrate Research*, 342, 2067–2074.

Tripathy, T., Pandey, S. R., Karmakar, N., C., Bhagat, R. P. and Singh, R. P. (1999). Novel flocculating agent based on sodium alginate and acrylamide. *European Polymer Journal*, 35, 2057–2072.

Trivedi, J. H. Kalia, K., Patel, N. K. and Trivedi, H. C. (2005). Ceric-induced grafting of acrylonitrile onto sodium salt of partially carboxymethylated guar gum. *Carbohydrate Polymers*, 60, 117–125.

Van de Velde, K. and Kiekens, P. (2002). Biopolymers: overview of several properties and consequences on their applications. *Polymer Testing*, 21, 433–442.

Wang, D. (2007, June). Superabsorbent Polymers Derived from Kenaf. Paper presented at the 2007 International Symposium on Kenaf and Allies Fibres, Xiamen, China.

Wang, W. and Wang, A. (2010). Synthesis and swelling properties of pH-sensitive semi-IPN superabsorbent hydrogels based on sodium alginate-*g*-poly(sodium acrylate) and polyvinylpyrrolidone. *Carbohydrate Polymers*, 80, 1028-1036.

Wong, M. (2004). Alginates in tissue engineering. In A. P. Hollander and P. V. Hatton, *Biopolymer methods in tissue engineering* (pp.77 – 80). US: Humana Press.

Xu, K. Q., Xu, X. L., Ding, Z. J. and Zhou, M. H. (2006). Synthesis and flocculability of sodium alginate grafted with acrylamide. *China Particuology*, 4, 60 – 64.

Yang, F., Li, G., He, Y. G., Ren, F. X. and Wang, G. X. (2009). Synthesis, characterization, and applied properties of carboxymethyl cellulose and polyacrylamide graft copolymer. *Carbohydrate Polymers*, 78, 95–99.

Yang, L. Y., Zhang, B. F., Wen, L. Q., Liang, Q. Y. and Zhang, L. M. (2007). Amphiphilic cholesteryl grafted sodium alginate derivative: synthesis and self-assembly in aqueous solution. *Carbohydrate Polymers*, 68, 218–225.

Yin, Y. H., Ji, X. M., Dong, H., Ying, Y. and Zheng, H. (2008). Study of the swelling dynamics with overshooting effect of hydrogels based on sodium alginate-*g*-acrylic acid. *Carbohydrate Polymers*, 71, 682 – 689.

Yoshimura, T., Uchikoshi, I., Yoshiura, Y. and Fujioka, R. (2005). Synthesis and characterization of novel biodegradable superabsorbent hydrogels based on chitin and succinic anhydride. *Carbohydrate Polymers*, 61, 322–326.

Zhu, S., Ma, M. and Zhou, W. (1996). Theory of non-random cross-linking: free-radical polymer grafting. *Macromolecules*, 29, 5688–5694.

Zohuriaan, M. J. and Shokrolahi, F. (2004). Thermal studies on natural and modified gums. *Polymer Testing*, 23, 575–579.

Zohuriaan-Mehr, M. J. and Kabiri, K. (2008). Superabsorbent Polymer Materials: A Review, *Iranian Polymer Journal*, 17, 451-477.